DV1.2 Lithology Assessment & Constitutive Model [NGI & Rockfield]

Organisation(s)	NGI and Rockfield
Author(s)	Lars Grande, Carl Fredrik Forsberg, Nazmul Haque Mondol, Dan Roberts, Dan Phillips
Reviewer	John Williams
Type of deliverable	Report
Dissemination level	SHARP Consortium only
WP	1
Issue date	29th September 2023
Document version	02b for SHARP website

Keywords: Lithology, mineralogy, uplift, glacial, diagenesis, *in-situ* stress, constitutive modelling

Summary:

This report focuses on assessments of lithological impact to present day *in-situ* stress state and integrating observations into constitutive models for application in subsequent tasks (WP1.3 and 1.4). This work is closely linked to WP3.2, and both reports seek to investigate the relative contribution of various processes (initial deposition and mineralogy, burial history including diagenesis, erosion, uplift and glacial loading) to the current *in-situ* stress in the North Sea basins. The content of the report includes exhumation studies using logs from DISCOS database in combination with lithology-dependent (rheological) compaction and uplift behaviour extracted from the NGI's database of soils and rocks, supplemented by rock mechanical data shared by the storage site operators. This report integrates the experimental laboratory results and empirical relationships from WP3.2 (report DV3.2), with the load

history from glacial loading and burial/uplift using stress indicators from geotechnical site investigations and exhumation analysis of logs respectively. Publicly available extended leak-off tests (XLOT) and leak-off tests (LOT) complemented by additional XLOT data provided by Equinor are used for comparison of empirical relationships defining the impact of mineralogy and burial and loading history on present day stress. We demonstrate how empirical relationships, logs and LOP data can provide useful additional insights into depth dependent and potentially lateral variations of stress within a basin, i.e. between fault blocks or CCS injection sites, and specifically in uplifted areas. Key laboratory data in report DV3.2 are brought into constitutive models to provide the link between the inferred stress history (imposed load/deformation) and the resultant stresses. A proprietary constitutive model has been applied and calibrated with laboratory datasets, which has been shown to satisfactorily capture the experimental response of various soils and soft rocks. This model calibration work is partly reported in DV1.1b, and the model is further tested and calibrated to field stress observations in this report. Workflows to assess stress from reginal trendlines in combination with a method for impact of lithology and burial history have been established and demonstrated for the SHARP CCS sites, with main focus on Aurora and Smeaheia in the Horda platform area, and the Lisa Structure in Denmark.

Contents

Appendix A- Tables with data and figures from Geotechnical Site investigations, detailed XLOT data and Poisson's ratio from lab testing (restricted for SHARP until published)

1 Introduction

1.1 Overview

This task focused on determining the relative contribution of initial deposition and mineralogy, burial history (including diagenesis), erosion, uplift and glacial loading, to the current in-situ stress in the North Sea Basin. This includes exhumation studies using supplied logs in combination with lithology-dependent (rheological) compaction and uplift behaviour extracted from the NGI/BGS database of soils and rocks, supplemented by the rock mechanical data shared by the storage site operators. This task integrates the results from WP3.2. SHARP report DV3.2 focuses on analysis of experimental database, whilst this report focuses on the application of findings from DV3.2 and calibration with field stress measurements, extended leak-off tests (XLOT) and leak-off tests (LOT) provided by operators or that are publicly available. Key findings summarized in report DV3.2 are brought into constitutive models for the forward modelling work. A proprietary constitutive model has been applied and calibrated with laboratory datasets, which has been shown to satisfactorily capture the experimental response of various soils and soft rocks. This modelling calibration work is partly reported in DV1.1b, and the model is further tested and calibrated to field stress observations in this report.

The study focuses on the upper sedimentary package where the calibration of available stress measurements from wells is possible (0-5 km). The potential for stress decoupling between the basement and upper sedimentary package can be dependent on the material contrasts in the base of the sedimentary package and within the basement rock. This has only been briefly discussed in this report and will be further evaluated in WP1.3. The outcome of this study will be a direct input to further modelling work on stress history to be done as part of WP1.3, which covers a regional 2D model of the east-west cross-section comprising the uplifted areas in the Horda Platform, across the Viking Graben and East Shetland Basin to the west. This report documents results from estimated load history from uplift and glacial loading analysis of field stress data and calibration of constitutive model for use in modelling studies in WP1. The work reported here provides direct input to the uncertainty and risk evaluation to be performed under WP5 and round 2 rock failure risk under WP4.

A detailed background study of the stresses in the selected SHARP CCS sites has been given in previous SHARP reports, concerning tectonic and sedimentary history and potential stress drivers (DV1.1a and b, DV4.1), stress orientations from observation in wells (DV2.2), and a summary of available field stress measurement data and state of the art understanding with respect to failure scenarios and monitoring (DV4.1). The primary study area used in this report is the uplifted Horda Platform in the northern North Sea, including the producing fields Troll in the east and Oseberg. Additionally, a wider cross-section covering Viking Graben and East Shetland Basin to the east was also chosen to evaluate the more regional impact of uplift. The study area is mature with respect to available datasets; high-quality XLOT tests, geotechnical data and rock mechanical test data are available from the long history of producing fields in this area. Also, the CCS storage sites Smeaheia (Alpha Beta and Gamma wells) and Aurora (Eos well) are relatively mature compared to other sites with respect to data and previous development studies and research. A map of the wider and central study area for this report is shown in Figure 1-1. The key calibration points are the XLOT data in a few wells provided by Equinor. These have been complemented with many LOT data

available from the NPD (Norwegian Petroleum Directorate) well database. Data from geotechnical site investigations (SI) of Troll and Oseberg were included to evaluate material behaviour and stress barriers in the shallow Quaternary and the potential impact of ice loading on the stresses in the older rocks below quaternary units.
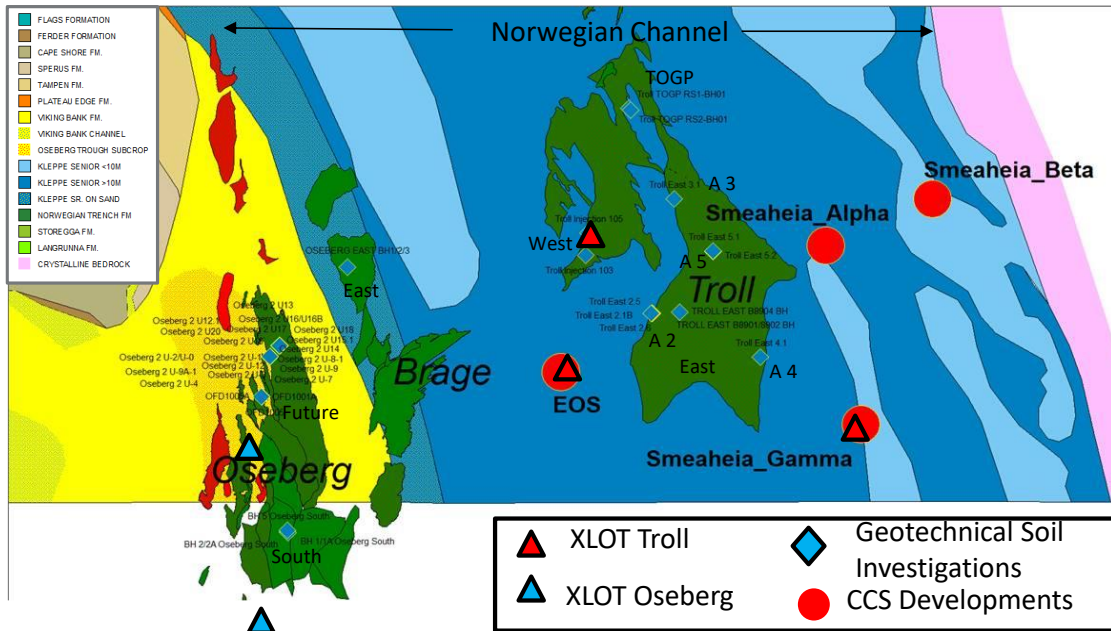

Figure 1-1 Central study area for this report is the Horda Platform stretching from the Norwegian Coast in East and through Troll and Oseberg fields including the CCS development sites of Smeaheia (Alpha Beta and Gamma wells indicated) and Auroura (Eos well indicated). The key calibration points is the XLOT data as indicated by triangled. Data from Geotechnical Soil Investigations has been included into the analysis of shallow Quaternary units (ca 200 m depth in Eastern part) (geological base map based on Rise et. al, 1984)

The report starts by describing the load impact from burial diagenesis and glacial loading on minimum horizontal stress (Chapter 2). Furthermore, a detailed evaluation of XLOT data and LOT data in the wider Horda Platform area is presented along with local trends of minimum horizontal stress in the E-W cross-section to evaluate potential impact of burial diagenesis and uplift on the observed trends (Chapter 3). The data and trends are compared with the recently published regional trends from the Equinor XLOT database, which is used as the reference throughout this analysis (Thompson et al., 2022a and Thompson et al., 2022b). Testing and calibration of the constitutive model developed and presented in DV1.1b are underlain based on recent laboratory datasets from the DV3.2 report and the XLOT field stress measurements (Chapter 4). To conclude, the general findings from this work on the Horda Platform are applied to other field cases to demonstrate the broader application of results to less mature fields in field stress data (Chapter 5). This highlights the expected trends based on regional published trends from high quality XLOT in combination with expected variation range based on lithological impact. For the Lisa field, information on lithology and mineralogy has been included in an updated plot and discussion into an example of the applicability of procedures to a

less mature field where site specific LOT data is not yet available (mineralogy data for Lisa is documented in the DV3.2 report).

Note that this report focuses on lithological impacts under uniaxial strain conditions and gravitational (mechanical) and chemical compaction effects on *in-situ* stress conditions, including minimum horizontal stress σ_h, total vertical stress σ_v and pore pressure P_p, and their resulting effective stresses throughout geological history. Potential tectonic effects on maximum horizontal stress σ_H and horizontal stress anisotropy are not covered in this report, as this is subject for further work on a regional model in WP1 and integration with stress focal mechanisms from basement earthquakes in WP2.

Early work in SHARP (for DV1.2 and DV3.2 report and Grande et al 2022) indicated that an empirical approach based on high stress uniaxial strain laboratory tests. These are commonly referred to as a K_0 test and directly measures the ratio between effective horizontal to effective vertical stress under uniaxial strain boundary conditions. K_0 in sediments fits rather well with range of K_0 measured in Norwegian Continental Shelf (i.e. Andrews et al 2016), and that majority of XLOT tests falls within the expected range of K_0 (0.6+/-0.2) same as what is expected from variations in lithologies assuming uniaxial strain conditions (see DV3.2 report). Also empirical relations of K_0 based on initial friction angle and plasticity of sediments undergoing mechanical uniaxial compaction capture the same variation range of K_0. In reality, the complex burial history of North Sea basins includes complex time and temperature dependent chemical creep from pressure and dissolution processes (i.e. Bjørelykke 1997, 1998, and Croize 2010), tectonically active periods with extensional stresses throughout early sedimentation history, and stress relaxation from both Neogene uplift and repeated glaciations in the Quaternary (DV1.1a, DV1.1b and DV1.4 report). Collectively these all play a role and add to uncertainty, however these processes are complex to test in laboratory and challenging for numerical modelling. Empirical methods therefore give valuable practical guidance on the lithological impact on stress, although all mechanisms are not captured or quantified. In this report we investigate further empirical methods from geotechnical engineering and laboratory studies based on uniaxial mechanical compaction, and constitutive relationships with extensions for impact on diagenesis, through testing and calibration with stress data from North Sea.

The stratigraphy of the Horda Platform is shown in Figure 1-2, and the cross-section of the Eastern part of the Horda Platform shown in Figure 1-3 provides the overview of the lithologies discussed in this report.
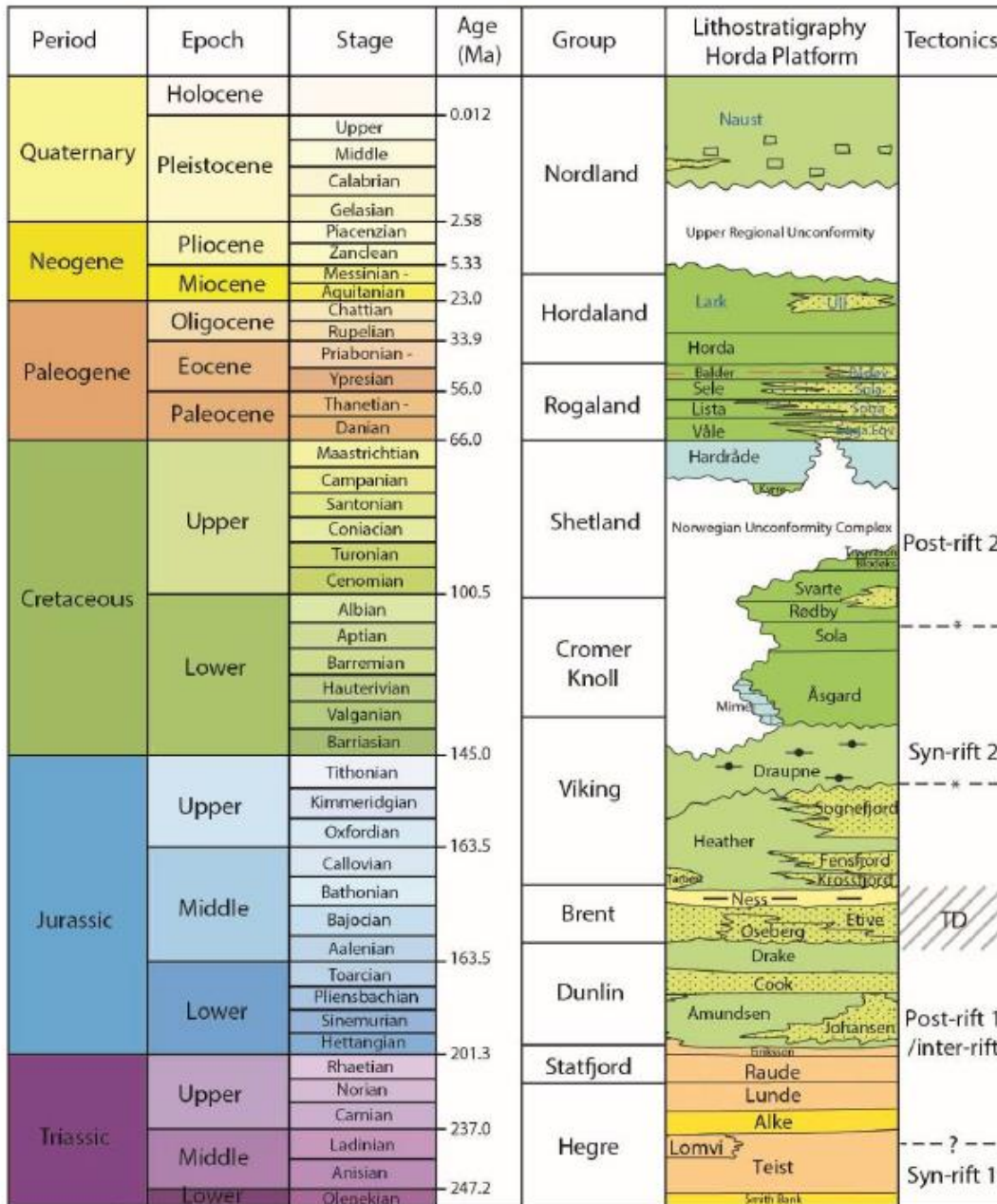
Period	Epoch	Stage	Age (Ma)	Group	Lithostratigraphy Horda Platform	Tectonics
Quaternary	Holocene		0.012	Nordland	Naust	
	Pleistocene	Upper				
		Middle				
		Calabrian				
		Gelasian	2.58		Upper Regional Unconformity	
Neogene	Pliocene	Piacenzian				
		Zanclean	5.33			
	Miocene	Messinian - Aquitanian	23.0	Hordaland	Lark	
Paleogene	Oligocene	Chattian			Ull	
		Rupelian	33.9		Horda	
	Eocene	Priabonian -			Balder	
		Ypresian	56.0	Rogaland	Sele	
	Paleocene	Thanetian -			Lista	
		Danian	66.0		Våle	
Cretaceous	Upper	Maastrichtian		Shetland	Hardråde	Post-rift 2
		Campanian			Kyrre	
		Santonian			Norwegian Unconformity Complex	
		Coniacian				
		Turonian				
		Cenomian	100.5		Svarte	
	Lower	Albian		Cromer Knoll	Rødby	
		Aptian			Sola	
		Barremian			Åsgard	
		Hauterivian			Mime	
		Valganian				
		Barriasian	145.0			Syn-rift 2
Jurassic	Upper	Tithonian		Viking	Draupne	
		Kimmeridgian			Sognefjord	
		Oxfordian	163.5		Heather	Fensfjord
	Middle	Callovian			Krossfjord	
		Bathonian		Brent	Ness	TD
		Bajocian			Oseberg Etive	
		Aalenian	163.5		Drake	
	Lower	Toarcian		Dunlin	Cook	
		Pliensbachian			Amundsen Johansen	Post-rift 1 /inter-rift
		Sinemurian			Eriksson	
		Hettangian	201.3	Statfjord	Raude	
Triassic	Upper	Rhaetian			Lunde	
		Norian			Alke	
		Carnian	237.0	Hegre	Lomvi	---?---
	Middle	Ladinian			Teist	Syn-rift 1
		Anisian	247.2			
	Lower	Olenekian			Smith Bank	

Figure 1-2 Stratigraphy of the Horda Platform area (Holden, 2021).
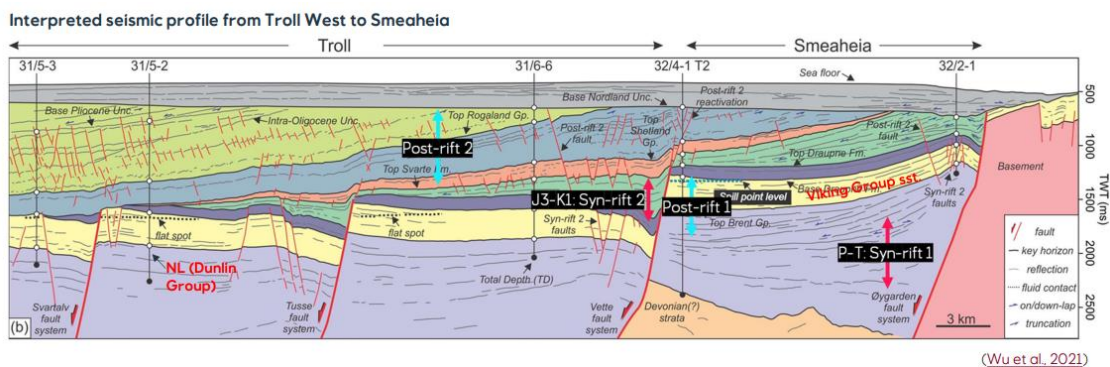

(Wu et al., 2021)

Figure 1-3 Cross section for the Eastern part of the Horda Platform (Wu et al., 2021)

1.2 Important Definitions

This subsection highlights key geomechanical definitions relevant to the clarity of the report. Foremost, an important parameter when considering the stress regime of the subsurface is the coefficient of Earth pressure at rest, K_0. This is defined as the ratio between the horizontal $\sigma h'$ and vertical $\sigma v'$ effective stresses under uniaxial strain conditions (Equation 1);

$$K_0 = \frac{\sigma h'}{\sigma v'} \qquad \text{(Eq. 1)}$$

The total minimum stress is measured in boreholes through *in-situ* hydraulic fracturing, where a pressurised fluid is injected into the desired bed until fractures are induced and subsequently closed. The orientation of the induced fracture gives an indication of the direction/configuration of stresses. Identifying the pressure required to initiate the propagation of fractures or, ideally, to close the fractures after injection approximates the magnitude of minimum total *in-situ* stress. In North Sea sedimatary basin general assumption is nomal stress regime, and minimum total stress then equals minimum horizontal stress σh . Effective horizontal stresses $\sigma h'$ can then be derived from this value with knowledge of *in-situ* pore pressure, and the $\sigma h'$ is among the most influential parameters in geomechanical stability and integrity evaluations. The σh is the key parameter often used to define the maximum capacity of the seal, i.e pore pressure in reservoir during CO_2 injection should not exceed the total horizontal stress in seal. Therefore, in this report we focus for prediction of σh , $\sigma h'$ and K_0 ratio.

Under normal mechanical consolidation, K_0 can also be approximately expressed as a function of the mobilised friction angle (ϕ') of a material (Equation 2). This angle describes the sum of resistance to interparticle sliding, or the slope of a linear representation of the shear strength of the rock.

$$K_0 = 0.95 - \sin \phi' \qquad \text{(Eq. 2)}$$

For isotropic materials *deforming elastically* the K_0 value can also be related to the Poisson's ratio (v) of a specific material, i.e the ratio of transversal/radial to axial strain: (3).

$$K_0 = v/(1 - v) \text{ (Eq. 3)}$$

Intuitively, one can see that these equations relate the stress conditions via strength properties or elastic properties. More generally, this relates the *in-situ* stress conditions of a specific horizon to the rheological properties.

One final noteworthy parameter to define is the Overconsolidation Ratio (OCR). This is the ratio of the maximum vertical effective stress a rock has been subjected to (preconsolidation pressure, $\sigma p'$), to the present-day vertical effective stress ($\sigma v'$) (Equation 4). In principle, lithologies with OCR values <1 represent an underconsolidation state, OCR values =1 represent a normally consolidated lithology and OCR values >1 are associated with an overconsolidated state. Hence, this value gives insight into the densification or stiffening of lithologies.

$$OCR = \sigma p'/\sigma v' \text{ (Eq. 1)}$$

2   Loading Scenarios 1D

The purpose of this chapter is to establish loading scenarios for modelling in the Horda platform area. This section only considers uniaxial loading conditions for the evaluation of lithological impact on stress.

2.1   Loading from Glaciers

A summary of geotechnical information and geology of Quaternary units from the Horda platform, Troll, Brage and Oseberg sites are reported in DV1.1a. A similar review is also given in Master's Thesis from NTNU (Jalali, 2023). Furthermore, examples of load history and 2D consolidation analyses in PLAXIS were given in the same thesis.

One main topic of interest is the highly over-consolidated Unit III in the Troll Quaternary units, which has a high OCR of 7 and a reported $K_0>1$ and to evaluate its regional appearance and behaviour. This layer with $K_0>1$ is of high interest from two perspectives; one is the indication of a large loading during ice ages, and the second is that such a layer can potentially be a stress barrier, preventing vertical leaks or distributing potential leaks laterally; this could affect the strategy and location of monitoring infrastructure. Another main interest is the pre-consolidation stress P_c' at the base of Quaternary or in highly overconsolidated layers. This is an indication of what may have been the maximum vertical effective load from ice on the older eroded and uplifted units below. The focus has therefore been to document observations of effective vertical stress (po'), pc', OCR and estimated K_0 in available geotechnical boreholes. Note that in this report we use both Po' and σ_v' for effective vertical stress (Po' from geotechnical standard terminology).

2.1.1   Quaternary Geology

A detailed presentation of Quaternary geology in the Horda Platform area was presented in SHARP Report DV1.1a. This chapter focuses on some key units and surfaces in the Troll and Oseberg areas that are of special relevance for stress history evaluations.

A map of the area, cross-section and profile analysed with the site investigations indicated are shown in Figure 2-1. The Upper Regional Unconformity (URU) represents the base-Quaternary and is a composite surface that variably follows the top of the Utsira Formation where present, the mid Miocene Unconformity (MMU) and underlying Hordaland group. Because the Norwegian Channel Ice Streams eroded and removed a large amount of the underlying sediments, the URU is synonymous with the base Quaternary horizon across much of the eastern Norwegian Channel. The Naust Formation sediments host several gas discoveries, including the Peon and Aviat fields (Mikalsen 2015; Rose et al. 2018), contain numerous shallow gas pockets and is the seal for CO2 sequestration in the underlying Utsira Formation (Halland et al. 2014; Lloyd et al. 2021). Intra-Norwegian Channel 1 and 2 (INC-1 and INC-2) are regional seismic reflectors.

The study includes geotechnical data from deep geotechnical boreholes at three sites from Troll and four sites from Oseberg (see Figure 2-1). For Troll the database includes data from Troll East (NGI 1984 and NGI 1989), Troll West (NGI, 1991) and TOGP location (NGI, 1997). The deep geotechnical borehole (no 8903) is also documented in

Lunne, 2006. The following sites from Oseberg are included in the evaluations; Oseberg 2 (Location 1 and 2) (NGI, 1987), Oseberg East (NGI, 1991), Oseberg South (NGI, 1996) and Oseberg Future (NGI, 2014).

The Troll area is positioned within Norwegian Channel with Tertiary sediments from the Oligocene (Hordaland Gp.) below the URU. The Oseberg wells are positioned on the flank of the Norwegian Channel and therefore represent a different lithology compared to Troll.
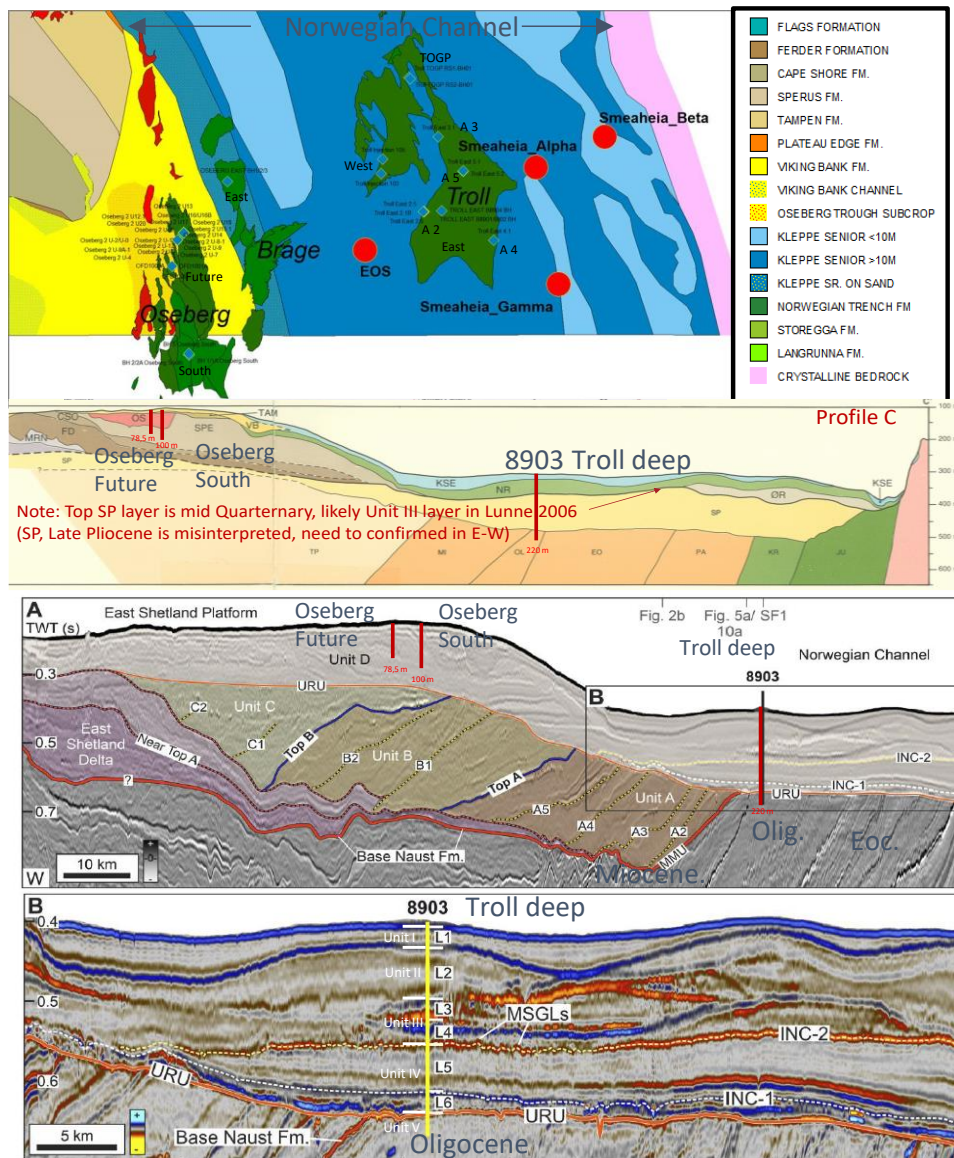

Figure 2-1 Map of area of interest and 2D E-W profile through Troll East, Brage (just south) and Oseberg. Major faults are indicated as tagged lines (map based on Rise et. al, 1984). Lower part of figure show seismic E-W cross section through geotechnical drillhole BH8903 at Troll and the more detailed stratigraphy (L1-L6 and Unit I-IV) within Quaternary are indicated from seismic horizons (Løseth et. al, 2022). Unit V below URU belongs to Tertiary older sediments of Oligocene Fm. Hordaland Gp. Figure Map of study area with wells Bore SI locations indicated.

The Troll Quaternary lithological units are well documented with respect to geotechnical parameters (Lunne et al., 2006) and Quaternary chronostratigraphy (Sejrup et al 2003). The naming of Units is slightly different, where the map above uses L1-L6, whereas this

report uses Unit 1-V according to geotechnical reports and Lunne et al 2006. L1 and L2 are concordant with Units I and II. L3 and L4 are the same as subdivided Unit III. Unit L5 and L6 correspond to Unit IV. The deep geotechnical borehole BH8903 indicated in Figure 2-1 is used as a reference for description of the key geotechnical Units III and V below.

<u>Troll Unit III (74 m – 135 m in bh8903)</u> is thought to be a series of glacial tills, and the top of is an erosional surface which is easily identified on seismic sections. This surface was caused by glacial advance which removed an unknown quantity of the sub-glacial strata. The high OCR could be due to a previous sediment load or glaciations. It is possible that the lowest sub-unit comprises a lodgement till, and that the upper zone was formed as a melt out till. The top of Unit III is a glacial erosion surface present in much of the Norwegian Channel and corresponds to the base of the Norwegian Trench Formation (NR) on Figure 2-1 where it can be seen to be exposed at the seafloor in NE parts of the map. This is probably related to erosion/non deposition caused by the Norwegian Coastal current.

<u>Troll Unit V (201-2020 m in BH8903)</u> represents the uppermost part of the Tertiary unit from the late Oligocene (Hordaland Gp). The transition from Unit IV to Unit V is defined as URU in this borehole. The Tertiary units are ca 1km thick in total, and the potentially Smectite rich layers of Oligocene and Eocene that define the Hordaland group are ca 0.45 km thick at this location. Unit V has V_{cl} (<2um) of 38%, of which 60% is Smectite, 20% Kaolinite, and 20% Illite (Lunne et. al., 2006). This layer may be characterized as Smectitic mudstone. Smectitic mudstones, mostly of Lower Tertiary age, and in particular Eocene and Oligocene mudstones representing distal facies, may have a very high smectite content (>50%) and almost no quartz or feldspar (Hugget 1998, Bjørlykke, 1992).

The lithologies at Oseberg South and Oseberg Future are more dominated by sand with a ca 10 sand layer at the top (Viking Bank Formation) and thicker layer of sand below ca 20-30 m depth (Oseberg Trough Formation). In between there is a 10-15 m thick layer of clay with sub layering Unit II, III and IV (ca 12-27 m) in Oseberg South and Unit II, III (ca 12-21 m) in the Oseberg Future location. Although there is different naming at the two sites, this clay unit is likely one regional clay unit covering the sand below, which likely belongs to the Oseberg Trough Formation (marked OS on the map in Figure 2-1). This is a local sand body with limited extent to the north, however the full extent towards the south is not mapped in the Oseberg South area (From original map based on Rise et. al, 1984). The thickness is ca 12 m in Oseberg South and 40 m in Oseberg Future, which may indicate that the sand also pinches out southwards.

2.1.2 Stress and Load History Profiles

The depth profiles of pre-consolidation stress P_c', overconsolidation ratio, OCR, and K_0 are shown in Figure 2-2 for Troll and Figure 2-3 for Oseberg respectively, and the profiles summarise all available information from the site investigation reports. Note that for P_c' and OCR these are a mix of data points based on various methods of direct interpretation from oedometer test data (Casagrande, Janbu methods) and empirical correlations with strengths etc. Recommended values (solid lines) for each formation based on engineering judgement are included based on original recommendations in

reports. No new interpretations are included here. There are some variations in depths between main units in the geotechnical sites evaluated in this study.
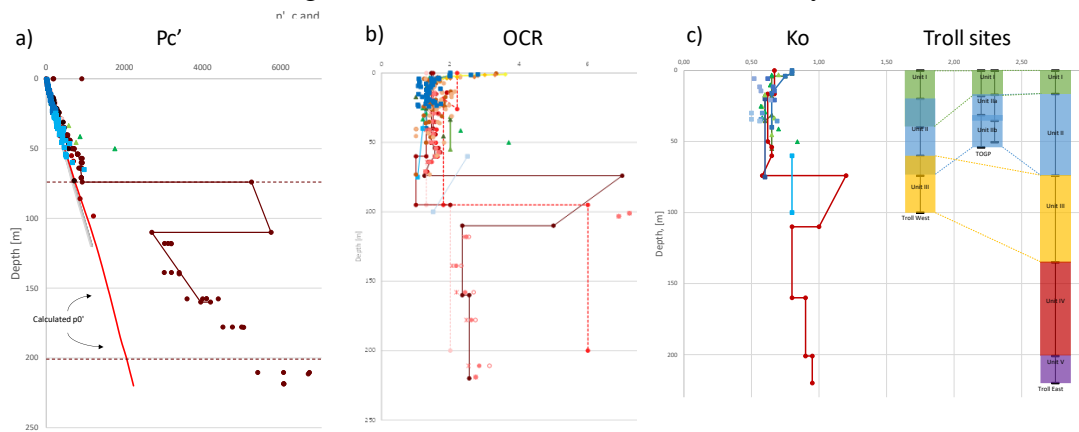

Figure 2-2 Stress parameters pc' and po, OCR and K_0 vs- depth in three Troll locations in plots a, b and c respectively. The legend refers to site investigation and areas in Troll, and interpretation method i.e. Casagrande for determination of pc'. All recommended trendlines from the different site investigation plots area included. The three main sites Troll East, Troll West and TOGP in Northern part is indicated with the coloured bars and indicate the depth in the boreholes within the areas (thin line within the coloured bars).
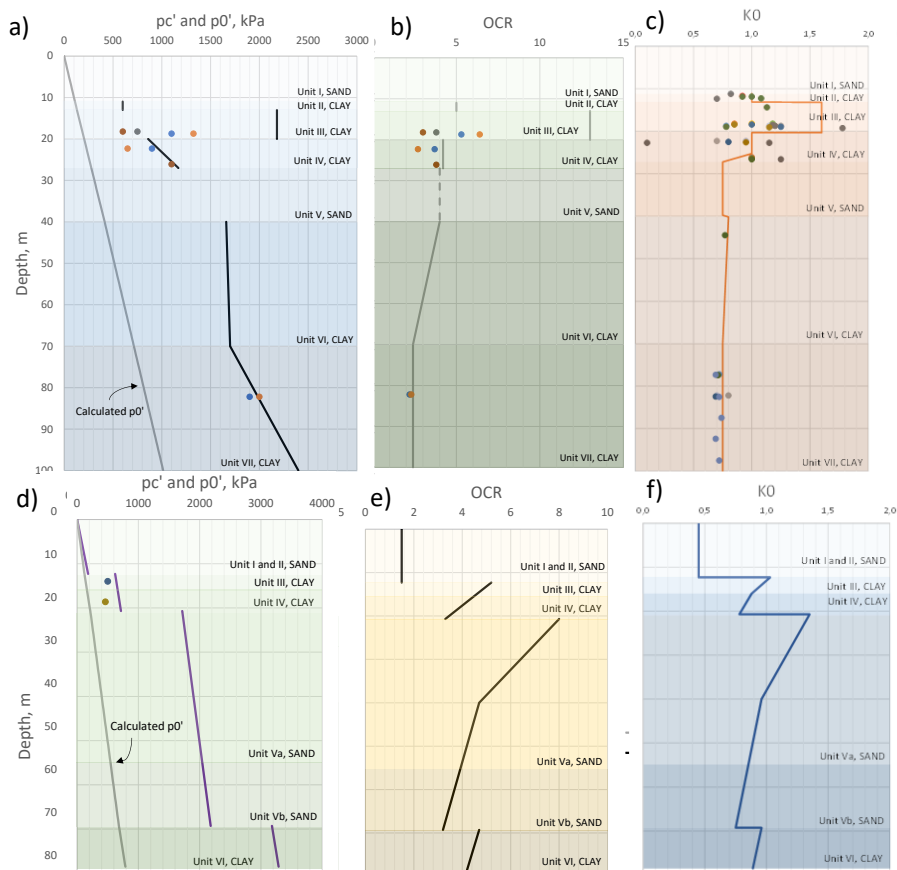

Figure 2-3 Stress parameters pc' and p'o, OCR and K0 vs. depth Oseberg Site Investigation locations, in Oseberg South (a, b and c) and Oseberg Future (d, e and f). Note that the names of the two main Units at the two locations are not the same but are local and taken from the referenced projects. Also recommended trendlines from the different site investigation are indicated by drawn lines.

A summary of depth, OCR and estimated K_0 at top Troll Unit III and Oseberg top clay unit (both with high OCR), and at maximum depths at selected locations are given in Table 2-1.

Table 2-1 A summary of depth, OCR and estimated K_0 at top Troll Unit III, Oseberg top clay unit (both with high OCR), and at maximum depths at selected locations.

Field	Soil Unit	Depth	OCR	Estimated K_0
Troll East (bh8903)	Top Unit III	74	7	1.2
	At max depth	220	2.55	0.95
Troll Area 2	Top Unit III	95	2	0.67*
Troll Area 3	Top Unit III	52	2-6	0.74-1.24*
Troll Area 4	Top Unit III	44	6	1.21
Troll Area 5	Top Unit III	56	2-6	0.65-1.1**
RS1-BH1	Top Unit III	50.5	2.0 (1.8)	0.79*
RS2-BH1	Top Unit III	54.1	2.3 (3-7)	0.79-1.17*
Oseberg 1996	Top Unit III (Clay)	13-20	13	1.6
	At max depth	100	2.4	0.75
Oseberg 2014	Top Unit II (Clay)	12.3-20.7	5.2	1.03
	At max depth	78.5	4.2	0.89

*Using $K_0=0.48Ip^{0.03}OCR^{0.47}$ (when Ip is reported, L'Heureux et al., 2017)
** Using $K_0=0.47OCR^{0.47}$ (when Ip not known, L'Heureux et al., 2017)

2.1.3 Discussion of Results

Regional stress barriers for fluid flow
Within the Troll area, when comparing Troll Unit III distribution at other locations they appear at shallower depths and with lower OCRs; in range 2-6 compared to BH8903 (Table 2-1and Figure 1-1 and Figure 2-1**Error! Reference source not found.**). In Area 2, just west of BH8903, Unit III is deeper (95m) and has a lower OCR of 2 and K_0 of 0.66. In Area 3, 4 and 5, Unit III is shallower 44-56 m with OCRs of 2-6 and K_0 in the range 0.65-1.24. In the northern part of Troll (RS1 and RS2) the Unit III is also shallow 50-54 m and the OCR 2 and 7 and estimated K_0 in the range 0.79-1.17. The boreholes further west at Troll West are shallower and do not penetrate into Unit III.

The high OCR and K_0 indicated in Troll Unit III seem to be of rather local occurrence and remaining boreholes have $K_0<1$. The influence of this layer as a stress barrier ($K_0>1$) may therefore be limited. However, it can still have significant impact on flow due to the larger permeability of this till unit. The mechanisms for developing high Pc' and OCR are complex and based on several mechanisms, not only the variation of the detailed composition of the sediment parameters such as Plasticity (Ip), clay content, permeability etc, but also the presence of drainage pathways in permeable layers around the overconsolidated zone is essential for low permeability layers to drain and distribute pore pressures.

There is some indirect evidence from historic gas seepages that western part of Troll is more permeable, and pockmarks are more frequent on the seafloor (Andersen et al., 1995, Forsberg et al., 2007, Mazzini et al., 2016 and 2017).

<u>Calibration of historical vertical stress at the base Quaternary at URU and MMU</u>
The high value of OCR of 7 near the top of Unit III is the maximum found over the entire Troll deep boreholes, and this is used as indicator of what the load from Ice could have been during glaciations. The pc' of 5.25 MPa on Top unit III is same as the p_c' at the URU surface at a depth of 201 m. The OCR at the depth of the URU is 2.55 and additional load of 3.19 MPa from ice loading is therefore expected to have influenced the Tertiary Units below URU (glacial load calculated from p_c'-p_o' at 201 m).

The Oseberg wells indicate a pc' of 2.4 MPa at 100 m in Oseberg South and 3.3 MPa at 79 m in Oseberg Future development. The exact depth of URU is not known as seismic data from this area is not available to the project. A reference is therefore made to the base NAUST (MMU) as reported from nearest explorations wells (526 m in 30/9-6 well Oseberg South and 526m and 491 m for Oseberg Future Development area). The estimated OCR at depth of MMU is then ca 1.5 with an additional load of 2.52 MPa from ice loading below MMU (glacial load calculated from p_c'-p_o' at 79 m). Utsira sand is the unit below at all locations and may therefore be overconsolidated at the top with an OCR of 1.5 correspond to weight of ice load during Quaternary. Note that an OCR of 1.5 is usually considered to be normally consolidated from aging effects and is not considered as a high value (i.e. Bjerrum. 1967). Drainage from the deeper mudstones below Utsira into Utsira sand is therefore also possible allowing for consolidation of mudstones from ice loads in this area.

There is no relevant geotechnical data for Smeaheia and Aurora sites. However, the reported values for Troll and Oseberg above are calibration points which can be used to calibrate empirical models of thickness of ice cap might have been for the larger area.

2.2   Exhumation Analysis Logs and Diagenesis

Exhumation analysis was targeted for wells spread along E-W cross section and for wells where XLOT data are available. Log data from DISKOS has therefore been collected for the same wells where XLOT data were available, giving 14 wells in total. First an evaluation in the eastern part of study area was done and reported in DV1.1b, covering the most uplifted areas; Smeaheia, Troll East and West, and Aurora. However, most of the wells where XLOT is collected are development wells with limited well log data available and not suitable for exhumation study. Where key log data for exhumation analysis are missing, we use data from exploration wells with good log coverage that are close by. Results from exhumation study are shown in Figure 2-4. The study is performed using 17 exploration wells from the Horda Platform area including the selected CO_2 storage sites Aurora and Smeaheia. To avoid uncertainties and to get better uplift estimates in every well location in the target area, the NCT (Normal Compaction Trend) technique is utilized in this study to construct the high resolution uplift map. The high resolution uplift map shows that the well locations in the study area have been subjected to different magnitudes of uplift. The estimated uplift values vary from 200 to 1400 m from west to west.
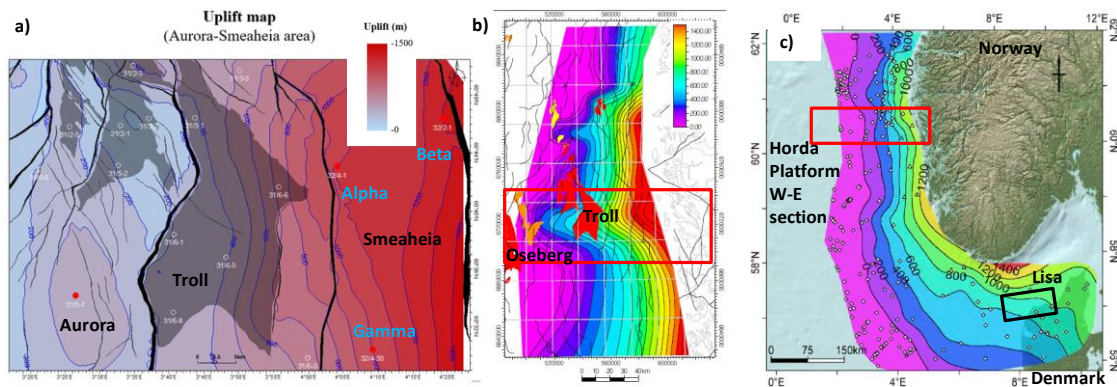
Figure 2-4 a) Contour map with estimated uplift (also reported in SHARP report DV1.1) and b) net uplift estimates based on sandstone modelling (Gateman, 2016) with a contour map of a larger area. Note that wells in the Oseberg were not included in either of these two studies. c) Uplift map based on sonic log along larger part of Norwegian coast with Hordaplatform and Lisa structure indicated (Baig et al 2019)

The accuracy of NCT-based uplift estimation strongly relies on the selection of NCT. Selecting differing NCT may result in uplift estimation variations in the order of several hundred meters (Gateman, 2016; Baig et a., 2018). Therefore, to construct a reliable NCT for the Horda Platform it is necessary to estimate compaction-based uplift in the area. A shale compaction trend is established by using a database of well characterized, mechanically compacted, reconstituted shales calibrated with a reference well. Overall, there are good agreements between uplift estimates reported in Gateman, 2016 and Baig et al., 2018 and uplift estimated in this study. Gateman (2016) reports close to zero uplift in the position of Brage and Oseberg based on analysis of sands in wells. This may indicate that only glacial loading is present in the western part of E-W cross section through Troll and Oseberg. From Baig et al 2018, the uplift seems to pinch out in same area as reported by Gateman 2016.

The work flow for computing exhumation was to compare Vp-depth trend for any target well with the established NCT (Mondol, 2009). The interface (TZ-Transition Zone) between the mechanical (MC) and chemical (CC) compaction zones was identified. This interface depth is the present day cementation depth. After aligning the velocity data trend of all wells with the established NCT, the exhumation magnitude was calculated. The overburden is important in a sense that it lies within the mechanically compacted zone making it possible to compare its compaction trend with the reference compaction trend obtained from laboratory experiments and reference well. The main problem faced in the analysis was absence of necessary log data at shallow depths (against the overburden) and data scatter without a conclusive trend. The exhumation method used here is simple but very helpful in showing a general uplift trend in the area. The inversion on particular block-bounding faults (e.g., Tusse and Vette) and the contour variations for each block are out of the scope of this study using this method.

The study area has been influenced by several phases of uplift and erosion episodes. Due to uplift, the rocks (source, reservoir, cap, overburden/underburden) in the area are not currently at their maximum burial depth. Uplift and erosion can have a wide range of effects, both positive and negative, on CO_2 storage sites. The uplift and erosion of the study area are associated with the opening of the Norwegian Greenland Sea since the earliest Eocene and with the Late Pliocene-Pleistocene glaciations, which span over

several million years. Using different uplift/erosion techniques (e.g., shale normal compaction trend (NCT), interval velocity, and thermal maturity), numerous articles discussing uplift/erosion of the Norwegian continental Shelf have been published (e.g., Baig et al., 2016; Baig et al., 2018).

Like other parts of the Norwegian Continental Shelf, the uplift episodes have significant consequences on CO_2 storage and petroleum systems in the Horda Platform area. The reservoir quality, maturity of the source rocks and the migration of hydrocarbons are affected by the processes. Owing to changes in the PVT conditions in a hydrocarbon-filled structure, uplift and erosion increase the risk of leakage (example of Bjaaland structure in the Barents sea) and expansion of the gas cap in the structure. Negative effects include spillage of hydrocarbons from accumulations, expansion of gas and evacuation of structures, potential for seal failure and cooling of source rocks. Therefore, understanding of the timing of uplift, faulting, diagenetic history and fault/seal/overburden rock properties are therefore significantly important to develop CO_2 storage in the study area.

2.3   Summary of Loading Scenarios for Modelling

Calibration points for ice loading at Troll and Oseberg were highlighted in Chapter 2.1. To evaluate ice loads on a more regional scale and at the CCS sites of Smeaheia and Aurora, extrapolation through empirical models of ice cap thickness has been completed. According to Figure 2-1, relevant formations at Aurora and Smeaheia are the Kleppe senior and Norwegian Trench formations respectively. The Eastern trench formation in the east is only relevant for Smeaheia. The Troll site is assumed to be the most representative sites for both Aurora and Smeaheia.

Figure 2-5 shows a schematic of a 2D cross section to illustrate some key subjects discussed in this report, where a complex load history and the relative impact of ice load vs. previous over-consolidation from burial diagenesis is highlighted. The rocks are uplifted more towards the east and experienced more mechanical compaction and diagenesis. The loading of the ice cap during ice age is also larger in the eastern part of where thickness of ice of 1-2 km is reasonable and with significant total load on sediments and rocks below. Effective load may however be close to zero in these unit if water cannot escape. i.e. long drainage path.

One key question is whether the (effective) load from the weight of ice acting on sediments below URU and MMU surface was larger than load of overlying sediments carried when the formation was at its maximum burial depth (MBD). In order for sediment to compact further the load from ice must be larger than the load from sediment (po'$_{ice}$> po'$_{uplift}$). Another key question is whether these clays below URU were able to drain during glacial loading or if there was a buildup of excess pore pressure. The presence of potential draining layers below URU are then of high importance. The drainage in layers below MMU and URU can be variable based on the lateral position in relation to the presence of permeable sand or silt layers capable of draining excess water pressure. In western parts below the URU in the Oseberg location, the Quaternary sediments (NAUST Fm.) had experienced limited compaction prior to glacial loading which give high permeability of clays and presence of drainage layers of sand and silt,

which in combination may drain excess pore pressure during consolidation of clays. Eastwards below URU at the Troll location, more consolidated and smectite rich layers in Oligocene and Eocene with low permeability and limited access to draining sand layers may have experienced excess pore pressure during glacial loading.
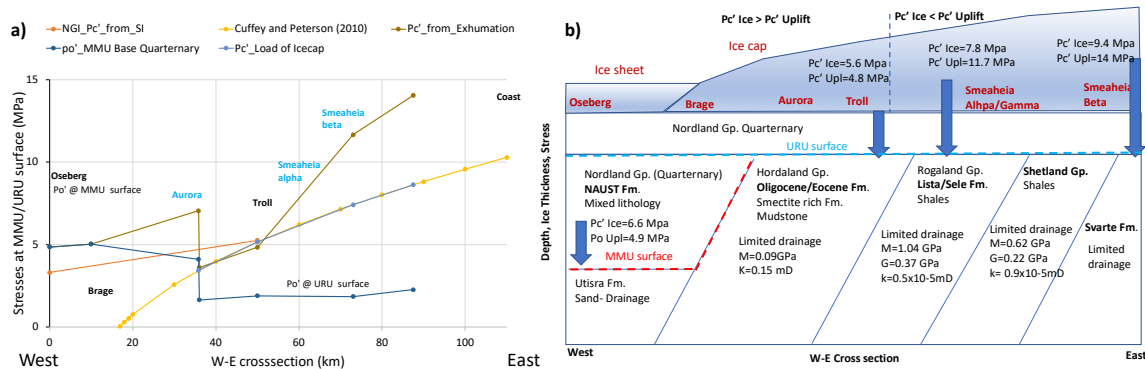

Figure 2-5 Simplified sketch of the complex load and the relative impact of ice load vs. previous over-consolidation from burial diagenesis. The figure shows uplifted inclined lithologies below the Quaternary URU and MMU interface. Note that the pc' Ice at URU is here termed as effective stresses, this is based on the assumption of total stress from estimated thickness of ice and hydrostatic pore pressure assuming drained conditions. At the time of glaciation, there has likely been significantly excess overpressure and close to zero effective stress at URU interface and in over pressured units above and below.

Potential areas where pc' Ice> pc' uplift is Oseberg, Troll West and Troll East, and potentially also the Aurora CCS storage site. In these areas cyclic loading from ice may have been enough to consolidate the units below and if impermeable units with lack of silty/sandy drainage layers inbetween (i.e smectite rich Oligocene layers below URU) excess pore pressure might have been generated. However, in Smeaheia, although ice cap is likely thicker and weight of ice larger, the weight of overburden sediments during maximum burial depth exceeds the weight of ice load (i.e pc' Ice> pc' uplift). In this case cyclic loading from glaciers may have less impact based on the overconsolidated state of these more compacted sediments. However, these are speculations and consolidation modelling would be beneficial to address these questions.

Impact of ice loading on the pore pressure on a basin scale has previously been modelled in the Barent sea (Lerche et al., 1997) and pore pressure effects in Tertiary units in North Sea are evaluated also for North Sea areas (Gyllenhammer 2003). However, the combined impact of pre-consolidation from large burial depth and uplift, glacial loading on pore pressure in the Horda Platform area are not found from literature.

3   Calibration of Log Methods and Field Stress Data

This chapter covers an analysis of LOT and XLOT data in the wider Horda platform area. A comparison between high-quality XLOT data with less accurate LOT data are done in this relatively mature area where both types of data are available. A more detailed well-based evaluation based on log-based methods has been applied to the XLOT data points where gamma logs are available and to key wells around Smeaheia and Aurora. The workflow used for stress estimation is based on the rock physics relationship of clay content, smectite content, and over-consolidation ratio (OCR), and

well log data has been established as part of SHARP project WP3.2 (Grande et al. 2022). In this section, further analysis and application to more wells have been done based on the updated rock physics model summarized in SHARP report DV3.2.

Geotechnical field stress data are not included in this evaluation, although such data are available from several sites offshore and onshore. WP3.2 includes a work task and discussion of results from laboratory tests (triaxial K_0) and empirical relations with field stress data from Onsøy test site at 6 m depth (Gundersen et al., 2019). Experiences from offshore North Sea tests are summarized in NGI 1990, and approximately 10 field stress test are from Troll during site investigations (taking place in 1987, 1988, 1989) using Fugro McClelland Packer system as well as Marchetti Dilatometer test (Lunne et al., 2006).

3.1 Method for Analysing Trends of LOT and XLOT Data

3.1.1 Method

Extended leak of tests (XLOT) released for SHARP project and leak of pressure (LOP) from the Leak Off Tests (LOT) derived from the NPD well database have been analysed with respect to fields, geological structure, and fault segments. The fields evaluated are in an East-West (E-W) orientation from East Shetland Basin (ESB) in the west, crossing Rugne Sub-Basin (RSB) and Viking Graben (VG), to Lomre Terrace (LT) and the Horda Platform (HP) in the east. This includes the following fields: Martin Linge, Oseberg, Oseberg East, Huldra, Veslefrikk, Brage, Aurora, Troll West, Troll East and Smeaheia. LOT data from Gullfaks and Statfjord in the East Shetland platform are also included, although they are located to the north of the main study area (see Figure 3-1, Section A and B).
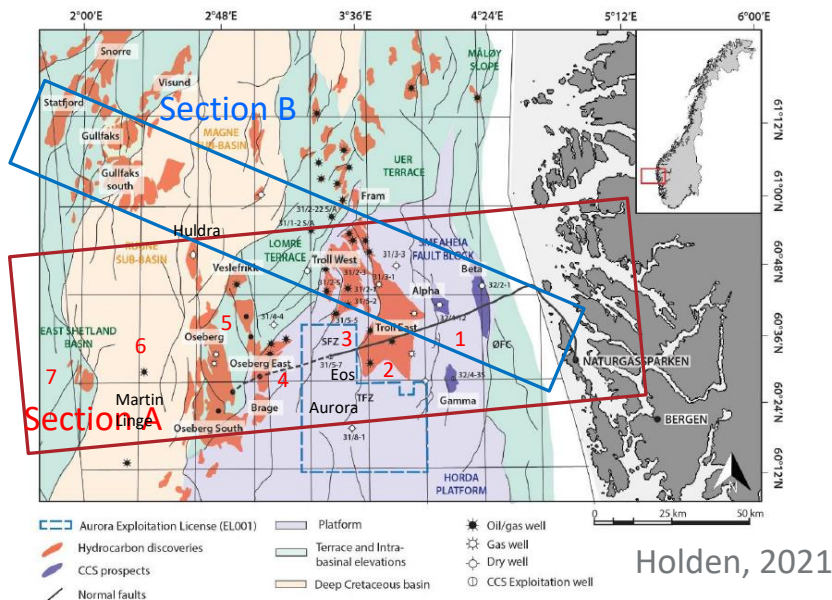

Figure 3-1 Study areas A and B. The oil and gas fields and CCS sites are indicated. East Shetland Basin and Lomre Terrace (green), Viking Graben (yellow) and Horda platform (violet). Structures/fault segments are indicated with numbers 1-7.

A selection of LOT data from a previous NGI compilation of LOT tests from the NPD database for entire Norwegian Shelf from have been utilized (NGI, 2019). More recent (post 2019) wells are not included in the database. The original database contains 2919 LOT tests from both exploration wells and deviated wells. This study includes 946 LOT tests from the selected area of interest. The database contains only the LOT interpreted value as reported in NPD database. A further evaluation of LOT test data and test quality is not done, as pressure data or interpretations report are usually not available from the NPD database.

The XLOT data released for SHARP includes in total 14 tests where 3 tests are already published (Thompson et al. 2022 and Wu et al., 2022). The new data includes 2 tests from Martin Linge, 6 tests from Oseberg area and 3 tests from the Troll area (Appendix A, restricted for SHARP projected until publication). The XLOT data are from the Equinor database, which has been interpreted according to Equinor procedures and quality system (Andrews et al., 2016). Tests with pore pressure (Pp) deviating more than in 10 % from hydrostatic are excluded from the evaluation of minimum horizontal stress σ_h trends. Out of 14 XLOT tests received, only 5 tests can be regarded as high-quality data (+/-10% after criteria used in Thompson et al. 2022a and b). These have been used in the further evaluation of σ_h. These data are sorted for the eastern part of the Horda platform (HP-E, Segment 1-3, marked green), the western part of the Horda Platform (Segment 4 and 5, HP-W marked blue in Table). The two deep XLOTs of Martin Linge are included to demonstrate the effect of pore pressure on σ_h trend below 3 km in the area of East Shetland Basin.

Trends of minimum horizontal stress (σ_h) for all segments (1-7) have been established for all XLOT and LOT data and compared with published trends of σ_h from Equinor's XLOT database from the Horda Platform (HP) wider area similar to E-W cross-section A in Figure 3-1(Thompson et al. 2022a) and the entire North Sea database (Thompson et al., 2022b).

The overall target for analysis was to evaluate the lithological impact on stress, and the following tasks were investigated.

- Find local trends within each main structure and faulted structure (Figure 3-1) and evaluate if local trends differ from regional trends
- Check how LOT data compares with XLOT data and if such data can be utilized to increase the amount of data for uncertainty evaluation and for other areas where XLOT data are not available.
- Evaluate the more detailed lithological impact on stress σ_h based on information on clay content from mineralogy or volume clays from cores or from log-based method (Grande et al., 2022).
- Evaluate impact of uplift and erosion and glacial loading, by plotting E-W trends and N-W trends of datasets of the main lithologies (Drake, Draupne, Sele/Lista and Hordaland) and using results from exhumation study and the concept for over consolidation ratio (OCR) for log-based method (Grande et al. 2022)

Results from the study are also shown in Appendix B in a factual format for more detailed documentation. The key results are highlighted and discussed in this chapter.

3.1.2 Background Data

A background for in-situ stress was given in SHARP report DV1.1b for Horda Platform and for all sites in the DV4.1 report. This study focuses on the Horda platform area where most XLOT data are available compared to other SHARP sites. Published trends of σh from XLOT database from the Horda platform (HP) wider area (Section A) are shown in Figure 3-2 and *Table 3-1*.

 (Thompson et al. 2022a and Wu et al. 2022). Three trends are identified based on depth and sorting criteria. When considering all data, a bi-linear trend is observed with a change in trend from below 3km. In this study, we use a reference to trendline a) for < 3km, trendline b) for >3 km depth, and trendline c) for data from the shallow interval (<3 km) where high pore pressure is less than 10% from hydrostatic.

Regional trendlines of minimum horizontal stress σ$_h$ and vertical stress σ$_v$ for the entire North Sea are also included for comparison all figures. The general expression of average linear trendlines for σ$_h$ used in the published results of XLOTs are shown in Equation 5. Relations may be corrected for pressure to mudline and excess pore pressure Pp according to general formula;

$$\sigma_h = WP_{@ML} + X*Depth_{mbml} + Y(Pp-Pp_{NORM}) \qquad (Eq.\ 5)$$

where WP@ML is the water pressure at the seabed/mudline, D = Depth$_{mbml}$ is the true vertical depth (TVD) below seabed/mudline (mbml – meters below seabed/mudline) and X is the slope of trendline of σ$_h$, and Y is the pore pressure correction factor. The variables are listed in tables below.
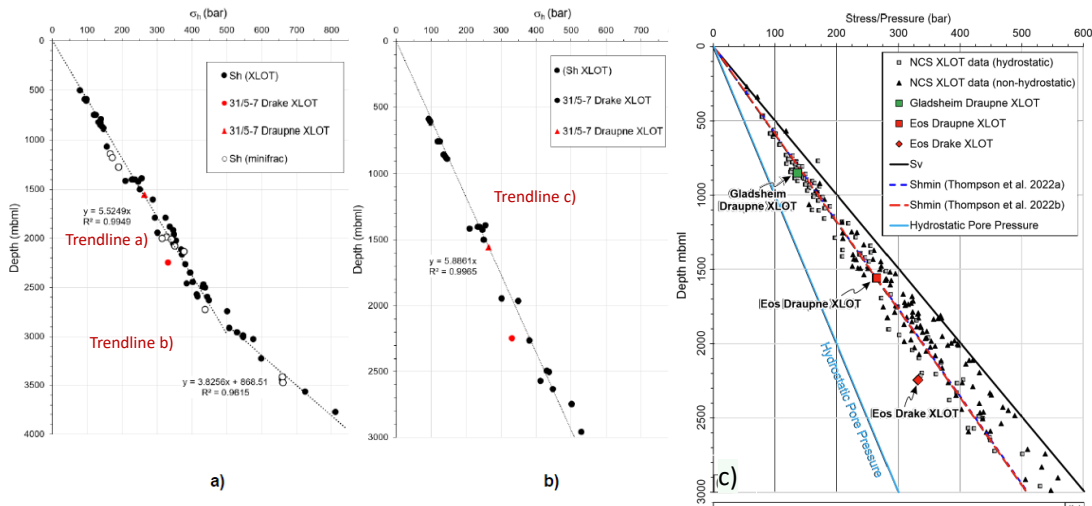

Figure 3-2 (a and b) Reference trend lines published by Equinor (Thompson et al. 2022). Three trendlines a, b and c are indicated. Figure a) All regional data and b) XLOT data < 3km with where pore pressure less than +/-10% from hydrostatic has been included. (c) Horda Platform XLOT data from same database but also including well 32/4-3 S (Draupne Formation) (Wu et al. 2022). Hydrostatic pore pressure gradient (0.103 bar/m) and vertical stress gradient (0.201 bar/m) are assumed. Data are plotted in meters below mudline/seabed, and stress from water column has been removed from all data.

Table 3-1 Summary of published trend lines of σ_h and OBG applied in this study from Thompson 2022a, b and Andrews, 2016. The X and Y- values refers to Eq. 5, where X is the slope of σ_h and σ_v trendline Y-is the pore pressure correction factor, and D= Depth$_{mbml}$ is the true vertical depth (TVD) below seabed/mudline (mbml – meters below seabed/mudline). High quality XLOT's Selected pore pressure less than +/-10% from hydrostatic

Structure	Trendline name used in plots	σ_h -Slope of trendline X-value	Pore pressure correction factor Y-value	R2	Comment
Horda Platform wider area (corresponds to SHARP profile E-W Section A) Thompson et al., 2022a	a	0.0181*D		0.9949	All XLOT data
	b	0.0261*D-22.703		0.9615	XLOT Below 3 km depth
	c	0.017*D		0.9965	High quality XLOT's
North Sea (NO) Thompson et al., 2022b	d	0.01684*D	0.526	0.987	All XLOT data
	e	0.01693*D	0.522	0.981	High quality XLOT's
	f	$1.66e\text{-}05*D^2+0.1408*D$		0.983	Including effect of depth variation due to pore pressure
	OBG	$7.36e\text{-}06*D^2+0.1924*D$		0.996	
Norwegian Continental Shelf (NCS), Andrews et al., 2016	OBG_high	0.22*D			
	OBG_low	0.2*D			

3.2 Results from Analysis of XLOT and LOT Database

The detailed plots of LOP and σ_h from XLOT vs. depth for all segments sorted from East to West and by key lithological units are documented in this Chapter. Figure 3-3 show stress data from the entire database evaluated, including 945 LOT test data and 14 XLOT data (left), and a selection of data from Eastern part of Horda Platform (Segments 1,2 and 3 combined). The σ_v from Troll East 31/6-1 is used for total vertical stress, which is slightly higher than regional trend for the Norwgeian sector (Thompson et al. 2022b), and falls between the OBG max and min trend (Andrews et al. 2016). The average trend from LOP shows slightly higher value than σ_h from XLOT. Also, LOP data in upper interval 0-700 m TVD from Troll show higher values than OBG. The examples in Figure 3-3 demonstrate that a more detailed sub-division of the large dataset into the smaller area will reduce uncertainty significantly and potentially pick out more local lithological or structural (tectonic) controls on stresses.
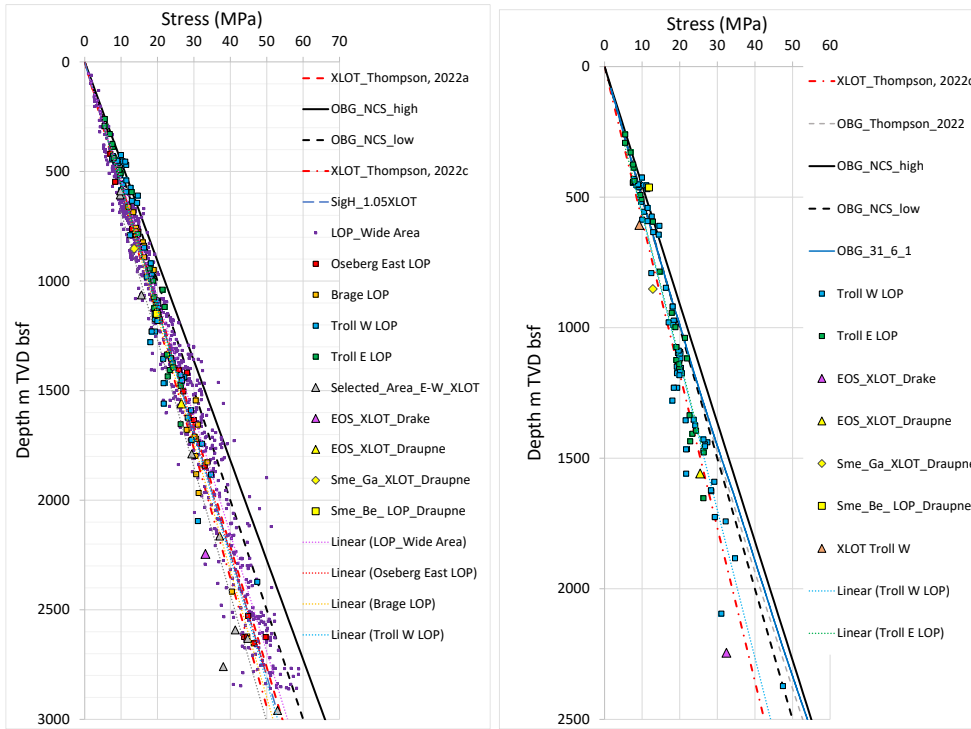
Figure 3-3 Summary of all data included in analysis covering both Section A and B (Left). Data from Eastern part of Horda platform area, showing LOT from Troll East and West together with XLOT data from same area (Right). Trendlines from Thompson et al (2022a and b) and Andrews (2016) are plotted for comparison.

3.2.1   Sorting of Stress Data by Segments

Figure 3-4 shows the stress vs. depth plot in the Eastern part of the Horda platform area, showing LOT from Troll East and West Segment 3 and XLOT data from the same area. This example shows that when using the four selected best quality XLOT data points lower trends are recovered (y=0.0151x) than trendlines a and c (Thompson et al., 2022a). Uncertainties related to Drake XLOT are reported in Thompson et al., 2022a. The slope of the average trend line from LOP data locally in Troll East and West are very close to the regional trendline from XLOT. The one LOP datapoint below 3km aligns with the shallow LOP trend.
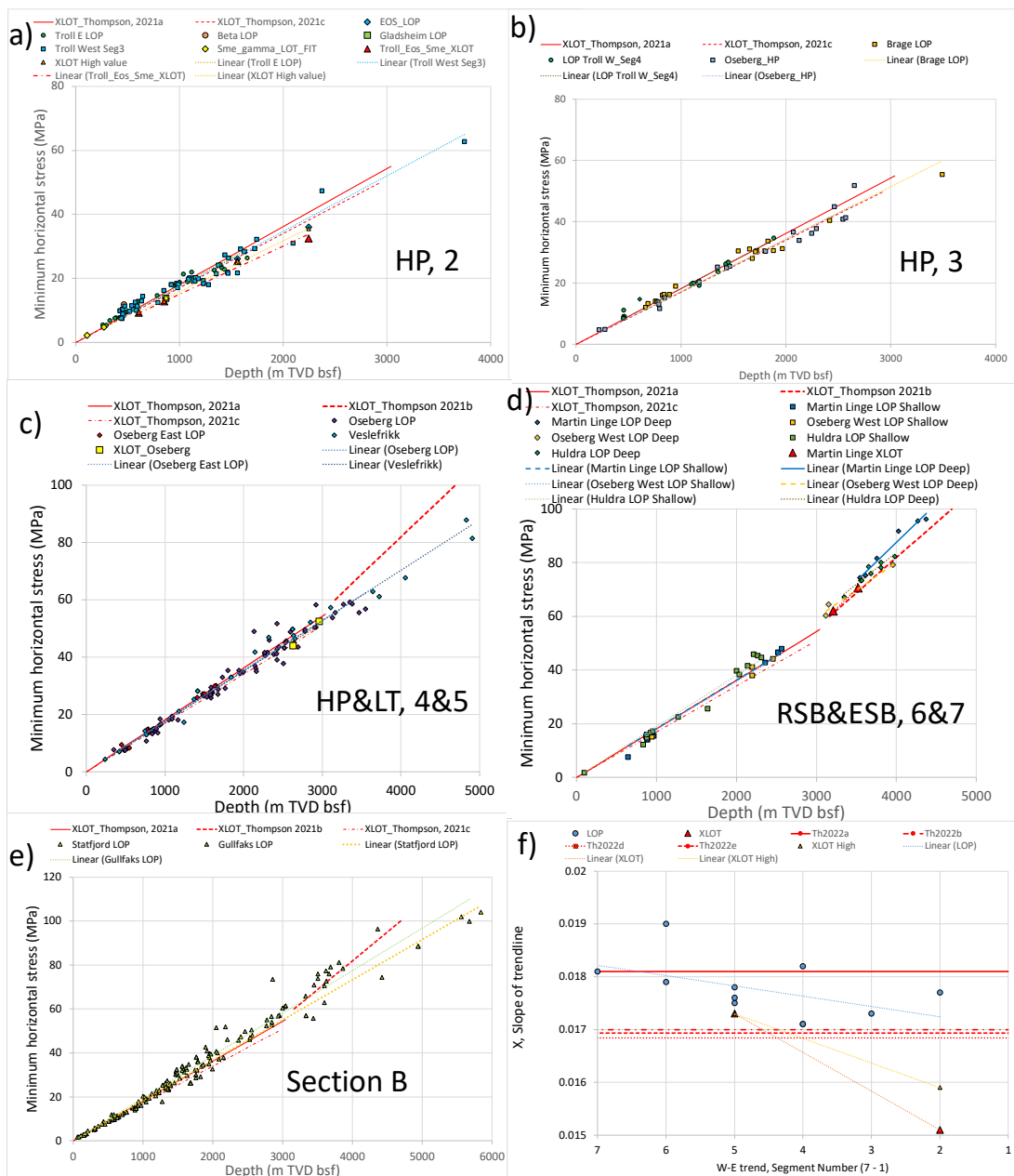
Figure 3-4 Stress vs. depth for Segments 2-7 along section A (E-W profile, in Plot a, b, c and d) and section B (Plot e). Data from both LOT and XLOT tests are plotted with trendlines (trend a and c) of minimum horizontal stress from Thompson et al (2022a). Minimum horizontal stress on Y-axis refers to stress from XLOT data in comparison with LOP pressure points. (Plot f) Summary of slope of trends (x) from section A (Plots a, b, c, d) where x-axis indicates segment number, 7 is west and 1 is east. A reduced eastwards average trend is indicated.

For the western part of the Horda platform, including Troll West, Brage and select Oseberg wells (Figure 3-4b, segment 4), the trends are in-line with the trend further east and the trendlines a and c (Thompson et al., 2022a). The one LOP datapoint below 3km is in line with the shallow trend. There are no XLOT data available for comparison. For Lomre Terrace including Oseberg, Oseberg East and Veslefrikk (Figure 3-4c, segment 4 and 5), the LOP vs. depth trends are similar to those in the Eastern part of the Horda platform and also close to XLOT trends a and c (Thompson et al., 2022a). The deep LOP data (D>3km) have the same trend as in the shallow section and are in line with the deep

LOP data points further east (Figure 3-4a and b). There is no shift in trend from deep elevated pore pressure, however, a few LOP datapoints at depth range 2-3 km depth show larger LOP values which may indicate locally overpressured units, and this agrees with pore pressures reported with XLOT in similar depth ranges (Appendix A). Western part of E-W Cross section in the Viking Graben and East Shetland platform (Figure 3-4d, segment 6 and 7, including Martin Linge in East Shetland basin, Oseberg West and Huldra in Rugne basin of Viking Graben) show a bi-linear trend with shift at 3km. The test data from Martin Linge are classified into shallow (<3km) and deep (D>3km) sections, and the average trendlines correspond well with shallow and deep trends from XLOT (trend a and b, respectively, from Thompson et al., 2022a). The same shift in trend is observed in area west of Oseberg and Huldra. The deep trend likely indicates overpressure at a large depth (D>3km). Overpressure in East Shetland subbasin are also reported for Gullfaks area (Nordgård Bolås et al., 2014 and Grollimund et al., 2001). The pore pressure is likely induced by diagenetic effects. LOP values in Gullfaks are high also in the depth 1.2-3 km, indicating overpressure in these formations. The deep trend >3km in Gullfaks is similarly high as in the western part of Section A (RSB and ESB) and likely indicates overpressure at large depth. Overpressure in this area is also documented previously (Nordgård Bolås et al., 2014, Grollimund et al., 2001)

In summary, the trend of LOP and σ_h in the E-W cross section (Section A) appears to be differentiated into three main areas. The western area (Segment 6 and 7, S6 and S7) have a shift in trend at 3 km, likely due to excess pore pressure from diagenesis. This includes fields located in the East Shetland basin and Rugne subbasin (Viking Graben). The middle area (S5 and S4), defined by Lomre Terrace and the western part of the Horda platform, shows a deep LOP trend consistent with the shallow trend for the entire depth range, including even below 3km. There are, however, some areas with reported overpressures also in the Oseberg area. The XLOT test data have indication of excess pore pressure in Balder and Heather in Oseberg West and East respectively (1.8-2.6km depth m TVD bsf). The same deep trend of LOP data is indicated in the Eastern part of the Horda platform (S3, S2 and S1) however, this is only from a single deep LOP test in Troll west; nonetheless, the shallow units (D<1km) show a higher trend.

The key trendlines from plots are summarized in Figure 3-4f. The data are sorted by LOP and XLOT trends for the plots sorted by structure (HP, LT, RSB and ESB) and Segment (1-7) in Section A from Figure 3-1. An E-W trend of the slope of trendline (X) is indicated from the LOP and XLOT data. The published slope of trendlines (a, c, d, e) in shallow units are plotted for comparison (from Thompson et al. 2022a and b). The trends in E-W horizontal effective stress can be linked to the work for WP1.3 in terms of calibration/comparison for the E-W cross section.

3.2.2   Sorting by Lithological Formations

The LOP for the HP area (Troll E, Troll W, Smeaheia, EOS and Brage) are sorted based on lithological formations: Drake, Draupne, Sele/Lista and Hordaland (group) where several LOTs were available in Figure 3-5. The average trend of the LOP vs. depth is similar in Draupne, Drake and Lista/Sele formation and also aligns with the general trendlines of the area (x=0.00171-0.00176). LOP trend vs. depth is higher (x=0.00191) in shallow Hordaland Group, which consists of Oligocene and Eocene shales and mudstones units where the content of smectite can be significant in these formations.

The trend of LOP/depth increases towards the East for all lithologies except for Drake; however, wells where Drake is present are located in rather narrow E-W positions with few observations. In Hordaland, there is a larger spread, and this may be from large variability in formations tested (as Hordaland is undifferentiated). The trend of LOP/depth also increases towards North for all lithologies except Lista/Sele, although generally larger scatter in the data in the N-S compared to the E-W orientation. K_0 estimated from LOP and XLOT vs. depth for the Lithologies Hordaland, Lista/Sele, Draupne and Drake.
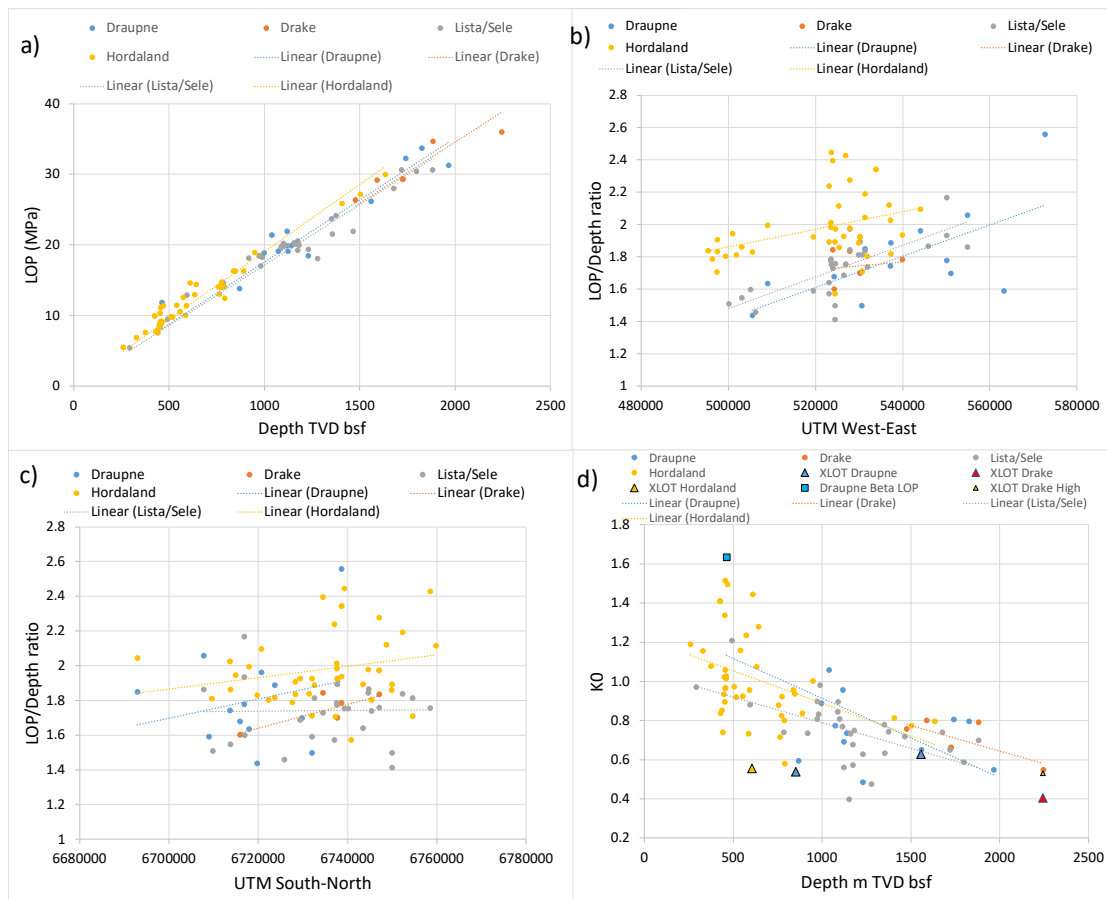
Figure 3-5 a) LOP vs. depth (TVD bsf) for various lithological formations/Groups. The order of trendline equations is same as listed in legend. LOP/Depth ratio vs. W-E location (UTM) (b), and S-N direction (UTM) (c) for various lithological formations/Groups. The order of trendline equations is same as listed in legend. d) K0 estimated from LOP and XLOT vs. depth for the Lithologies Hordaland, Lista/Sele, Draupne and Drake.

The higher LOP values observed in Hordaland may be related to a higher smectite content directly from lithological impact or indirectly from a high pore pressure due to low permeability. It may also be due to the effect of larger uplift in these shallow less consolidated mudstone formations from the OCR effect. The increasing LOP vs depth ratio in the Eastward direction supports this argument. There are now measurements of pore pressure in the upper part available for analysis in this report. Hydrostatic pore pressure down to reservoir is normally assumed for Smeaheia and Eos, and Troll may have a slight overpressure from the gas columns. However, there is some indication from completion reports where pressure gradients have been predicted above hydrostatic in the overburden.

3.2.3 Vertical Stress Trends

Total vertical stress for entire sedimentary packages and the effective vertical stress for depth are shown in Figure 3-6. The deep well 31/6-1 in Troll east have been used as a reference in this study. The density log is available for almost entire depth range, and a splice with nearby geotechnical well bh8903 was undertaken to ensure representative densities in the shallow units.

The general published trendline used for regional studies in North Sea (Thompson 2022b) based on integrated density logs is in line with the shallow Troll trend, although slightly lower than the local trend line based on the integrated log from well 31/6-1 and geotechnical borehole bh8903 (Figure 3-6b). At maximum depth of 31/6-1 well of 3754 m, the difference in total vertical stress is only 3%. At a depth of base URU of 200 m, the difference in total vertical stress is ca 4.7%, and for the effective stress, the regional trendline is 9.4% smaller at this shallow depth. When comparing the stress trends reported for geotechnical site investigations based on measured density data there are some small differences (Figure 3-6a).
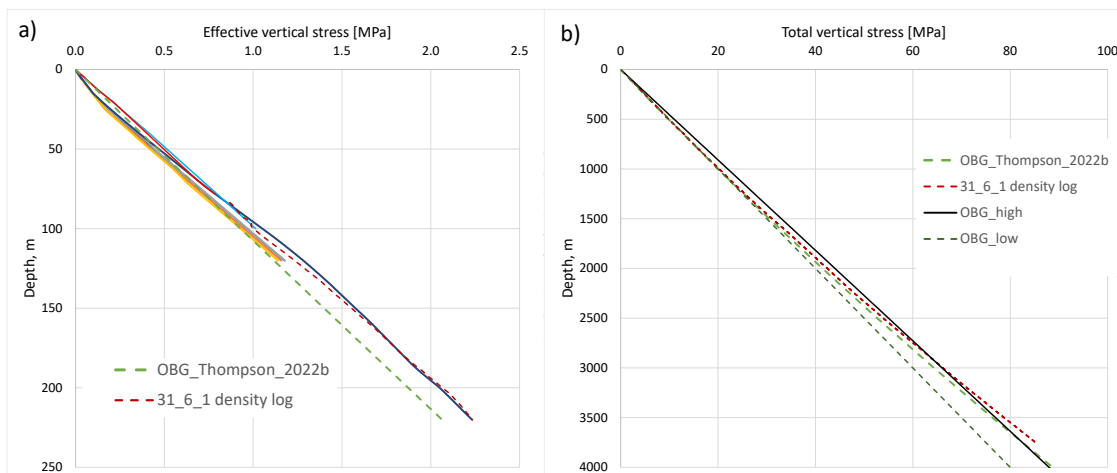

Figure 3-6 Comparison of effective vertical stress trends a) at shallow depth range typical for the Quaternary units (<250 m) and b) for the deeper units (<4km). Trends are from Geotechnical site investigations in Troll and Oseberg and one general published trendline used for regional studies in North Sea (Thompson 2022b) and one local trend line based on the integrated log from well 31/6-1 and geotechnical boring bh8903 in troll east (for at shallow depth where density log is missing). A hydrostatic pore pressure is used for calculating effective stress. The depth is from below mudline. OBG high and low is based on gradients 0.22 MPa/m and 0.2 MPa/m respectively after Andrews et al., 2016. The depth is from below mudline.

3.2.4 Uncertainties in Pore pressure Trends

Pore pressure is normally measured in reservoir units with high accuracy, but no measurements are available from mudstone or shale units where the actual XLOT and LOT have been tested. Indirect knowledge or assumptions of pore pressure in the investigated units need to be incorporated. A detailed analysis of pore pressure from sonic log or other methods has not been included as part of this report. Eaton's method is one of the conventional methods of the pore pressure prediction, which considers

compaction disequilibrium as the main mechanism of overpressure generations. Eaton (1975) proposed an empirical equation to quantify the pore pressure using well log data. This method assumes that overburden pressure is supported by pore pressure and vertical effective stress, as shown in Terzaghi's equation.

Analysis of the deepest wells 31/6-1 and 32/4-1 may give some further insights to the sensitivity of this parameter in the Aurora and Smeaheia area. Also, log analysis may be useful to further evaluate pore pressure in shallow units below quaternary. However, the V_p log in 32/4-1 is poor quality in upper part and for 32/2-1 there is no Vp log available (Grande et. 2022).

3.3   Analysis of XLOT Intervals Based on Borehole Logs

3.3.1   Method and Demonstration of Analysis on Wells

A workflow for stress estimation based on the rock physics relationship between clay content (V_{cl}), smectite content ($V_{smectite}$) Over-consolidation ratio (OCR), and well-log data has been established as part of SHARP project WP3.2 (Grande et al. 2022). The method was applied to logs from Eos, Smeaheia (gamma, alpha and beta) and Troll East well 31/6-1. In this section, the key plots from analysis are shown. A similar analysis was also done on remaining wells where both XLOT and gamma ray analysis were available in same well. Further analysis and application to more wells have been done based on the established rock physics model summarized in the report DV3.2.

For a complete description of the V_{cl} method see the more detailed description in Grande et al. 2022. The K_0 value is calculated from V_{cl} as obtained from gamma ray log, content of smectite from XRD or QEMSCAN on cuttings and the OCR from exhumation analysis or glacial load history (see Chapter 2). These parameters are input to the Equation 6 below;

$$K_0 = ((0.034 \cdot V_{cl} + 0.3681) + (0.003 \cdot V_{smectite})) \cdot OCR^{0.47} \quad \text{(Eq. 6)}$$

In WP3.2 further work was done to correlate plasticity index (Ip) to clay fraction from grain size analysis $< 2 \, \mu m$. This can give a useful relation when clay content is available from sieve analysis in geotechnical wells or gamma ray logs in deeper wells. Note that the clay fraction is not necessarily clay minerals, and using the gamma ray as source will give some source of errors. The following correlation equations for Ip (Eq.7) was established in WP3.2 which can be applied into general correlation from L'Heurex (2017) (Eq.8) also shown in DV3.2;.

$$I_p = 0.7995 \cdot V_{cl} \qquad \text{(Eq.18, fromWP3.2,)}$$

$$K_0 = 0.33 \cdot I_p^{0.17} \cdot OCR^{0.39} \qquad \text{(Eq.8, fromWP3.2,)}$$

K_0 profile from two key profiles are shown in Figure 3-7 and Figure 3-8, for Troll East deep geotechnical borehole BH8903 spliced with Well 31/6-1 from same area and well 31/5-7 (Eos) and 32/4-3S Smeaheia gamma.
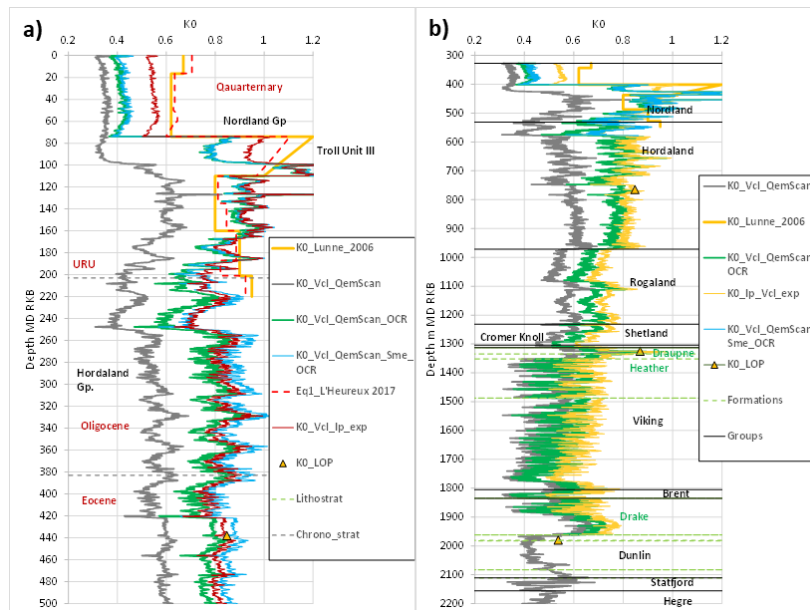

Figure 3-7 K0 vs. depth for Shallow geotechnical borehole BH8903 and gamma log from nearby well 31/6-1 in Troll East, where a) shallow section <0.5km and b) deep <4km. Different sets of gamma min and max values have been used in IGR calculations in different sections because the composite gammaray log had significant shifts between sections.
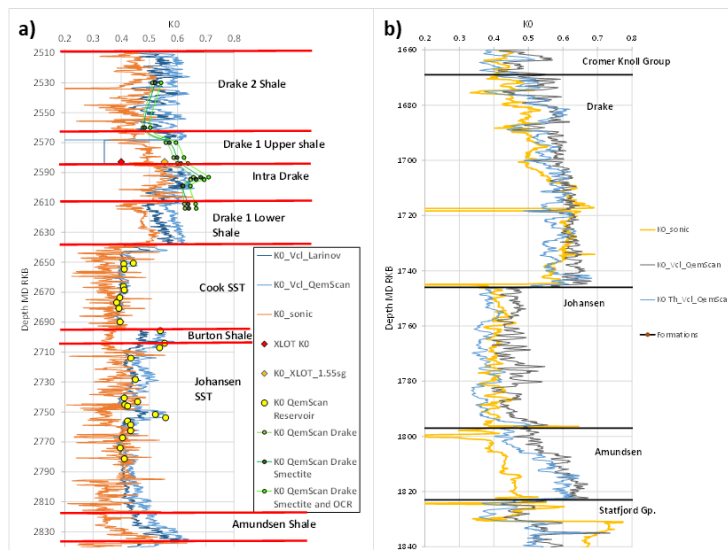
Figure 3-8 Eos 31/5-7 Well (Aurora) reservoir and Drake cap rock (left) and Well 32/4-3s (Smeaheia Gamma) with Draupne cap rock. Vcl method based on standard gamma log and gamma thorium curve (right) have been compared with sonic log method (Eaton) and XLOT tests.

3.3.2 Log Analysis of Intervals of XLOT Data

Table 3-2 show a summary of K_0 from XLOT intervals from analysis of gamma ray logs in the selected best quality XLOT's (Pp <+/-10% of hydrostatic). The logs are documented in Appendix B. Figure 3-9 shows a plot of K_0 vs. V_{clay} as interpreted from the Gamma ray log for the same data as reported in table.

Table 3-2 Analysis of XLOT intervals high quality tests (Pp<+/-10% from hydrostatic). Summary of K0 data, K0 Xlot is measured and other interpreted values from analysis of Volume clay (Vcl) from gammalog, smectite and estimated OCR.

General information			Summary of K0 data, K0 Xlot is measured, and other interpreted values are from analysis of Volume clay (Vcl) from gammalog, smectite and estimated OCR						
Field	Group/ Formation	CSG mTVD RKB	K0 XLOT	Vcl (frac)	Sme (%)	OCR	K0_Vcl	K0_Sme	K0_OCR
Aurora (Eos)	Drake	2583	0.41	0.61	9	1.12	0.58	0.60	0.63
Aurora (Eos)	Draupne	1897	0.63	0.68	15	1.18	0.60	0.64	0.69
Smeaheia (gamma)	Draupne	1175	0.54	0.68	15	2.19	0.60	0.64	0.87
TROLL West	Hordaland Gp. Oligocene/Eocene	962	0.56	0.5	25	1.34	0.54	0.61	0.69
OSEBERG SATELLITTER	Viking Gp. Heather Middle,Heather	3093	0.64	0.81	0.0	1.05	0.64	0.64	0.66
OSEBERG SØR	Shetland Viking? Draupne?	2763	0.61	0.52	0.0	1.05	0.54	0.54	0.56

From Figure 3-9 it is indicated the K_0 from XLOT in Oseberg area are closer to the expected trend based on expected K_0 from V_{cl} interpreted from gamma ray log. For Horda Platform East there is deviation from this trendline. A major difference between these two areas is that Oseberg has only experienced compaction and minimal uplift, and therefore represents normal compaction throughout geological history. The Horda Platform east is uplifted to various extent and are all overconsolidated with a larger maximum burial depth compared to present day depth. From considering only the best quality data points, it may be indicated that the various mechanisms of uplift and glacial loading play a significant role on the present day depth dependent stress profile in this area. However, more study might be necessary to support this hypothesis.
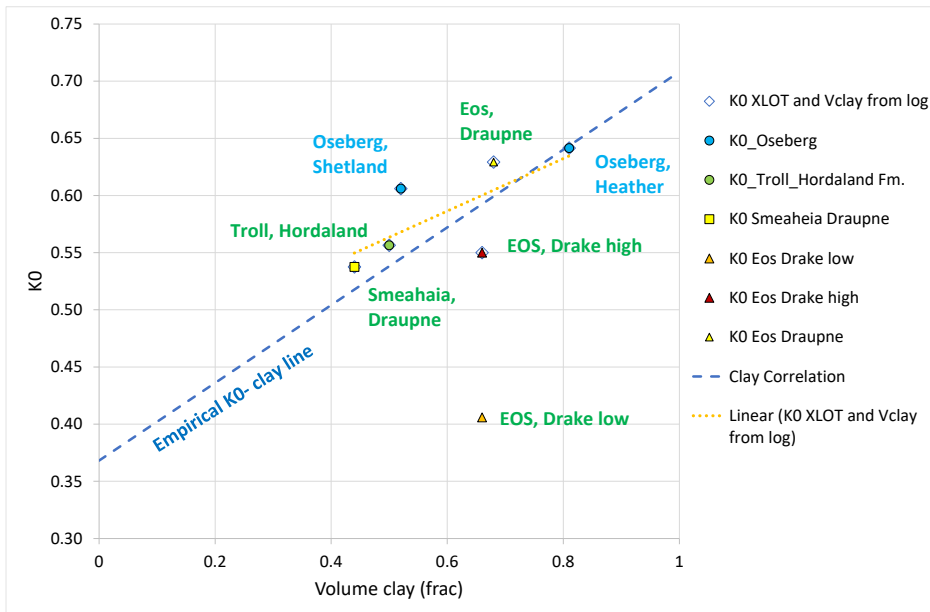
Figure 3-9 K0 vs. volume clay for available XLOT data analysed in this study. Measured K_0 data from normally consolidated but chemically altered formations in Oseberg show a rather good match, while K_o in Uplifted and overconsolidated Horda platform are not matching the predicted trend based on normally consolidated clay. Note that the Vcl from gamma ray log are also questionable for some intervals, which may not be well calibrated for all sections in well (i.e. Troll XLOT test in Hordaland show very low gamma value at same depth interval). Vcl of 0.68 was used for Draupne in Eos well (no Thorium curve available) based on XRD data for Draupne in Smeaheia area (Rahman et al., 2020). The V_{cl} of 0.44 from Smeaheia Gamma thorium curve may also be on low side.

3.3.3 Poisson's Ratio – Sensitivity for Modelling

A key parameter for modelling of the K_0 and lateral stress is the Poisson's ratio. Dynamic Poisson's ratio (undrained) and the resulting K_0 are calculated for key lithologies from Vp and Vs log data in Eos well and Smeaheia Gamma well, and presented as a function of Vp and Vs in Figure 3-10. Examples of drained Poisson's ratio and the K_0 during load and unload from K_0 tests are shown in Appendix A.

The Poisson's ratio and resulting K_0 is clearly decreasing from shallow to the deeper formations. For the Eos well, the shallow clays of Nordland and Hordland Gp. including Skade and Green clay Fm's. show the highest values of Poisson's ratio (0.37-0.47) and K_0 (0.6-0.9) and the typical sealing formations Draupne and Drake have lower Poisson's ratio (0.25-0.37) and K_0 ratios (0.35-0.6). There is a depth dependency also in K_0 derived from Poisson's ratio, in line with observations from K_0 indicated from LOP data (Figure 3-5 d).

For the more uplifted Smeaheia Gamma well, there is a larger span Poisson's ratio (0.25 -0.42) and K_0 ratio (0.35-0.7), and notably higher values of K_0 compared to Eos. I.e. for Draupne K_0 is in range 0.65-0.72 compared to 0.5-0.6 in Eos (only few log points), and for Drake K_0 is in range 0.35-0.65 compared to 0.35-0.58 in Eos. This may potentially indicate an influence of uplift (OCR) on K_0 from Poisson's ratio between the two field, which have experienced a similar maximum burial depth. Possion's ratio in Drake (0.25-0.38) are inline with rock physics analysis of Drake in Eos well (Mondol et al 2022a).

The regional variation for Drake from analysis of 17 wells is slightly larger with a range of K_0 of 0.2—0.42, with the deepest wells having the lowest Poisson's ratios (Mondol et al 2022a). The Heather Fm. have low values of K_0 in range 0.45 to 0.55.
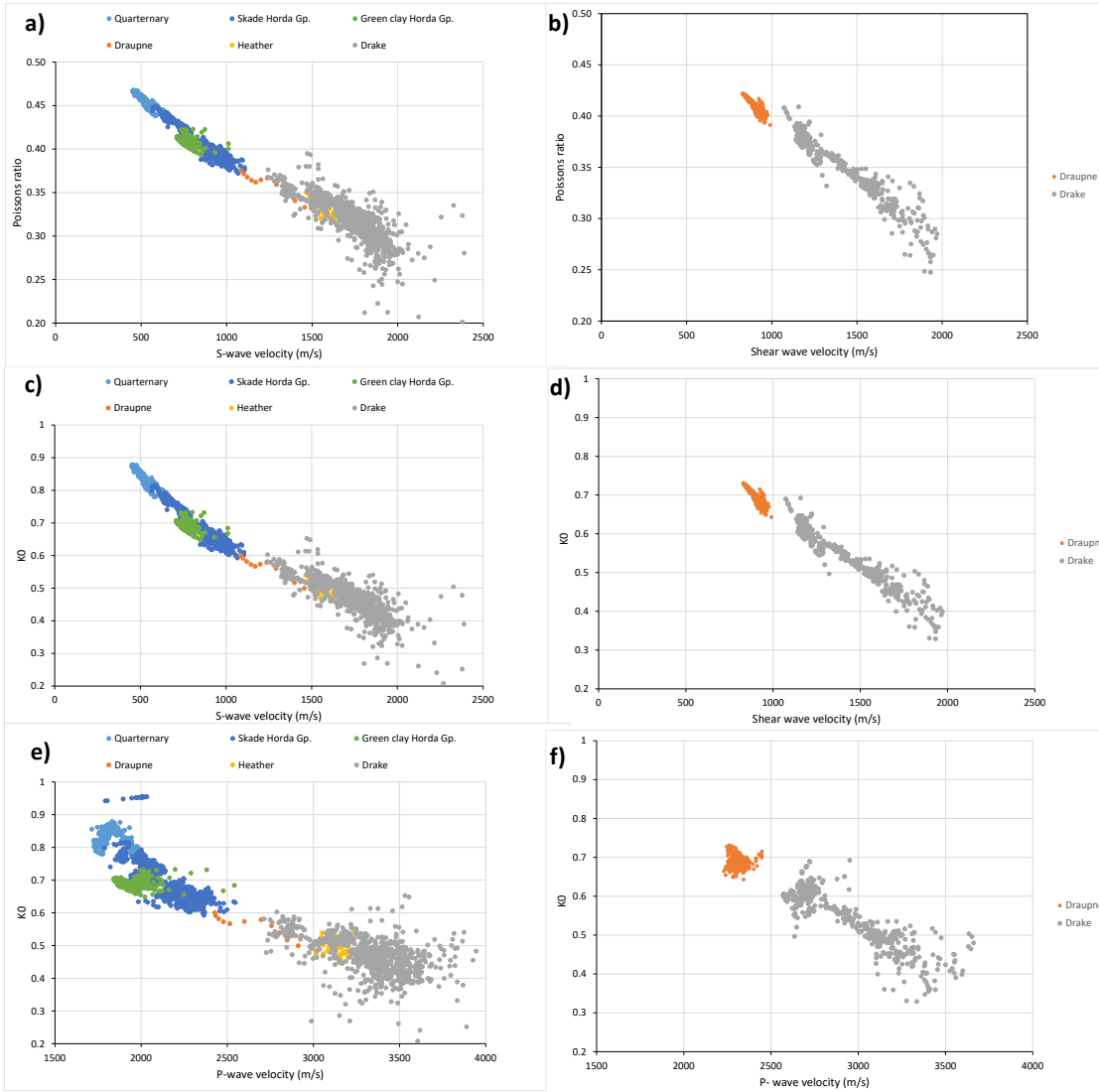

Figure 3-10 Dynamic Poisson's ratio vs S-wave velocity calculated from velocity logs in EOS well (a) and Smeaheia gamma well (b) for various lithologies. K0 vs. S-wave velocities calculated from velocity logs in EOS well (c) and Smeaheia gamma well (d) for key lithologies. K0 vs. P-wave velocities calculated from velocity logs in EOS well (e) and Smeaheia gamma well (f) for key lithologies.

The Green clay in Hordaland Gp. is typically known as a Smectite rich Eocene/Oligocene clay, have K_0 in range 0.65- 0.72. Green clay show a small drop in the calculated K_0 vs. P-wave velocity. In general, low values of P-wave velocity compared to depth, can be indication of high smectite content and or potential excess pore pressure.

3.3.4 Comparison Sonic log and V_{cl} method

A comparison between K_0 from the Vcl and the sonic log method for the Eos 31/5-7 Well (Aurora) and Well 32/4-3s (Smeaheia Gamma) are shown in Figure 3-11. The figure shows a good correlation between the methods for Drake shale formation, and less favourable correlation for Cook and Johansen sandstone intervals. These correlations are not expected to give a perfect match, especially in Cook and Johansen reservoir units where there are intra clay layers. Clay automatically gives high K_0, however, these layers have like limited lateral extent and actual K_0 will likely be the same as for the sandstone. However, a rather good correlation in Drake is promising for evaluation of Drake and thicker sequence of clays, mudstones and shales in general. Also, these relations may be useful for the purpose of upscaling from seismic data.
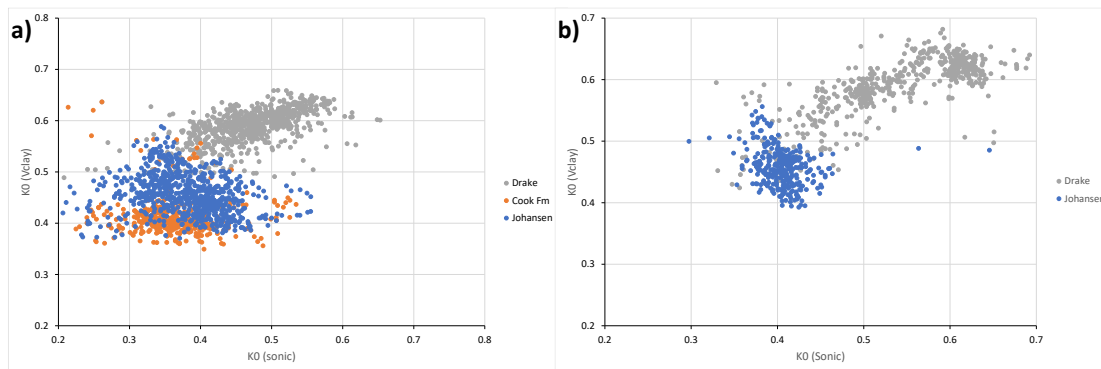

Figure 3-11 Comparison sonic log method (Eaton) vs. Vcl method for the Eos 31/5-7 Well (Aurora) (left) and Well 32/4-3s (Smeaheia Gamma) (right)

4 Insights from Constitutive Modelling

4.1 Overview

The intention of this section of the report is to describe how the inferred lithological component can be incorporated into constitutive models, with some consideration of supplementary diagenetic processes that are active at significant depths. The rationale for developing calibrated constitutive models is:

- Development of such characterisations will permit numerical investigation of trends and insights developed in Section 3 concerning the influence of deep diagenesis and overpressure in shallow Tertiary units; these are targeted as part of WP1.3.
- Working towards incorporating the diagenetic processes in laboratory experimental studies is difficult and therefore numerical modelling allows for conceptual investigations of what such changes should mean for K_0 during loading and unloading during/subsequent to diagenesis.
- The characterisations can be applied fairly widely within the North Sea basins, and potentially beyond, to minimize uncertainty and risk for sites where data is scarce.

It should be noted that whilst explicitly incorporating chemical compaction processes is not possible in experiments, experimentation on altered samples can provide useful information on how these processes affect fundamental properties e.g. stiffness, compressibility, strength; see Nygard et al., 2004, Grande and Mondol, 2013). A description of the source data used for the present characterisations can be found in both SHARP DV1.1b and DV3.2b and draws heavily from earlier NGI experimental databases (Grande, Mondol, and Berre 2011; Grande and Mondol 2013).

4.2 Mechanical Compaction

Mechanical compaction is defined as changes in rheological properties of sediments as a result of an increase in burial stress. This effect is especially prominent during temperatures below 70°C, and porosity reduction is observed synchronously with increase in rock strength.Critical-state based constitutive models are an obvious choice for calibrationand validation as they effectively couple volume change and strength. The finite element software Elfen® is used and the Soft Rock 3 constitutive model is selected to represent the various materials. The reader is referred to SHARP DV1.1b for details of the computational framework and the constitutive model formulation.

4.2.1 Synthetic Samples – Mechanical Properties

The reference data set includes re-sedimentation under K_0 triaxial conditions of slurries composed of:

- Two sandstones; quartz arenite and volcanic arenite.
- Clay mixtures featuring varying ratios of illite and kaolinite.
- Silt-clay mixtures that contain varying ratios of illite and silt. Additionally a mixture of smectite and silt is tested.

The results of the calibration process for the sand samples (quartz arenite and volcanic arenite) presented in Figure 4-1. The upper image shows the comparison between

experimental and numerical porosity changes with increasing effective vertical stress for both sands. The sands exhibit different mechanical characteristics such as stiffness, preconsolidation pressure and hardening owing to differing mineralogical compositions as documented by others; see Chuhan et al., 2003 for example. The calibration is generally satisfactory. Small creep stages were included in the experiment where additional porosity loss at constant stress was observed, and this behaviour is not accounted for in the applied rate-independent constitutive model. The lower image shows how K_0 changes during loading and unloading stages and again the match appears favourable.
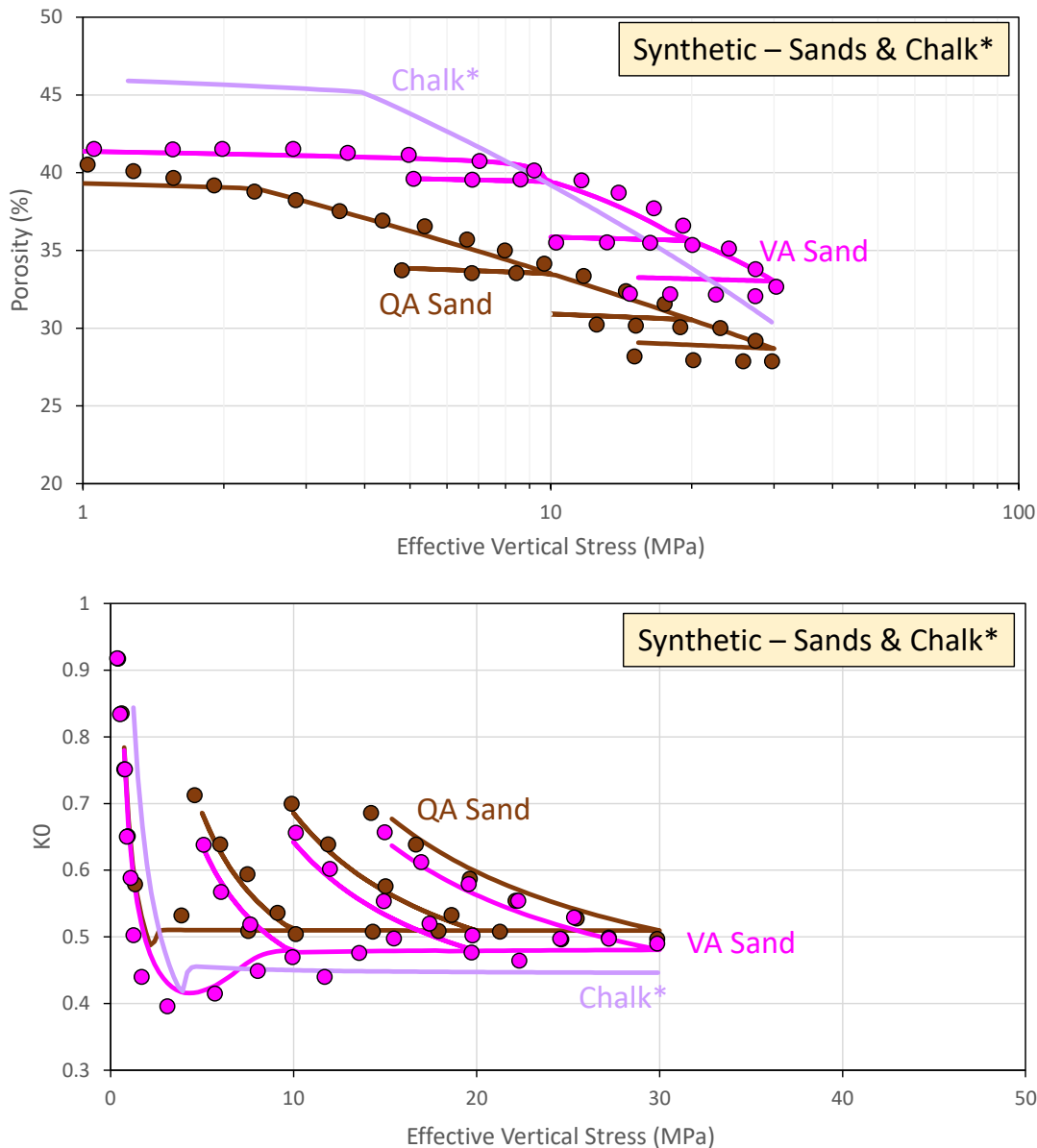

*Figure 4-1 Comparison between experimental (circles) and numerical (bold lines) responses for Quartz Arenite (QA) and Volcanic Arenite (VA) sands. Upper image – compaction trend. Lower image – K_0 ratio. * Reference data from Crook et al., 2008 is used to develop a characterisation for a porous chalk which is also included for reference.*

Also included in Figure 4-1 is a characterisation developed based on previous work modelling Lixhe chalk, a highly porous analogue for North Sea chalks (Crook et al.,

2008). Whilst this has not been resedimented, and therefore likely retains some naturally developed structure/fabric, it is of comparable initial porosity to the other synthetic samples. The purpose for including it here will become more obvious later in the text when discussing samples with low/negligible clay contents, and sequences of Cretaceous chalks are encountered elsewhere in Norwegian sectors and the Southern North Sea. This permits the characterisations to be applied more generally across North Sea sites.

Equivalent plots for synthetic samples of clays are shown in Figure 4-2. Differing proportions of the clay minerals illite and kaolinite are used. The upper image confirms appropriate calibration of volume loss with increasing imposed vertical stress. The lower image also indicates a favourable match to the reported experimental K0 values, and these are clearly higher relative to the sandstone.
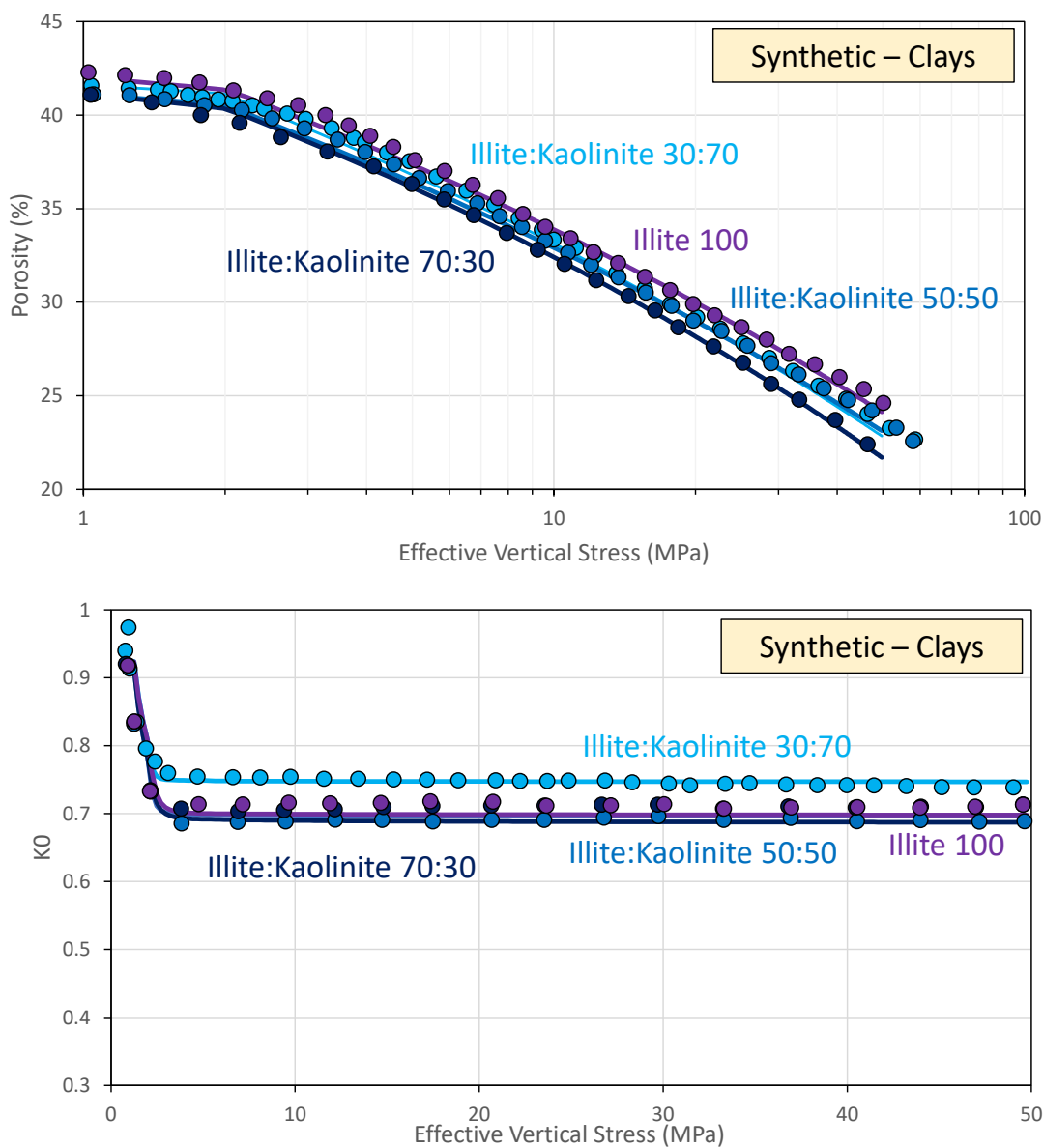

Figure 4-2 Comparison between experimental (circles) and numerical (bold lines) responses for various clay mixtures. Upper image – compaction trend. Lower image – K_0 ratio.

The silt:clay mixtures exhibit interesting trends with initial porosity and compaction behaviour clearly sensitive to the relative proportion of silt relative to illite as shown in the upper image of Figure 4-3. Comparison of the trends for smectite:silt 50:50 and illite:silt 50:50 reveals a considerable shift in porosity for a given level of stress. The lower image indicates the K_0 ratio which is again well approximated by the numerical tests and there is a strong dependence on the relative ratio of clay and silt in the lateral stress ratio, with increasing clay content elevating the lateral stress ratio. It is clear that the presence of smectite also has a significant impact on K0, increasing this value by ~0.15 relative to the same ratio of illite and silt.
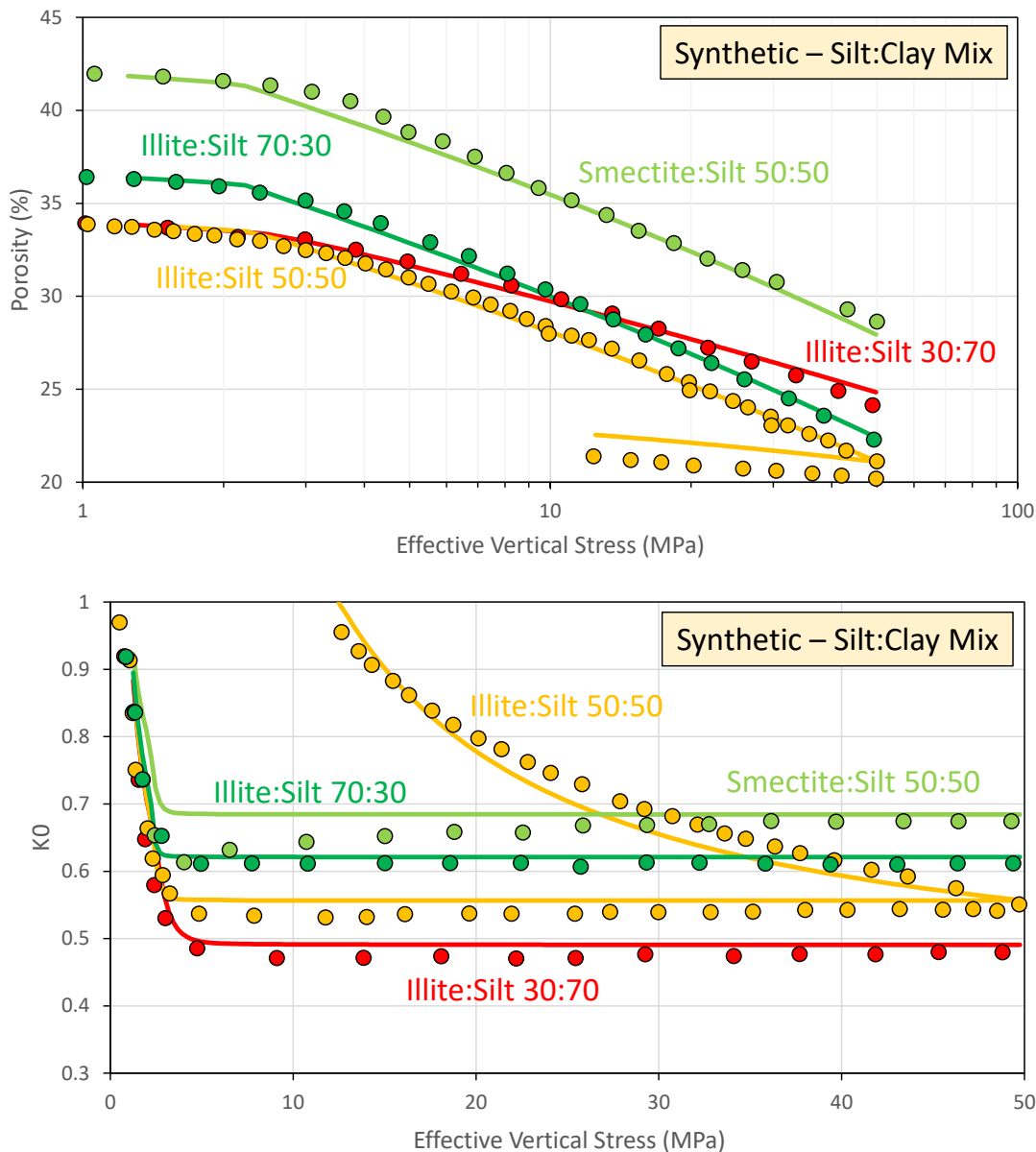

Figure 4-3 Comparison between experimental (circles) and numerical (bold lines) responses for various clay and silt mixtures. Upper image – compaction trend. Lower image – K_0 ratio.

4.2.2   Synthetic Samples – Hydraulic Properties

The reference data sets also include data for permeability at select stress levels during the test, with strong permeability decreases observed as stress increases. As noted by

Grande et al., 2013, this is due to porosity reduction through compaction as observed in Figures 4-1 to 4-3. It is therefore possible to construct a porosity-permeability relationship for each of the samples, and several popular forms may be used as a foundation; refer to DV1.1b for an introduction to some common forms. The relationship proposed by Yang & Aplin, 2010 has been adopted which relates void ratio and permeability through clay fraction. The calibration process involves selecting a clay fraction that approximates the general form (slope) of the data and then apply a scaling factor was incorporated to improve the fit. The fit for both clays and silt:clay samples can be found in Figure 4-4 and 4-5 respectively.

Sand permeability trends were not presented but representative curves can be generated quite easily. It is clear that all samples exhibit very low permeabilities. Whilst the samples are synthetic a comparison to resedimented Kimmeridge Clay data (Nygard et al., 2004) is also shown. This clay is a stratigraphic equivalent of samples investigated as part of WP3 such as the Draupne shale and has a clay fraction of approximately 55%. It is clear from the lower image that the smectite:silt 50:50 sample quite closely matches the Kimmeridge Clay data, highlighting that the synthetic samples provide realistic data for natural, unaltered samples. It is noteworthy that whilst the resedimented Kimmeridge Clay already has very low permeability, diagenetic changes may result in fabric and pore space changes that can further reduce permeability by 5-6x (Nygard et al., 2004). This should be considered when contemplating the rate of loading and unloading events, and the ability of pore pressures to dissipate efficiently In either scenario.
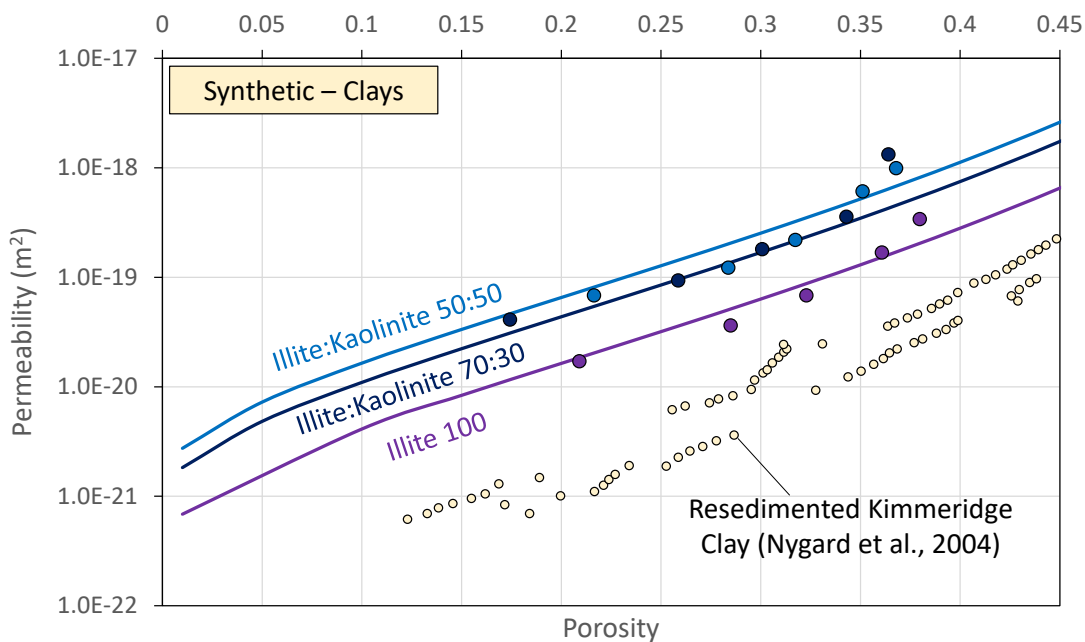

Figure 4-4 Developed porosity-permeability relationships for synthetic clay mixtures. For reference a resedimented natural sample (Kimmeridge Clay) is also shown; refer to Nygaard et al., 2004 for description.
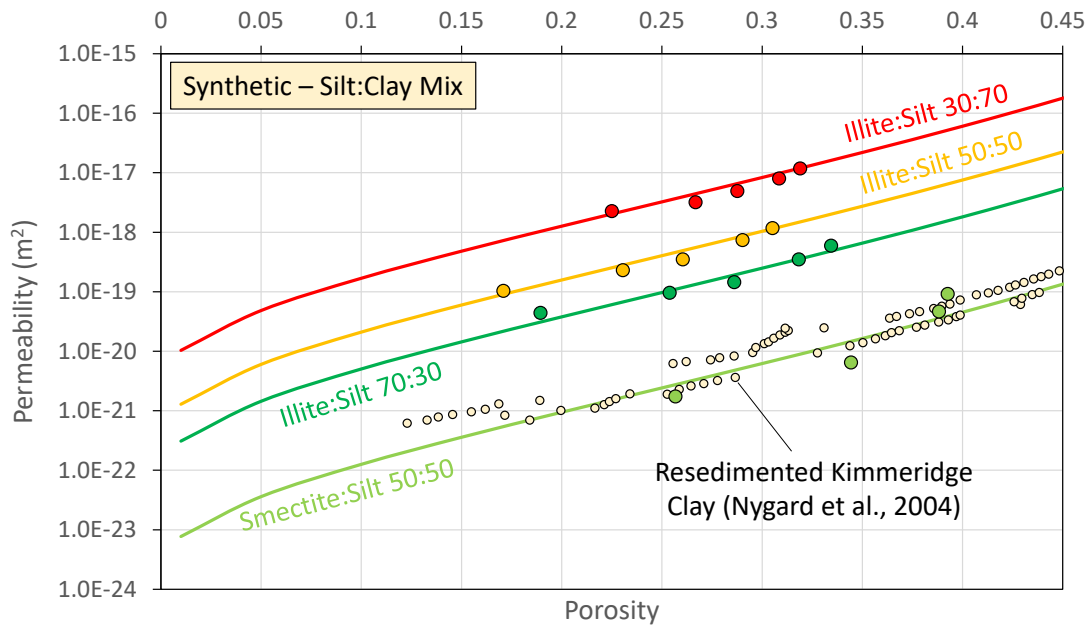
Figure 4-5 Developed porosity-permeability relationships for synthetic silt:clay mixtures. For reference a resedimented natural sample (Kimmeridge Clay) is also shown; refer to Nygaard et al., 2004 for description.

4.2.3 Review

This section has developed characterisations that can satisfactorily approximate the behaviour of various lithologies in the mechanical compaction regime. As noted the constitutive parameters are documented in the appendix and contrasting the parameters required to produce satisfactory fits allows for an appreciation of the critical constitutive parameters influencing K_0.

Firstly, Poisson's ratio is important which is intuitive as it provides a relation between deformation and, by extension, stress changes normal to the direction of the applied loading during elastic deformation. Secondly, Failure/dilation parameters such as the profile of the failure surface and plastic potential are important in determining K0 beyond the onset of plastic yielding. This is further demonstrated in Fig 4-6 which explores the significance of amount of smectite on constitutive behaviour. The presence of smectite is understood to be very relevant as it may give high K_0 directly because of its constitutive properties or indirectly through pore pressure increases (DV3.2, Section 6.1.2). The reference 50:50 smectite:silt is shown and represents a 50% smectite characterisation. Overlain on the plot are experimental data points for various North Sea claystones reported by Wensaas et al., 1998. To allow for comparison the data points have been normalised to an *inferred* preconsolidation pressure (refer to DV3.2, Section 4.3.1 for equivalent techniques applied to sandstones) that would conform to the failure surface fit, and then scaled to the initial strength of the 50:50 smectite:silt sample (2 MPa). The data points shown for North Sea Claystones and London Clay fit well to this surface and have comparable quantities of smectite. A reference Mohr-Coulomb envelope would imply a friction angle of around 18°. The lower image shows the stress path followed in deviatoric (*q*) versus effective mean stress (*p'*) space. The K0 for this material is 0.684.
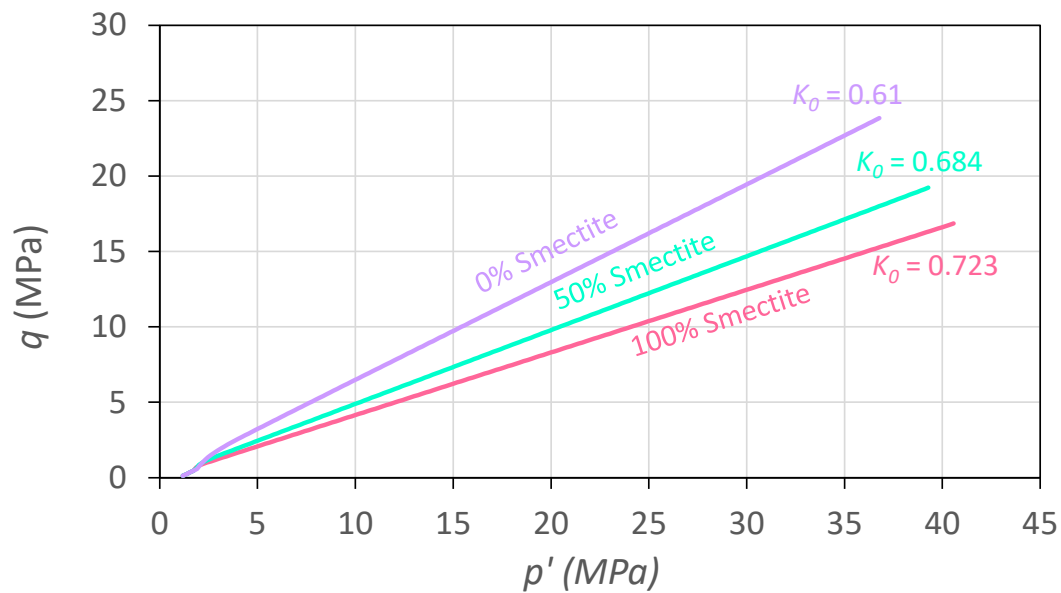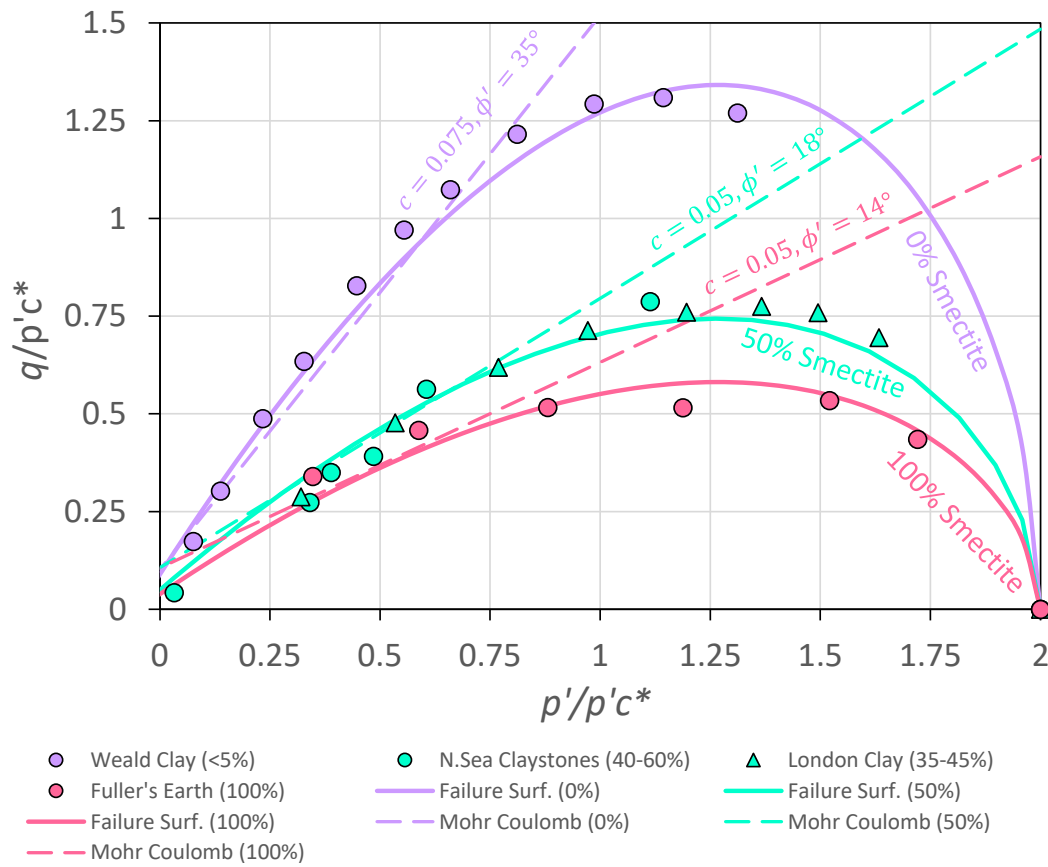
Figure 4-6 Upper image – failure surfaces for smectitic claystones modified after Wensaas et al., 1998. Symbols indicate test data for various samples, with smectite content shown in brackets. Failure surfaces are normalised to the estimated preconsolidation pressure for each sample constrained by the known data points. An additional scaling to the initial preconsolidation pressure of the smectite 50:50 characterisation (2mPa) is also included for comparison.

Retaining the same general shape of the failure surface but modifying the friction parameter only (analogous to friction angle for a Mohr-Coulomb model) allows for failure surfaces for Weald clay (<5% smectite) and Fuller's Earth (100% smectite) to be reasonably fitted. This modification has quite a significant impact on the K_0 values which are now 0.61 and 0.723 for 0% and 100% smectite contents respectively. From this assessment it is clear that the friction parameter/angle is very significant in determining K_0, and worth noting here that changes to other parameters (Poisson's ratio) have not been considered. For example Weald clay has a slightly lower K_0 than predicted here (DV3.2 report) which could be accounted for by altering additional parameters. Developing an appreciation of the significance of smectite content is important as there is the possibility of presence of highly plastic clays (high smectite) in Tertiary age sediments that likely influence pore pressure and K_0; understanding how to account for them in a constitutive sense permits systematic investigation later in the project.

4.3   Chemical Compaction

4.3.1   Assessment of Natural Samples

In the mechanical compaction realm synthetic samples such as those described above give good indicators of minimum stress evolution during both loading and unloading. There is some uncertainty as to how more deeply buried and chemically altered sediments will behave during unloading in particular, and numerical modelling offers the potential to explore such influences conceptually. A precursor to such investigations is some assessment of relevant data sets in which unloading is assessed and understanding the key constitutive parameters.

Barents Sea Mudstones (Grande, Mondol & Berre, 2011)
The reference data set also contains natural mudstone samples from the Hekkigen and Fuglen formations of the Barents Sea. These samples are reported to be cemented and analysis of natural samples is useful as it may indicate what changes in fundamental mechanical properties can be expected through diagenesis. Due to the more limited reported data for these samples, and particularly an absence of data to constrain volume changes with increasing stress, basic characterisations have been developed with minimal constraint to demonstrate some of the important aspects. With additional data the characterisations may be refined. wo samples are considered for characterisation, denoted here as Barents Sea 1 and Barents Sea 2 – see Figure 4-7. Discussion of the samples (Grande, Mondol & Berre, 2011) indicates that the mudstones tested have variable burial and uplift histories which is reflected in their present density. The Barents Sea 2 sample has a very high density which likely reflects significant porosity reduction and cementation. Some irrecoverable (plastic) deformation has taken place for the Barents Sea 1 mudstone as the path followed during unloading is different from that followed during initial compression.

By integrating insight developed in the previous section, the characterisation has been performed by using the illite:silt 50:50 characterisation as a foundation and adjusting the key parameters identified in Section 4.2.3:

- *Preconsolidation pressure (strength)* – the samples have higher strength owing to their deep burial and cementation. The inflexions marked by the blue arrows in Figure 4-7 mark the onset of plastic deformation. This location is sensitive

to the preconsolidation pressure as this largely sets the size of the failure surface. Additional information would allow for better constraint of this parameter.

- *Friction angle/dilation angle* – these parameters also influence the elastic-plastic transition and relative stress changes during plastic flow. It was found that both samples could be recovered with the same dilation angle. The Barents Sea 2 has a higher friction angle than Barents Sea 1, which is perhaps justified by the apparent higher degree of alteration (high bulk density). This is another area in which a more realistic characterisation could be developed using triaxial testing data for example.
- *Poisson's ratio* – this value is calibrated to approximate the loading/unloading response. The selected values for Barents Sea 1 and Barents Sea 2 were 0.29 and 0.15 respectively. The Barents Sea 2 sample is noted to be high density. The Barents Sea 1 sample could potentially have lower Poisson's ratio than assumed above.

The recovered numerical responses in Figure 4-7 are in good agreement with the experimental data, and as noted could be refined with the availability of additional information to better constrain various parameters, and this can be targeted in later phases of the project. The lower image in Figure 4-7 shows the evolution of K0 as a function of the overconsolidation ratio (OCR). This trend confirms the good unloading response predicted by the model. Several trend lines are also shown that indicate how different Poisson's ratio values would affect the response during unloading assuming the same value of K0 prior to unloading *(denoted as $K_0^{initial}$)* of 0.521. Lower Poisson's ratio values result in smaller incremental changes in the horizontal effective stress relative to the vertical effective stress and by extension higher K_0 values for a given OCR. As the value is reduced these relative differences are altered. Interestingly, if a Poisson's ratio is selected such that;

$$K_0 = \nu/(1-\nu) > K_0^{initial}$$

then it is possible for the value of *K0* to reduce during the unloading process as opposed to increase. This is shown in Figure 4-7 for the case where $\nu = 0.35$ as;

$$K_0 = \nu/(1-\nu) = 0.35/0.65 = 0.538 > K_0^{initial}.$$

There are some conclusions that can be drawn from these investigations and incorporated into conceptual studies that include the influence of burial diagenesis. Firstly, cemented mudstones can exhibit elastic behaviour even at stress levels exceeding their maximum burial stress. This is indicative of a pseudo-overconsolidation that arises from pore space rearrangement and/or cementation during diagenesis. This is an important consideration for constitutive models representing deeply buried samples as outlined in SHARP DV1.1b and this is discussed further in following sections. However, the degree of overconsolidation may be more subtle than indicated by these specimens and will vary depending on the specific mineralogy and burial history.
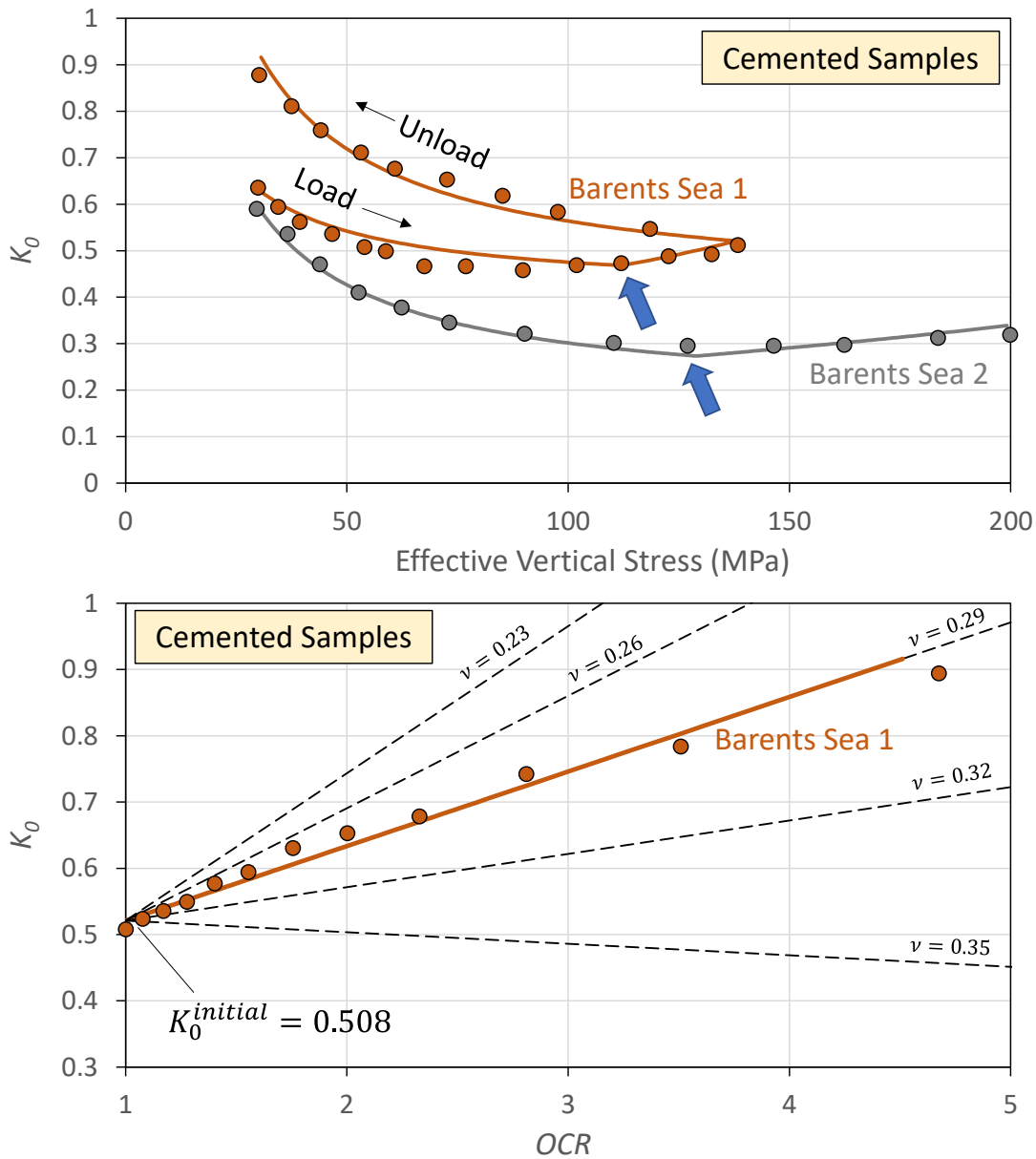
Figure 4-7 Comparison between experimental (circles) and numerical (bold lines) responses for natural cemented mudstones from the Barents Sea. Upper image – K0 ratio evolution for two samples, dashed lines reflect the influence of different Poisson's ratio. Lower image – relationship between K0 and OCR for Barents Sea 1 mudstone. Again, dashed lines represent unloading trendlines for different Poisson's ratios.

Secondly, the value of Poisson's ratio is an important parameter in predicting the unloading behaviour. This seems obvious given that it is well acknowledged that under conditions of zero lateral strain the ratio of horizontal to vertical effective stress can be expressed simply as a function of Poisson's ratio (refer to Eq. 3). The demonstrative characterisation of the Barents Sea mudstones reinforced that this is a key parameter for unloading behaviour of both cemented and uncemented rocks, and this has been discussed relative to experimental data in Grande et al., 2011. When discussing the Barents Sea mudstone trends Grande et al., 2011 suggest that K_0 correlates more favourably with bulk density relative to trends that use friction angle and OCR. It might therefore be argued that there exists a relationship between Poisson's ratio and porosity,

with a modification of the Poisson's ratio of the sediment as porosity and fabric are modified via diagenesis.

Cemented Shale (Berre et al;., 1995)
Berre et al., 1995 discuss the behaviour of both uncemented and cemented clay-shales tested in both loading and unloading in K_0 triaxial tests. The uncemented samples exhibit behaviour consistent with the behaviour described for the synthetic samples with increasing K_0 during unloading. However, the strongly cemented clay-shales exhibit the opposite behaviour with a noticeable reduction in K_0 on unloading – Figure 4-8. In the summary of the *drained* triaxial extension tests the determined Poisson's ratio values are reported, *which are high* in the range [0.37, 0.47], giving;

$$K_0 = \nu/(1 - \nu) = [0.587, 0.88] > K_0^{initial}$$

Therefore, a reduction in K0 during unloading would be expected in the same manner as is shown in Figure 4-8. This is confirmed when examining Figure 4-8 where the Poisson's ratio of 0.43 (mid-range of reported values) clearly results in a reduction of K_0 during unloading that is generally a good match for the experimental data. A value of 0.30 produces an increase during unloading that is typical for uncemented samples.
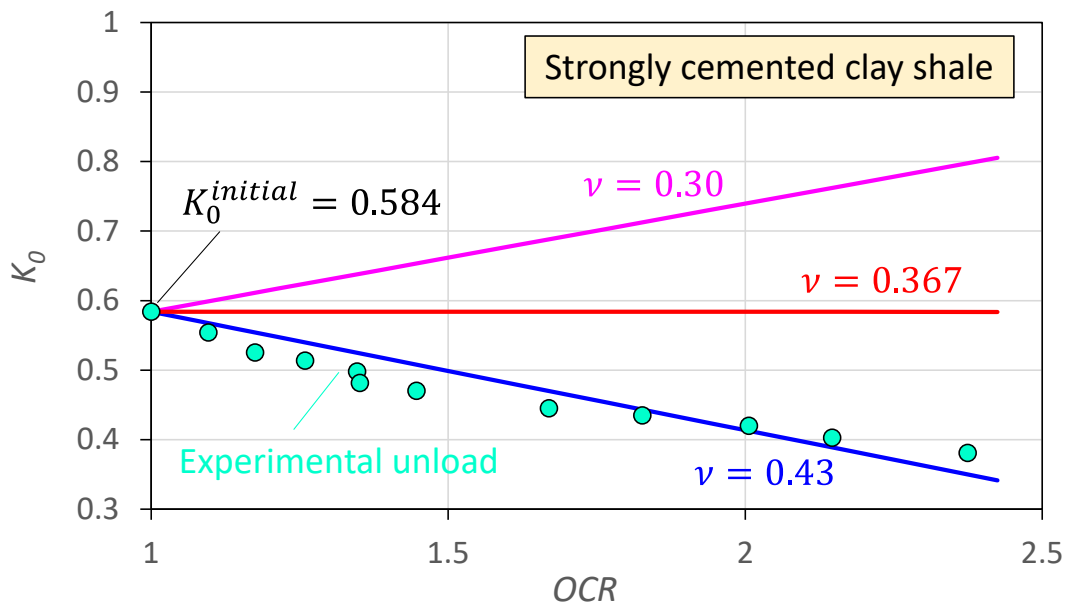

Figure 4-8 Unloading behaviour of a strongly cemented clay-shale (developed from data presented in Berre et al., 1995). Points represent K_0 unloading from $\sigma'_v = 96MPa$. The K_0 value prior to unloading was approximately 0.58. Lines represent calculated trends for differing Poisson's ratio values (as shown).

Berre et al. surmise that the unloading behaviour observed for the strongly cemented sample is likely resulting from the strong bonds in the material that are of a non-frictional nature. This suggests that Poisson's ratio changes during diagenesis may be quite complex and specific to the precise microscale processes at play. The availability of more experimental data and microstructural analysis might allow for better understanding in this area. Figure 4-8 reveals a further interesting aspect in that if the value of Poisson's ratio is such that;

$$K_0 = \nu/(1 - \nu) = K_0^{initial}$$

and *no change in K0 is predicted during unloading*.

New Experiments on Mudstones and Shales (WP3.2)
New experimental testing undertaken within WP3 (DV3.2, Figure 3-23, Figure 3-24) for natural samples is shown in Figure 4-9. The new experiments consist of a natural shale and a mudstone (70:30 clay:silt composition) loaded to vertical effective stresses of 50 and 25 MPa respectively. The mudstone has not been deeply buried (<1km), whilst the shale has been buried deeper (>2.5km) and subject to chemical diagenesis. Whilst the K_0 for both samples is not judged to have completely stabilised, they are suggested to be sufficiently close to the stabilised values to be representative. Also shown are a variety of calculated unloading curves for Poisson's ratio values in the range [0.1-0.32]. Poisson's ratio values of 0.29 and 0.26 look to be reasonable fits to the mudstone and shale respectively, though there appears to be some stress dependency for the mudstone as confirmed in Figure 3-23.

What the curves clearly demonstrate is that if a Poisson's ratio value of 0.32 was assumed for both samples the mudstone would exhibit K_0 increase during unloading, whereas the shale would show a decrease in K_0. Therefore, to predict the unloading response it is necessary to accurately capture the pre-erosion ratio of stresses and key constitutive parameters such as Poisson's ratio, both of which are likely to be affected by diagenesis. In essence more deeply buried samples appear to have reduced K0 values during normal consolidation which is also reported by others e.g. Nygard et al., 2004, and consequently they will exhibit less sensitivity to unloading for a given Poisson's ratio.
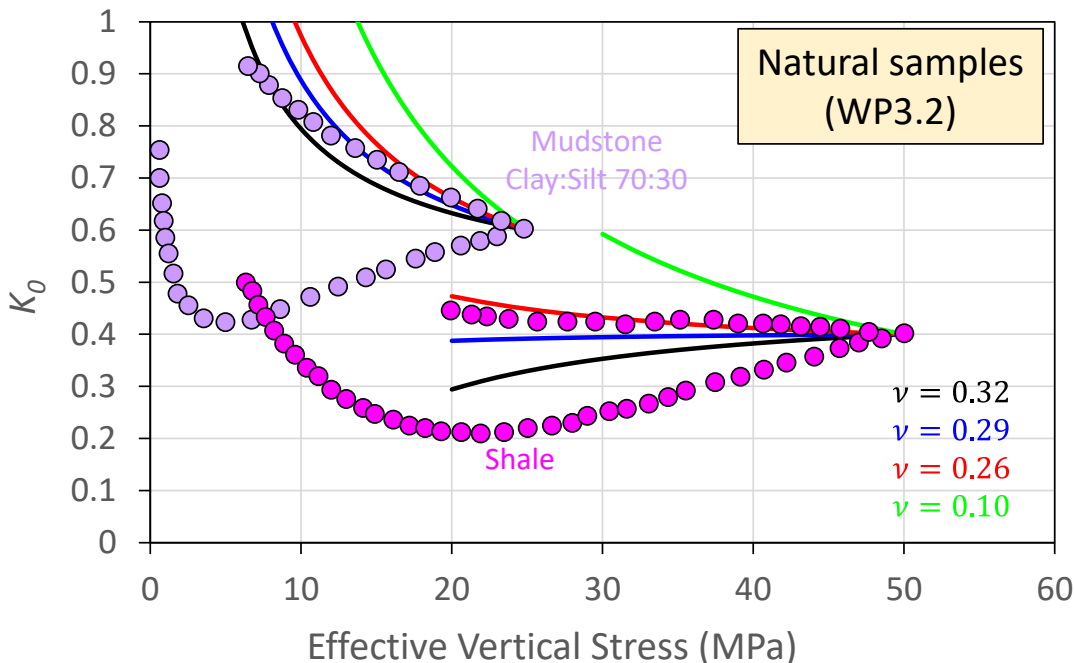

Figure 4-9 Loading and unloading response on a natural mudstone and shale, redrawn from Figure 3-23 and Figure 3-24. Coloured curves represent calculated unloading responses for different Poisson's ratio values, accounting for the initial K0 values of ~0.6 and ~0.4 for the mudstone and shale respectively.

4.3.2 Investigation – Drake and Draupne Shales, Horda Platform Area

The stress conditions in the Draupne and Drake Shales are important as they represent some of the primary caprocks for Horda Platform storage sites. Here we demonstrate some of the important insights developed in the previous sections. We begin by assuming an unaltered material with relatively high K_0. We choose the smectite:silt 50:50 sample as this was discussed with respect to the failure surface profiles in section 4.2.3. Incrementally we modify the input constitutive parameters based on known/likely values for both the Draupne shale and Drake shale based on published data and new insights developed through specific SHARP experimental testing. The changes implemented can result in a quite significant change in K_0 when accounting for changes to Poisson's ratio, hardening characteristics and friction angle; Table 4-1. When incorporating lower bound properties for Drake shale for instance the predicted K0 is 0.447 which reflects a change in K_0 of -0.237 (-34%) relative to the base characterisation.

Outputs from this exercise are used as input to theoretical unloading curves for Draupne and Drake shales in Figures 4-10 and 4-11 respectively for Eos, Troll East, Smeaheia. For each shale two plots are generated based on initial K_0 values and Poisson's ratio values derived in Table 4-1. The calculated initial and uplifted stress conditions are based on Figure 3-12 for overburden stress, with uplift estimates established in Section 2.2 and reported by Grande et al., 2022. Also shown on the plots are in-situ stress indications outlined in Section 3.2 in the form of LOP (leak-off pressures) and XLOT (extended leak off test) measurements.

Referring to Figure 4-10 it is clear that with lower bound Poisson's ratio inputs the Eos well *in-situ* stress data is well approximated; changing Poisson's ratio does not have a significant impact on the initial K_0 value and there is very modest uplift at this location. Lower bound Poisson's ratio inputs give a quite satisfactory match to the high LOP value (K0 ~1.25) recorded at the Smeaheia Beta well which has experienced a more appreciable uplift. Maximum burial is equivalent at Smeaheia Gamma but uplift is smaller; it is clear that in the low Poisson's ratio case the K0 value is overestimated. Assuming high Poisson's ratio inputs results in a subtle increase in K0 from the initial value but this is still somewhat higher than the *in-situ* tests indicate. In both scenarios the conditions at Troll East are underestimated. The poor correlation at Troll East and Smeaheia Gamma can be explained in various ways (e.g. non-uniaxial conditions) however it is noteworthy that these two locations experienced the shallowest and deepest maximum burial. It may therefore be suggested that Draupne at Troll East has not been very altered resulting in a higher initial K_0. Similarly, the Draupne shale at Smeaheia Gamma experienced greater burial, which may have provided the conditions for more significant alteration and lower initial K_0. Consideration should also be given to the high organic content in the Draupne shale which may make it more sensitive to local conditions.

Considering now Figure 4-11 we see that considering the lower bound Poisson's ratio values gives very satisfactory results for both locations where *in-situ* stress measurements are available. Adopting upper bound Poisson's ratio values overestimates the current K_0, especially at Eos where high quality XLOT data is available.

Sim Ref.	Poisson ratio	Hardening parameter $(\lambda - \kappa)$	Friction parameter β (MC)[a]	Dilation parameter, ψ	Final K0 $(\Delta K0)$[b]
Smectite:Silt 50:50	0.38	0.074	45° (18°)	58°	0.684 (-)
Draupne Shale – High PR	0.38	6.0E-3[d,e]	45° (18°)	58°	**0.650** (-0.034)
Draupne Shale – Low PR	0.26[c]	6.0E-3	45° (18°)[f]	58°	**0.595** (-0.089)
Drake Shale – High PR	0.38	6.0E-3	58° (27°)[h]	58°	**0.617** (-0.067)
Drake Shale – Low PR	0.09[g]	6.0E-3	58° (27°)	58°	**0.447** (-0.237)

Table 4-1 Progressive modification of a synthetic characterisation to reflect changes in fundamental properties due to diagenesis based on known/inferred properties for Draupne and Drake shales. Two realisations of each shale are developed to represent uncertainty and variability in Poisson's ratio.
[a] Mohr-Coulomb (MC) friction angle shown in brackets for comparison
[b] ΔK0 indicates change relative to the reference characterisation
[c] Poisson's ratio supplied by NGI for Draupne shale
[d,e] values for Kimmeridge Clay reported by Prats et al., 2019 and comparable to values back-calculated for Draupne Shale (Soldal et al., 2021)
[f] reported by Soldal et al., 2021
[g] value reported from K0 triaxial tests of Drake shale reported by NGI (WP3.2)
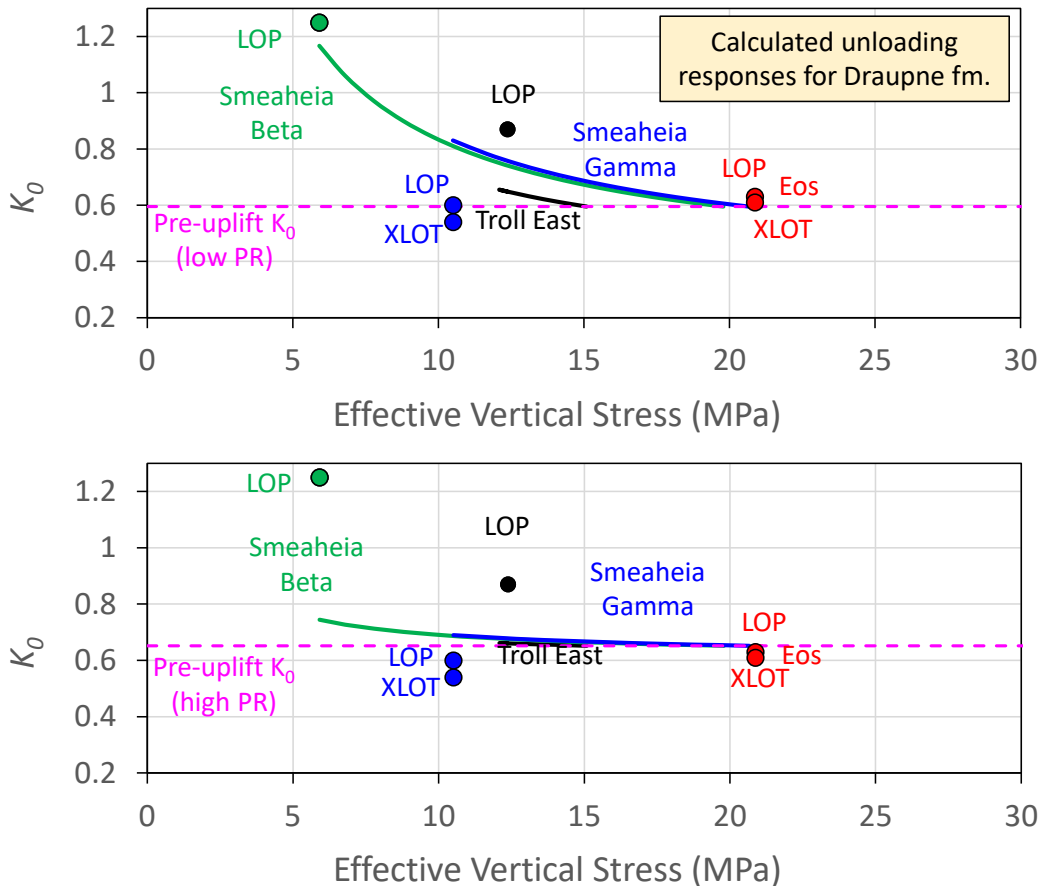*[h] reported for reconstituted Drake shale in Section 3.3.2*

Figure 4-10 Theoretically derived unloading responses for Draupne formation with comparison to in-situ stress data. Upper image uses the pre-erosion K0 and Poisson's ratio values assumed for the Draupne – Low PR properties in Table 4-1. Lower image uses the pre-erosion K0 and Poisson's ratio values assumed for the Draupne – High PR properties in Table 4-1.
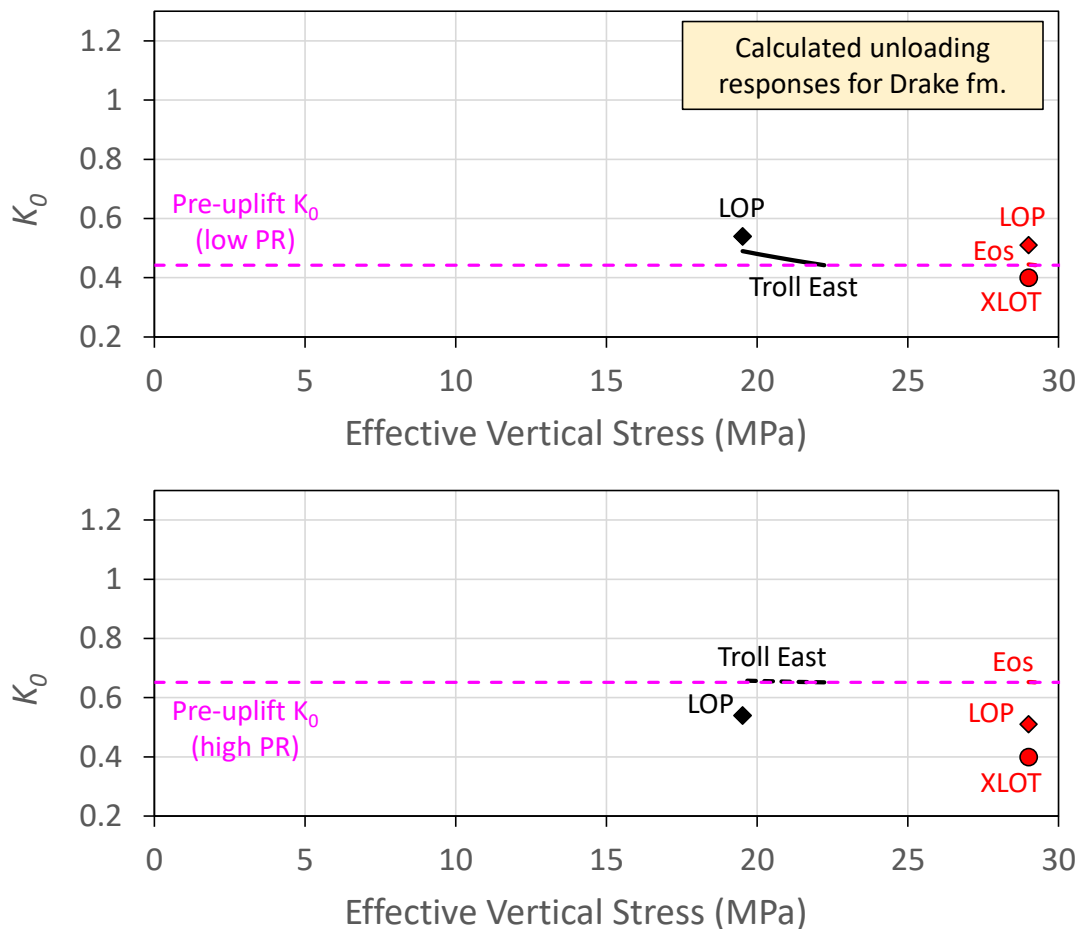
Figure 4-11 *Theoretically derived unloading responses for Draupne formation with comparison to in-situ stress data documented in Grande et al., 2022. This data is also reported in Chapter 3. Upper image uses the pre-erosion K0 and Poisson's ratio values assumed for the Draupne – Low PR properties in Table X. Lower image uses the pre-erosion K0 and Poisson's ratio values assumed for the Draupne – High PR properties in Table 4-1.*

The general methodology for representing diagenesis within geomechanical simulations has been outlined previously (refer to DV1.1b). Concisely the modelling methodology extends the conventional critical-state based constitutive modelling framework by coupling mechanical and chemically sourced volume changes. Whilst the current level of functionality has been shown to be effective, there are several areas that merit extension given the target investigations. Prats et al., 2019 use a very similar general modelling workflow within the finite element code Parageo, and make some important modelling contributions that are very relevant in the context of the SHARP project:

- The hardening law for their constitutive model is allowed to change as a function of diagenesis. This is important as observation indicates the compaction trend post-diagenesis for shales is usually much shallower i.e. they are "stiffer" (Nygard et al., 2004; Ewy et al., 2021).
- The framework described in Roberts et al., 2013, 2014 accords mechanical and chemical compaction processes equal contributions to strength changes. In terms of the preconsolidation pressure this appears a reasonable assumption for cementation processes in sandstones for instance, but changes in strength for shales appear more subtle (Nygard et al., 2004, Ewy, Soldal et al., 2021).

- A scaling factor to apportion the contribution from diagenetically-sourced volume changes to strength is therefore recommended (Prats et al., 2019). The effect of cementation on cohesion-like state variables is also discussed by Prats et al., but is less relevant for the current work. These changes however would have important implications for caprock integrity.

Some additional novel extensions to the framework are also proposed:

- The modified Cam Clay nonlinear elasticity law already makes provisions for diagenetically-induced stiffness changes (DV1.1b). Poisson's ratio has been shown to be a key variable in determining the unloading response, and there is some evidence that this may be altered during diagenesis-related fabric changes (Rahman et al., 2022).
- Modifications to the failure surface and dilation parameters are suggested as these will likely change in response to diagenesis, mineralogical changes and cementation.

Development of the modelling capability to address many of these aspects is underway and due to be reported in DV1.3 and/or DV1.4. A further aspect that has not been adequately addressed is the significance of anisotropy; some caprocks such as the Drake shale exhibit very pronounced anisotropy, yet most modelling frameworks do not accord this due consideration. Whilst modifying constitutive models to account for developing fabric/anisotropy may be beyond the scope of the project, consideration can be given to the implications on unloading behaviour in particular (similar to theoretical investigations in section 4.3.2).

5   Discussion

5.1   Lithological impact

In summary from selected high quality XLOT's (overpressure <10%) and for test performed in sediments close to its maximum burial depth (i.e Oseberg) observed K_0 are close to expected K_0 from mechanical compaction and normal consolidation of sediments governed by a basic equation of friction angle and plasticity of the sediment at initial deposition and with compaction. Although the area has a complex history, one hypothesis is that during aging and diagenesis the processes of creep, dissolution and precipitation will adapt to the initial stresses generated within sediment at early stage of compaction and not change significantly towards larger burial. Empirical correlations for normally consolidated sediments presented in this report and DV3.2 and workflows to estimate stress from logs (Grande et al., 2022) can work well, and the K_0 is then dependent on initial plasticity and initial friction angle of remoulded sediment. In uplifted or glacially overconsolidated areas the OCR can be applied to depths of ca 1 km, however, the OCR term is however not valid below a certain depth when lithification becomes significant (>1-2km). Evidence is that the K_0 may be insensitive or even reduce more deeply buried shales after diagenesis and chemical alterations (> 2-2.5km) (see Chapter 4). We discuss also whether K_0 in diagenetically altered shales can be reduced during uplift (Chapter 4), however, so far based on limited real observations mainly from three high quality XLOT test; this includes the two Draupne XLOT's, where K_0 in highly uplifted Smeaheia gamma are lower compared to Eos, and the low range K_0 value of 0.4 in Drake (Eos) which is far below the K_0 for the expected normally consolidated state of Drake and shales in general (based on clay content, mineralogy). However, the Drake upper range K_0 of 0.55 fits very well with expected K_0 for a normally consolidated state based on mineralogy. Alternative explanations for the low value of $K_0 = 0.4$ could be technical/operational in nature and related to validity of the XLOT test (see Thompson et al., 2022) or explained by geological mechanisms not yet captured in this evaluation. Such effects could potentially be:

- a strong diagenesis effect during uplift (see chapter 4)
- a small extensional component (slightly reduced compared to uniaxial strain) related to uplift
- local effects in the fault blocks or stress dominated by the thick sequence of sandstone above and below Drake (Brent sandstones are located above and Cook and Johansen Fm. Below). More high quality stress data calibration points are needed to have better confidence in interpretations.

5.2   Stress profile in uplifted and Glacially Loaded Areas

5.2.1   W-E Cross section trends

Figure 5-1show the slope of the average trendline of LOP and XLOT in comparison with a figure of LOT's vs depth from another study further south with examples from data in Quadrant 7, 8 and 9 and quadrant 15, 16 and 17 (Baig et. al. 2018), and from this figure a similar trend of reduced slope of LOP vs. depth can be recognized when mowing eastwards from Quadrant 15-17 within the uplifted areas.
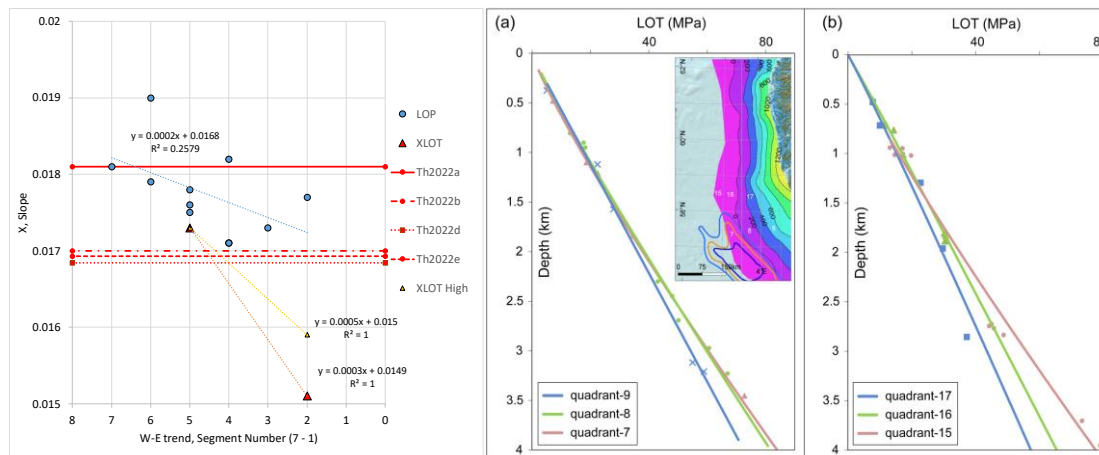
Figure 5-1 a) West-East average trend of LOP and σ$_h$ from XLOT vs. depth trend (from Figure 3-4). b) A similar trend of reduced slope of LOP vs. depth is observed further south with examples from data in Quadrant 7, 8 and 9 and quadrant 15, 16 and 17 (Figure from Baig et. Al. 2018)

In uplifted and glacially loaded areas it may therefore be generalized (from this study and Figure 3-4) that local changes in average and depth dependent stress trend may occur, with a tendency of reduced average σ$_h$ vs. depth trend when uplift increases (i.e. eastwards toward the Norwegian coast). A non-linear depth dependent σ$_h$ vs. depth trend may be more realistic in such areas, and such a trend may be simplified as a tri-linear σ$_h$ vs. depth trend, where high σ$_h$ and K$_0$ in shallow depths below 1km maximum burial depth (i.e K$_0$ in range 0.6-0.1, positive OCR effect). For sediments that have experienced more 2 km maximum burial depth diagenetic effects may have resulted in reduced σ$_h$ and K$_0$ during uplift (i.e K$_0$ in range 0.4-0.6, negative OCR effect). However, from field tests data it seems that although there is a diagenetic impact of stress >2km, the final stress after uplift will keep within expected range from lithological impact K$_0$=0.6+/- 0.2.

5.3   Uncertainties and Impact: Input to WP5

5.3.1   Uncertainties in the *In-itu* Stress Trends

Figure 5-2 shows a summary of trendlines and examples of data for uncertainty evaluations in the Horda Platform eastern area, including CO$_2$ storage sites Aurora and Smeaheia. The example illustrated has emphasis on the shallow (<1 km) and the deeper part (>3 km), which are not covered directly by XLOT data. There are only four XLOT data points to fill the local trend in the eastern part. A low value in Eos well of K$_0$=0.4 will give a trend lower than the regional trends for the Horda Platform. Also, LOT data supports the same observation but are closer to the regional trend. From the LOT data in the deep >3km, it is suggested Pp is close to hydrostatic, and this is supported by the linear trend of the entire depth compared to the clear shift in LOT trend as observed at Martin Linge, where XLOT and LOT clearly show a bi-linear trend. Also, there is no indication of reduced velocities from high pore pressure from sonic log vs. depth (i.e. 31/6-1 deep well). High LOT values close to lithostatic are present in the shallow lithologies of Hordaland. However, there is a large scatter in the data, and the effect may be local with higher values in the Troll West area (segments 3 and 4). Excess pore pressure from glacial loading on low permeability the sub-glacial units may develop differently in the in lithologies ranging from Quaternary in the West (Naust Fm.) to

Tertiary smectite-rich formations (Oligocene, Eocene) and shales from more compacted Rogaland, Cromer Knoll and Shetland to the east. Lithologies in the eastern part which experienced larger maximum burial depth likely have a tendency of lower permeability and compressibility.

The K_0 may then vary based on smectite, permeability, local drainage conditions etc. Hence, further knowledge requires detailed knowledge of geology with respect to content of clay, smectite, permeability and potentially draining layers of sands and silts allowing shales to consolidate and drained behaviour. Excess pore pressure due to low drainage may affect the LOP in this shallow environment.

Figure 5-2 also point to areas of interest for further evaluation of stability and uncertainties related to basement faults (i.e Vette and Tusse) and top fault leakage. Shallow LOT data from Hordaland fm. are highlighted for shallow depth (<1km) and summary of all deep data (> 3km) from both Horda platform (HP) and Lomre terrace (LT) are high-lighted.
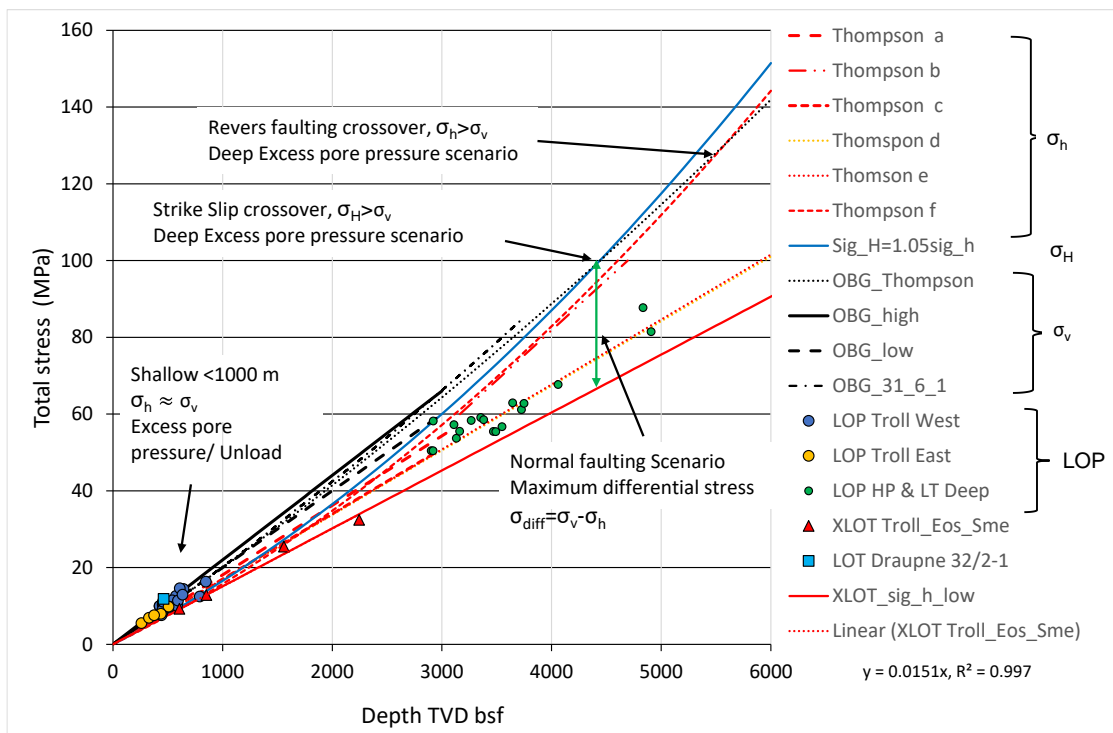

Figure 5-2 Summary of trendlines for discussions of Uncertainty.

The impact of increased σ_h in shallow units may give reduced shear stress and improved seal capacity in upper part of stress profile. For deep units, increased σ_h from pore pressure may result in a stress regime closer to strike slip or reverse faulting and a full switch may be possible with some impact also possible from basement lateral stress component (i.e. Thompson et al., 2022b). A switch in stress regime may be more likely for deep highly pressurized units, however potential coupling to basement will be further investigated in SHARP (WP1.3). It should be noted that the understanding within Equinor based on regional experience is that Horda platform pore pressure system is governed by hydrostatic pore pressure from surface all the way down to basement (Wu et al. 2022 and Equinor pers.com). However, pore pressure may still vary locally in shallow overburden from impact of glacial loading, and deep pore pressure trend i.e.

below lowermost pressure measurements and below depth of deepest well were geophysical logs are available are not documented previously. Performing uncertainty analysis in deep parts of sedimentary sequence is therefore still relevant to demonstrate impact of high pore pressure in general, although main assumption is hydrostatic pore pressure is governing for this specific area.

5.4   Schematics of mechanisms and uncertainties

Figure 5-3 to Figure 5-5 illustrates schematically the potential impact of unloading in shallow and deep lithologies on the shape of the stress profile based on observations in eastern part of HP area and the discussion in this report. Figure 5-3 show the potential impact on mechanical compaction and burial diagenesis on present day stress and K_0 profile in uplifted areas, where the arrows illustrate uplift for shallow (green), intermediate (yellow) and deep (red) lithologies respectively. The resulting stress trend after uplift may then be depth dependent and tri-linear rather than linear.
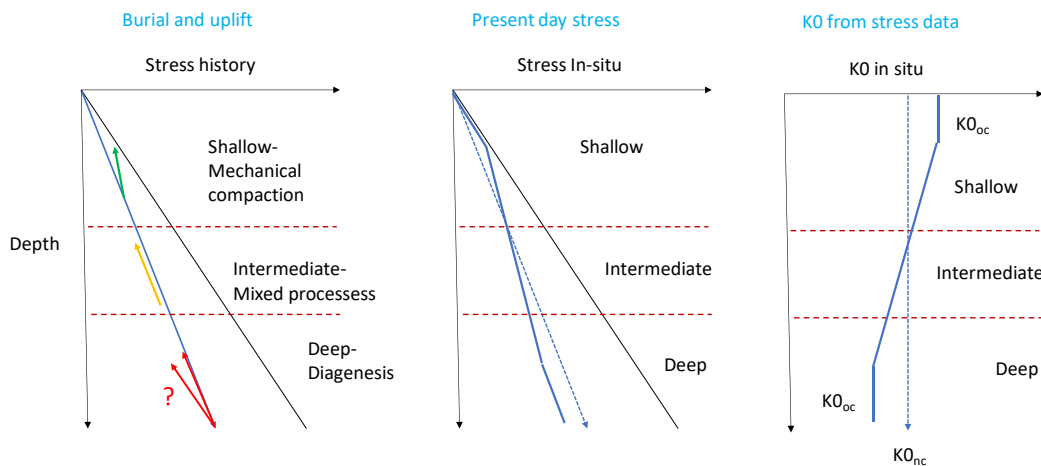

Figure 5-3 Schematic illustration of potential impact on mechanical compaction and burial diagenesis on present day stress and K_0 profile in uplifted areas. The arrows illustrate uplift for shallow (green), intermediate (yellow) and deep (red) lithologies respectively.

Figure 5-4 illustrates potential impact of uplift on present day stress and K_0 profile in the Horda platform area from West to East and how uncertainty may vary. In the western part with no uplift, the σ_h trend is linear, and in the eastern part with uplift the trend is tri-linear. The detailed gradient may vary depending on amount of uplift and properties of the shallow units below quaternary, where stiffness and permeability will vary along E-W profile, and whether the lithologies were deeply buried and diagenetically altered prior to uplift. When using and average trendline the uncertainty range will be larger in the eastern profile with large uplift compared to western area with no uplift.
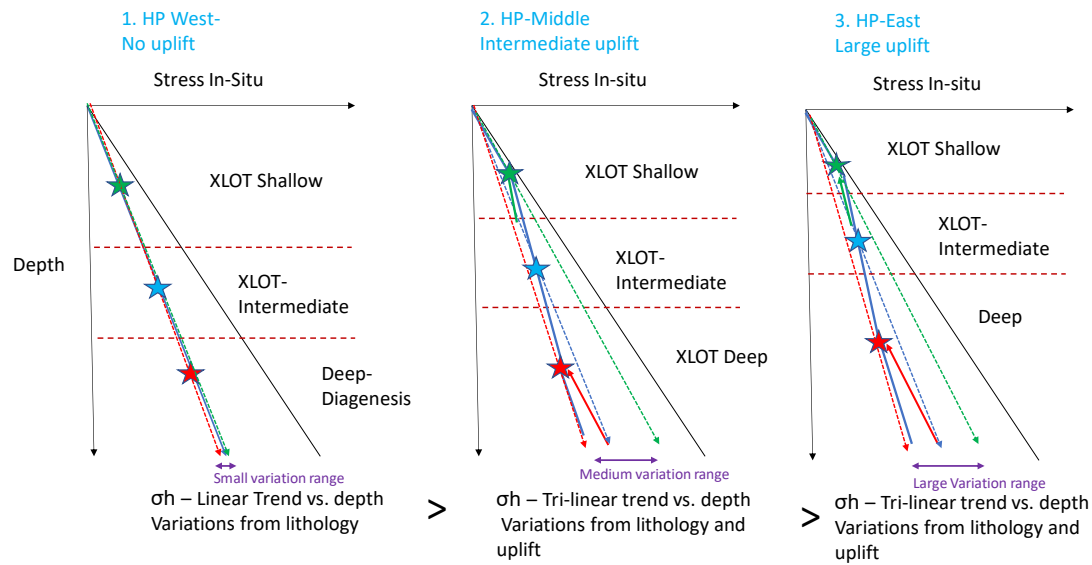
Figure 5-4 Schematic illustration of potential impact of mechanical compaction and burial diagenesis on the uncertainty range in the present day stress and K0 profile in the Horda platform area from West to East. The gradient and uncertainty range is varying depending on depth of XLOT and variable amount of uplift along E-W profile.

A flexural bending of sedimentary package with compressional component in the top and extensional component in bottom would potentially increase and reduce σ_h in upper and lower parts respectively.

5.5   Relevance of findings in Geomechanical analysis

Figure 5-5 illustrates schematically the relevance of the findings from this study for further evaluation on earthquake hazards, stress barriers for vertical flow, and variation in confinement along the fault that would influence stability and leakage evaluations. These findings may impact uncertainty and risk evaluation (WP5) and for various hazard and monitoring evaluations (WP4);

1. Earthquake hazards and basement coupling (left).
2. Shallow stress barriers and leakage monitoring systems (centre).
3. *Fault stability of the larger faults where depth dependent profile varies with depth (right).*
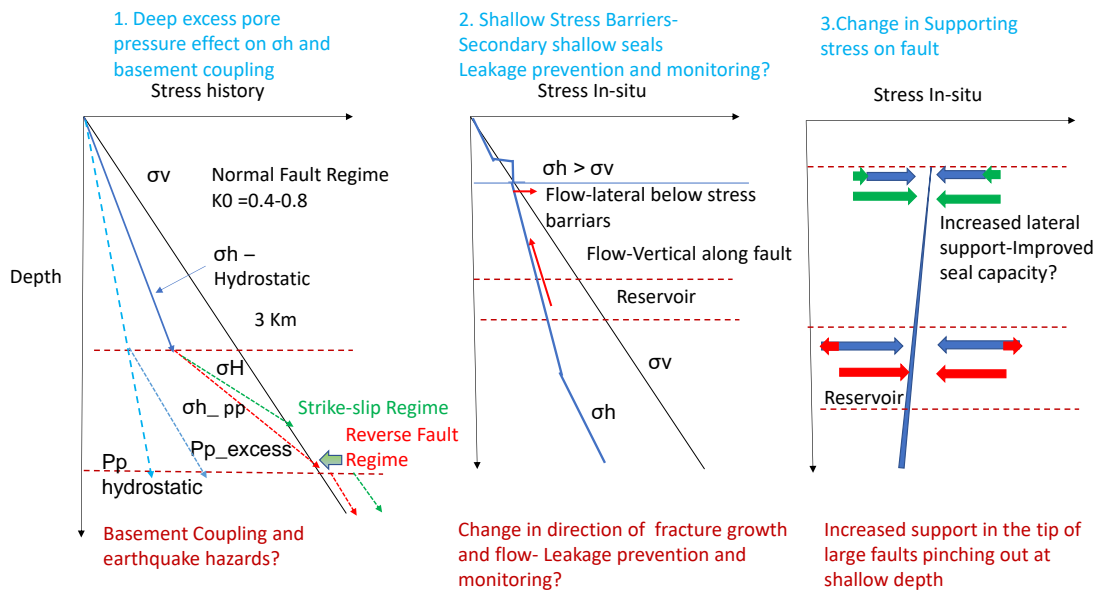
Figure 5-5 Examples of relevance of the findings from this study for further works on earthquake hazards, stress barriers for vertical flow and variation in confinement along fault for fault stability and leakage evaluations.

The average linear trend of σ_h from surface to reservoir level may be sufficient for analysis of sealing capacity of CO2 storage reservoirs (seal often in the range i.e. 1-3km), and useful in analysis for induced fracturing and fault reactivation from injection of CO_2 at depth of seal. However, analysis for impact of earthquake on fault reactivation of basement faults would likely benefit from more detailed understanding at large depth > 3km, i.e. deep excess pore pressure and σ_h from burial diagenesis (as illustrated in Figure 5-5, left figure). Evaluations of along fault fluid flow above reservoir, secondary seals and shallow stress barriers will benefit from more detail in the shallower intervals <1 km (as illustrated in Figure 5-5, middle and right figure). Hence, a continuous best estimate log based profile or tri-linear depth dependent stress trend with corresponding uncertainty range for respective interval may be useful to capture all aspects for various types of analysis at various depths. Such understanding may develop progressively under development of a CO_2 site based on availability of data;. For early assessments (Round 1, DV4.1 report) linear trends and typical uncertainty ranges may be sufficient. Improving the assessments through addition of more local/detailed datasets and site specific understanding may form part of Round 2 (due later in the SHARP project).

5.6 Assessment of stress state in CO2 sites

5.6.1 Early assessment and lithological bounds

Based on experiences from this study we may suggest a procedure for early assessment of stress in North Sea settings as summarized below. Suggested trendline from North Sea XLOT database can be used for a start (see Table 5-1). Included in this comparison is some specific consideration of the lithological impact using lithological bounds for normally consolidated sediments as defined under DV3.2: Sand 100% line $K_0=0.4$ and Clay 100% line $K_0=0.8$.

Table 5-1 Summary of published trend lines applied in this study from Thompson 2022a, b (Th2022a and Th2022b respectively). WP@ML is the water pressure at the seabed/mudline, D=Depth$_{mbml}$ is the depth below seabed/mudline (mbml – meters below seabed/mudline).

Area	Trendline reference	X-value	R2	Comment
Horda-platform	Th2022ac	σ_h=WP$_{@ML}$ + 0.181*D	0.9965	High quality XLOT Selected pore pressure less than +/-10% from hydrostatic
North Sea (NO)	Th2022be	σ_h=WP$_{@ML}$ + 0.1693*D	0.981	Best quality datasets for NO
	Th2022bf	σ_v=WP$_{@ML}$ + 1.66e-05*D^2+ 0.1408*D	0.983	Including effect of depth variation due to pore pressure
	Th2022ab	σ_h=0.0261*D-22.703	0.9615	Below 3 km depth in over pressured units (i.e Viking graben and east Shetland platform)
	Th2022bg	σ_v=WP$_{@ML}$ + 7.36e-06*D^2+ 0.1924*D	0.996	
United Kingdom (UK)	Th2022bh	σ_h=WP$_{@ML}$ + 0.1760*D	1.0	2 datapoints
	Th2022bi	σ_v=WP$_{@ML}$ + 0.2140*D	0.998	

The following steps are suggested.

- Minimum horizontal stress: Use available XLOT and LOT form area. Local stress trend from a few wells close to and within main structure is preferred. The reference should be seafloor when comparing LOT from different wells in different areas (i.e Thompson et. al., 2022b. Need to correct water depth and RKB pr. well.
- Vertical stress: Include local overburden gradient (OBG) when available. Normally there are only small variations in OBG between different areas (Andrews et al., 2016)
- Pore pressure: Document pore pressure info with LOT data if available. A pore pressure correction may be applied according to Thompson et. al., 2022b. Deep excess Pp >3 km from diagenetic effects are common, and shallow excess pore pressure can also be especially significant in tight formations due to rapid loading and poor drainage characteristics.
- Lithological bounds impact on K$_0$: Establish sand 100% line K$_0$=0.4 and Clay 100% line K$_0$=0.8 from best estimate OBG and Pp gradient. This is the expected natural variation for siliciclastic sediments. For average lines use Thompson et al 2022b regional trendlines from XLOT (average K$_0$ in range to 0.63 for North Sea). Presence of plastic clays i.e Smectite rich clays of Paleocene, Eocene, Oligocene should be identified as this may give high K$_0$ from high plasticity or from excess pore pressure due to poor drainage. High K$_0$ values can be common also in Halite rich formations, and lead to modified stress conditions in adjacent sediments.
- Uplifted areas: A tri-linear σ_h vs. depth trend may be present, where high σ_h and K$_0$ in shallow depth < 1km (positive OCR effect). For sediments experienced > 2 km maximum burial depth, diagenetic effects may have resulted in reduced σ_h and K$_0$ during uplift (negative OCR effect). The K$_0$ may then be different from expected range from lithological impact (K$_0$ of 0.4-0.8), i.e. variation ranges of K$_0$ may then rather be 0.6-1 for shallow and 0.6-0.4 for deeper units.

- Tectonic or structural impact: When LOP or XLOT falls outside expected variation range from lithological impacts of K_0 of 0.4-0.8 (or $K_0=1$ if halite), or average trend deviates significantly from $K_0=0.63$, structural or tectonic effects may be checked further.

It should be emphasized that leak-off pressure from LOT test does not strictly provide a direct measure of σ_h, especially when the raw data are not available for QC. As well as lithology and rock strength, drilling fluids and wellbore stability can impact the reported values (Raaen et al., 2006). Some lower values may also be failed LOT's, more comparable to Formation Integrity Tests (FIT's) where breakdown of the formation is not achieved, and there is a lack of pumping pressure charts to verify them. In general we assume that such errors (+/-) may cancel out when including more data points and that average trendline can be a useful indicator for regional trend, despite these being normally slightly higher relative to the more accurate XLOT. Therefore, analysis should not be focused for individual LOT outliers, but a trend from a larger number of datapoints. In this section we use reported values directly to demonstrate the method (pressure vs. time curves are not available) and a more detailed quality check on LOP data will be beneficial to improve confidence.

5.6.2 Detailed assessment on stress, lithological impact, depth dependency, lateral variations and upscaling

For shallow lithologies the impact of uplift may be reproduced using empirical relations using OCR term (SHARP report DV3.2, Grande et al., 2022) or calibrated constitutive models (Chapter 4). For, deeper diagenetically altered lithologies impact of diagenesis on constitutive behaviour may be accounted for (Chapter 4, DV1.1b) and will be investigated further as the SHARP project progresses. The exact transition between upper and lower regimes (1-2 km) is not known and may depend on the individual shales and combined mechanical and may be influenced by early diagenetic processes that start the transformation from mudstone to cemented shale.

This analysis indicates that LOP data can give useful additional insights into variations in average trends in an area i.e between fault blocks or injection sites or as function of depth. Although such tests are acknowledged to be less accurate than XLOT, the larger number of datapoints may give valuable insight to local variations in average trends as well as depth dependent variations related to lithology and uplift. Empirical methods based on laboratory studies (DV3.2 report) in combination with log based methods can give additional insights for depth dependent stress profiles (i.e. sonic method Eaton, Grande et al 2022).

Finally, similar methods may be applied through upscaling of seismic data, through inverted seismic cubes using density, poisons ratio and volume of clay in combination to constrain the $\sigma v'$ and K_0. However, a good understanding of governing mechanisms (diagenesis and 3D effects) must be then also accounted for, and these mechanisms at this stage are not sufficiently understood to derive quantitative 3D cubes of stress with a high degree of confidence.

Consolidation and basin analysis for local and regional pore pressure effects may be necessary and useful in order to reduce uncertainty of total and effective stress state.

6 Demonstration early assessment- SHARP Field Cases

Stress data from the North Sea sites have been plotted and compared with the regional trends from XLOT data (Thompson et al 2022b). In this comparison we use trends from North Sea (NO) and United Kingdom (UK). These trends have been compared with plots of large regional datasets of LOT data from UK, NL and DK within the WP4 DV1 report. A more detailed assessment of the sites Endurance (UK), Aramis (NL) and Lisa (DK) where a selection of data are highlighted and compared with regional trends is offered here. Included in this comparison is some specific consideration of the lithological impact through lithological bounds as defined from experimental data under DV3.2. Sand 100% line $K_0=0.4$ and Clay 100% line $K_0=0.8$. There is large scatter in the LOT vs. depth datasets in UK and NL when plotting all LOT's for a larger area (DV4.1 report).

6.1 Horda Platform Area (Norway)

Results from analysis of Horda platform datasets are shown in detail in previous chapters. Examples of estimation of K_0 for reference lithologies are reported in DV3.2 based datasets where mineralogy, plasticity and OCR are well known. These are not calibrated with field stress data directly. However, the estimated values were integrated with data and results from XLOT and LOT data.

Figure 6-1 shows a summary of XLOT data in the Horda-platform area. The Sand100% ($K_0=0.4$) and Shale100% ($K_0=0.8$) lines based on expected variation from lithological variations of normally consolidated sediments. K_0 is calculated from the published regional overburden gradient for North Sea (Thompson et. al 2022) and assuming hydrostatic pore pressure. The best estimate σ_h from Thompson equation's a and d are shown for comparison. All XLOT data except one data point are within this expected variation range. A similar procedure may be useful also for other sites to define the expected variability from lithology under assumption of drained conditions and uniaxial compaction.
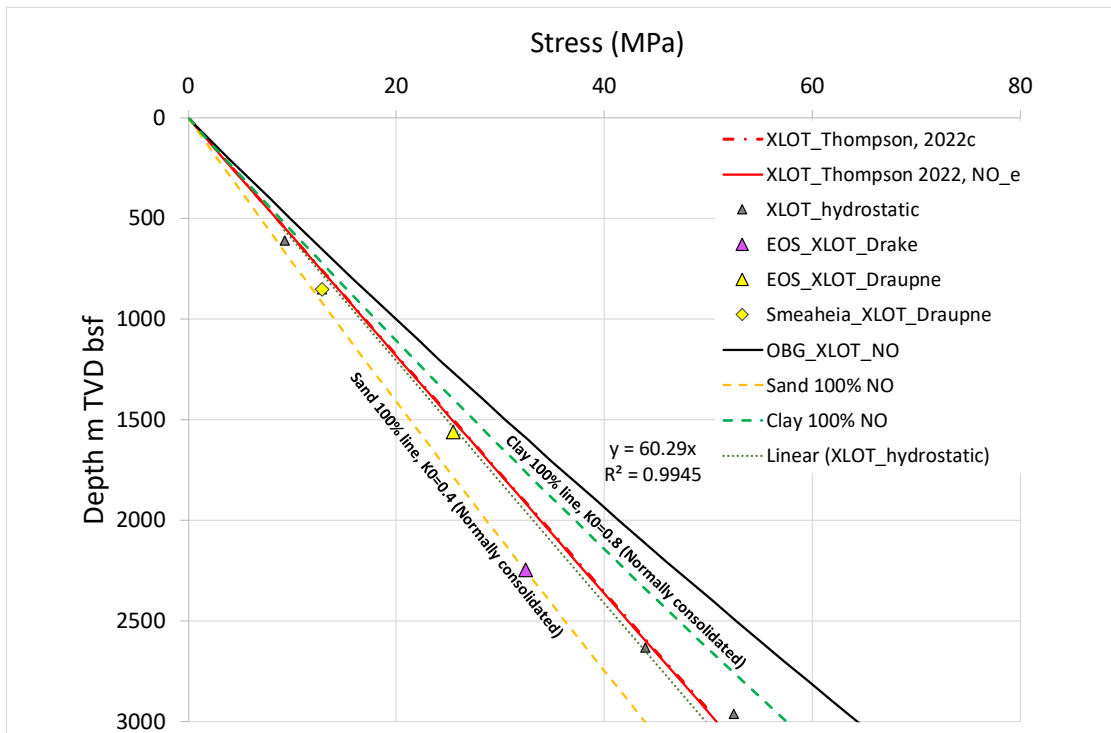
Figure 6-1 Summary of XLOT data in the Horda-platform area. The Sand100% (K0=0.4) and Shale100% (K₀=0.8) lines based on expected variation from lithology changes. K0 is calculated from the published regional overburden gradient for North Sea (Thompson et. al 2022) and assuming hydrostatic pore pressure. The best estimate σₕ from Thompson equation's a and d are shown for comparison.

6.2   Lisa Structure (Denmark)

There is no LOT data from the Lisa field, however, LOT data from Denmark has been plotted with depth in SHARP DV4.1 report. The location of wells with LOT from Denmark are shown in Figure 6-2. An updated plot of LOP data are shown in Figure 6-3 where datapoints are compared with trendlines for North Sea (Thompson et. al., 2022b) and reference lines for sand 100% and clay 100%. The LOT data are grouped in the main groups Clay/Shales, Silt/Sandstones and Chalk. The LOT data are in good agreement with regional trendlines from North Sea. Most LOT data plots within expected variation range of lithological impact (K_0=0.44-0.75). The two LOT's in sand and siltstone plot close to sand line, and most of claystone and shale are close to clay line.

LOT in chalk plots in the expected variation range for sandstone and clay. For the deeper LOT's (>0.5km), three are close to sand line (K_0=0.45) and three are close to clay line (K_0=0.4). The Chalk sediments are not present in the other sites evaluated. Whilst specific laboratory re-sedimentation data is not available for chalks as it is for sands and clays (SHARP Report DV3.2), K_0 triaxial testing of porous chalks (including Maastrichtian age chalk from Stevns Klint, Denmark with porosities >47%, reported by Omdal et al., 2010) indicate K_0 values generally between 0.45 and 0.51. This may provide an explanation as to why the application of the 100% sand line is generally a good match to the *in-situ* data in the chalks. These values also agree with the numerical K0 test simulated on characterised Lixhe chalk (Section 4.1, Figure 4-1).

The two sites Felicia and Thisted are closest to Lisa and highlighted in Figure 6-3. The two LOT from Felicia-1offshore west of Lisa in Claystones at depth 863 and 2112 m plots close to and above OBG, respectively. The pore pressure is assumed to be hydrostatic for lower depth and slightly over pressured for the deeper test depth. This may indicate some additional stress beyond lithological impact at Felicia-1. The two LOT in Thisted onshore south of Lisa show LOT values according to expected trend from lithological impact in one claystone and one siltstone. It should be emphasized also here as highlighted in introduction, that LOT data have uncertainties and individual LOT datapoints may vary from various reasons (Raaen et al., 2006), and we therefore recommend rather using the average trend for LOT datasets, and LOT data (and especially outliers) should be quality checked if possible to improve confidence.

Mineralogy and uplift data are reported in SHARP DV3.2 report. There is a significant uplift of c. 0.8 km in the Lisa structure. This corresponds to an OCR of c. 1.5 at top Gassum Fm. sandstone reservoir. Present day depth of 1.55 km m BSF and maximum burial depth of ca 2.3 km. Some chemical alteration may therefore be relevant in both Gassum Fm. and the sealing Fjerritslev Fm and OCR effect from uplift is not expected. There are also a shallow (ca 100 m thick) unit of Pleistocene sediments above chalk reported as gravel and sand (J-1x completion report). Prescence of Oligogene Smectite rich sediments is not yet known although indicated from regional maps (see SHARP DV3.2, map of Smectite rich layers in Oligocene). In general, the DK stress data are well in line with trends from XLOT database in North Sea. However, Felicia-1 well close to Lisa deviates from this trend with high values from LOT. A further evaluation and quality check of available LOT data and especially around Lisa structure would be beneficial for improved local confidence.
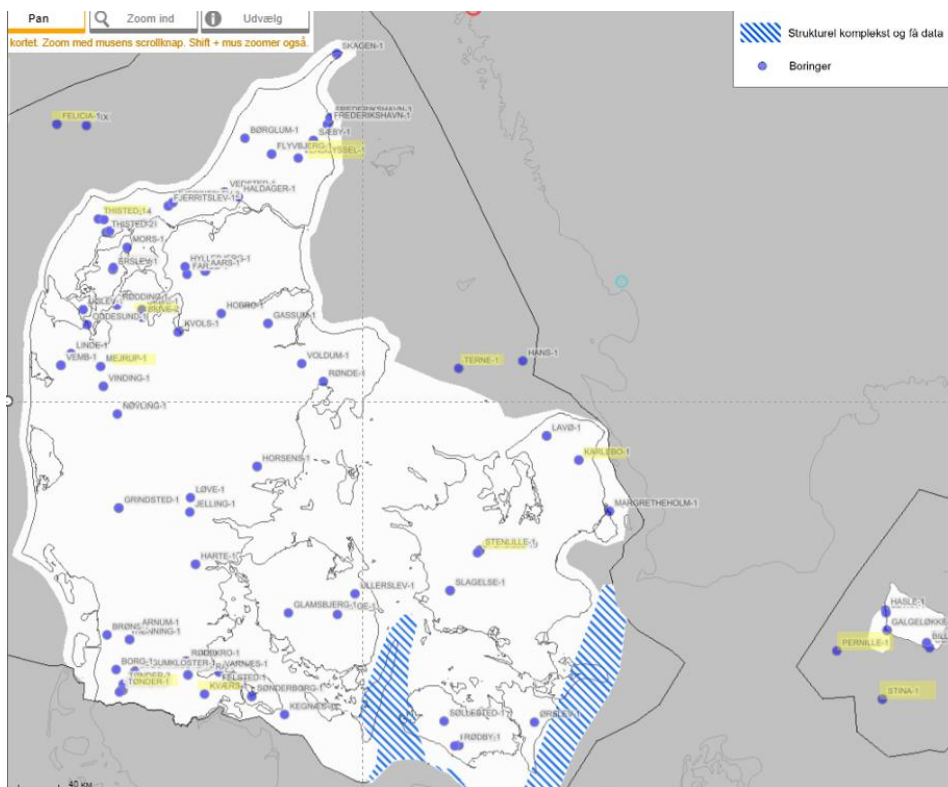

Figure 6-2 Map with the location of wells with LOT from Denmark (source GEUS)
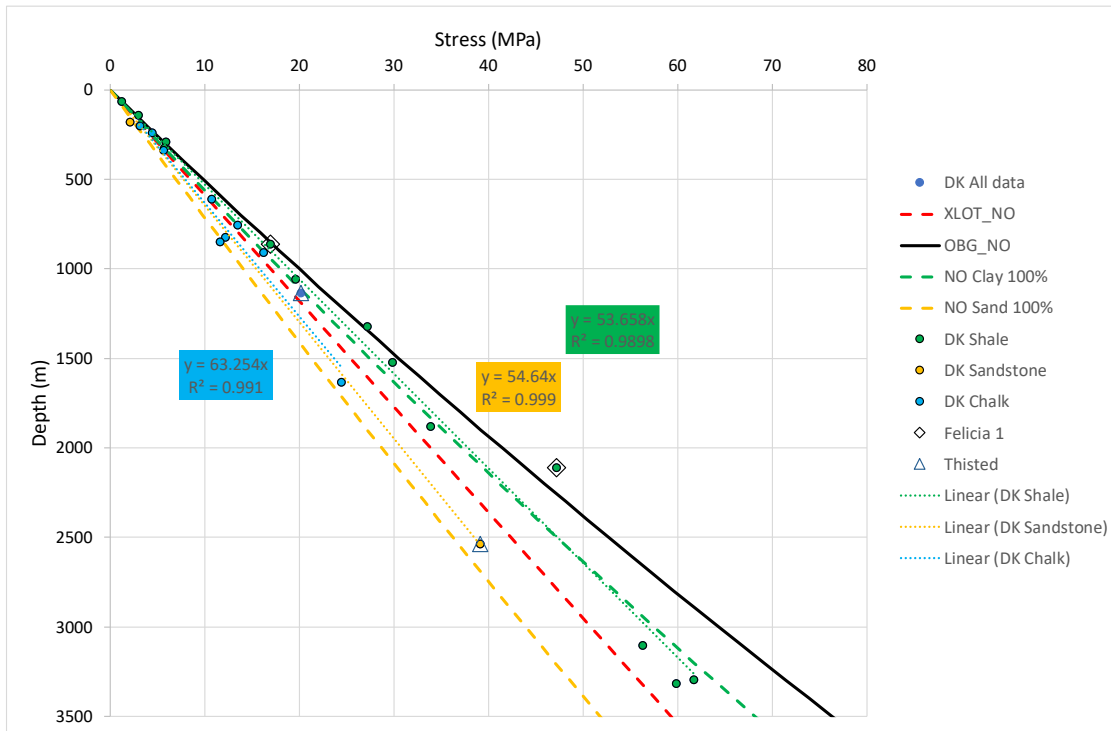
Figure 6-3 LOT data from locations is Denmark compared with trendlines for North Sea (Thompson et. al., 2022b) and reference lines for sand 100% and clay 100%. The LOT data are grouped in the main groups Clay/Shales and sandtones and Chalk. LOT Data were compiled by N. Springer, L. Kristensen, T. Laier, and P. Frykman at GEUS.

6.3 Endurance Structure (UK)

The Endurance structure is a salt-cored anticline in the southern North Sea. It has received extensive attention as a potential site for Carbon Capture and Storage. Plots of LOT stress data with depth are shown in the SHARP DV4.1 report. In Figure 5-1 the same data are compared with regional trendlines based on XLOT data for North Sea and UK wells (Thompson et. al., 2022b, trendline e, h and I in Table 5-1) and reference lines for sand 100% and clay 100%. The LOT data are grouped in the main groups Anhydrite, Claystone, Carbonate and Halite. The LOT and FIT data are quite spread and show more variation compared to LOT data than in the Horda platform area and several LOT data plot outside expected variation range of lithological impact for siliciclastic rocks (K_0=0.4-0.8). The LOT and FIT in Halite plots in the high range and close to OBG as expected due to viscoplastic creep reducing stress differences over geological time.
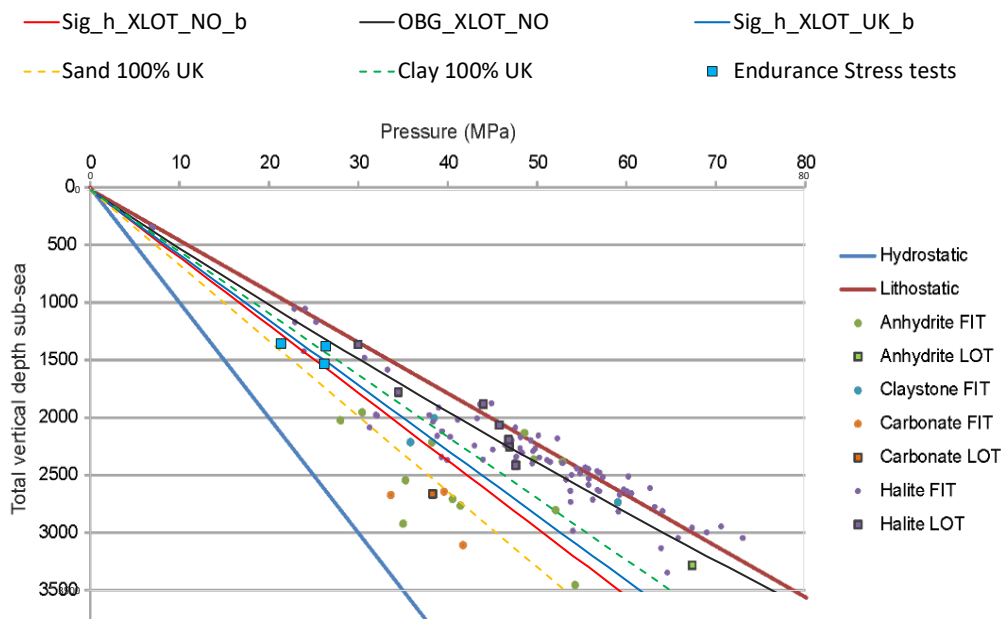
Figure 6-4 UK LOT and FIT data reported under DV4.1 compared with published reginal trendlines based on XLOT data for UK and North Sea (NO). LOT and FIT by dominant lithology in the Zechstein Group. A hydrostatic gradient of 10 MPa/km is shown along with a notional overburden gradient of 22.5 MPa/km. XLOT is an extended LOT, for which only a single measurement is recorded. LOT data reported in SHARP DV4.1 report in background, and that Figure was reproduced from Williams et al., 2015. BGS © UKRI (2022).

Three tests are available from well 42/25d-3 Endurance appraisal well (White Rose, 2016) close to Endurance structure. The datapoints from MiniFrac are in good agreement with general trendlines and within sand-shale 100% reference lines. The average trend of σ_{min} is in line with the UK XLOT trend (Thompson et al. 2022b). There are only 8 XLOT datapoints included for UK and a reference to NO trendline is also shown for context. Horizontal stress information estimated from minifrac data are shown in SHARP WP4.1 report, and here reproduced including derived K_0 values in

Table 6-1. The Röt Halite FIT showed no indication of leak-off or fracturing, and stresses are likely closer to lithostatic (K0=1) within the pure halite layers. The acquired minifrac data from the Bunter Sandstone BSF and Solling Claystone provide high quality stress measurements and estimated K_0 is 0.58 and 0.75 for the BSF and claystone respectively. Two gradients for OBG is reported 24 and 22.5 MPa/km for UK sites (White Rose 2016 and Williams 2015), both are higher than the XLOT OBG trend of 21.4 MPa/km.

So although complex structural history in the area from salt tectonic etc, the K0 values in tested units in 42/25d-3 Endurance appraisal well are reasonable close to what is expected from lithological effect and normally consolidated sediment only.

Table 6-1 Minifrac tests *FIT and minifrac data acquired from the 42/25d-3 Endurance appraisal well (White Rose, 2016). Depths are given in units of m True Vertical Depth Sub-Sea (TVDSS).*

Unit	Depth (m TVDSS)	S_{hmin} (MPa)	S_{hmin} gradient (MPa/km)	OBG_UK* 21.4 MPa/km	K0* field	OBG** 22.5 MPa/km	OCR	K0 ** field	Regional S_{Hmax}/S_{hmin}	Type
Röt Halite	1339	21.4	16	28.65	0.52	30.13		0.48	-	FIT
Solling Claystone	1363	26.4	19.4	29.17	0.82	30.67		0.75	1.2	Minifrac
Bunter Sandstone Formation	1520	26.2	17.2	32.53	0.63	34.20		0.58	1.15	Minifrac

*Thompson et. al 2022b
**Based on OBG from Williams 2015

More XLOT/Minifrac data on the Endurance will be beneficial to confirm trends. The local OBG trend of 0.24 bar/m reported seems high and should be confirmed from density logs, and also to evaluate/confirm deep pore pressure for evaluation of basement coupling.

6.4 Aramis (Netherlands)

The Dutch Geological Survey (TNO) has published an extensive dataset of LOT pressures compiled from wells in the Netherlands (see SHARP report DV4.1 report)). The LOT data are coloured according to Formation names e.g. Zechstein (Ze), Rotligende (Ro) etc. The aquifers in the Aramis AOI are hydrostatically pressured. The gas fields considered for CO_2 storage are in some cases depleted to about 10% of their initial pressure. An updated plot of LOT data is shown in Figure 6-5 where most relevant datapoints are compared with trendlines for North Sea (NO) and UK wells (Thompson et. al., 2022b) and reference lines for sand 100% and clay 100%.

There is a big scatter in the dataset and more evaluation of LOT and XLOT's from local wells in ARAMIS area will be beneficial to evaluate the effect of lithology on stress in the ARAMIS field. Furthermore, better understanding the local trend of OBG and deep pore pressure will help to narrow down the range of uncertainties.
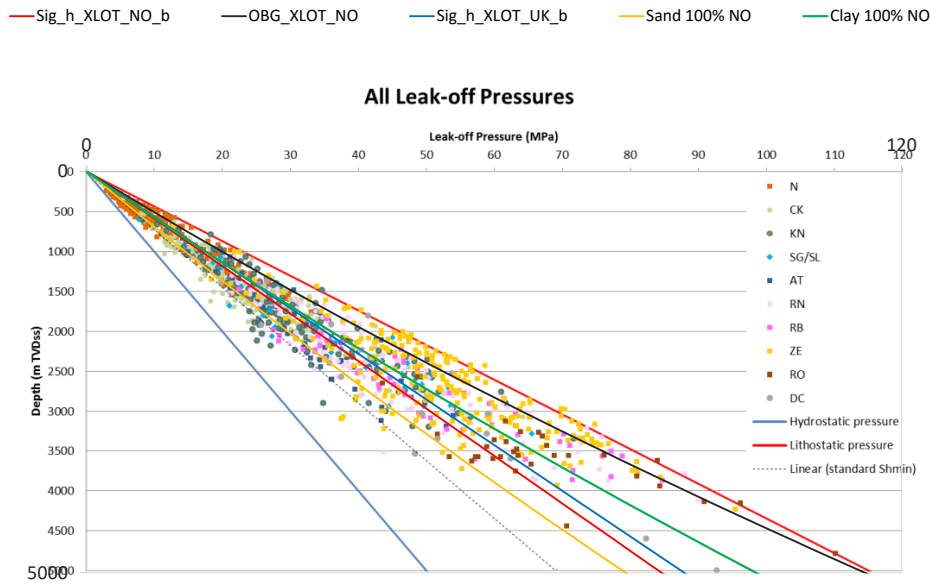
Figure 6-5 LOT data from locations is Netherland compared with trendlines for North Sea (Thompson et. al., 2022b) and reference lines for sand 100% and clay 100%. The plot shows all leak-off pressure points that are publicly available in The Netherlands, coloured by lithology (LOT data from SHARP WP4.1 report).

6.5   Rajasthan Region (India)

Bhagewala oil field in Rajasthan is the only site outside of the North Sea setting and currently no reference stress data is available for SHARP from this area. However, the geological setting and lithological column are reported in DV4.1 and shortly summarized below (for references see DV4.1)   The Bikaner-Nagaur basin is relatively shallow, with maximum depth to basement estimated to be 1.5–2 km, and contains a 1 to 1.5 km thick Infracambrian to Cambrian mixed evaporite, carbonate, and siliciclastic sequence overlain by a thin sequence of Permian to Holocene rocks. From the stratigraphic column of Baghewala-1 well the basal Jodhpur Formation sandstone are present at a depth interval of 1103–1117 m, and represent the heavy-oil reservoir. This clastic depth interval underlies laminated, organic-rich Infracambrian dolomites of the Bilara Formation. Crude oil similar to that encountered in the Jodhpur Formation occurs at Bilara, Hanseran Evaporite, and Upper Carbonate formations as well.

In comparison with North Sea there are multiple lithologies of sandstones, shales, dolomite, limestone, halite and conglomerate in the overburden, and there is a comparatively short distance to the basement (i.e 160 m in Baghewala-1 well) where lithologies are dominated by shales and volcanic intrusions.   We recommend the following:

- Start documenting the field as described in the introduction of Chapter 6.
- Determine the total vertical stress from integrating density logs and obtain best estimate pore pressures all way down to basement if possible.
- Use the global empirical relation to describe σ_h and σ_v (from Thompson et., al 2022b);

$$\sigma_v = WP@ML + 5.46e\text{-}06*D^2 + 0.2002*D$$
$$\sigma_h = WP@ML + 0.1659*Depth_{mbml} + 0.589(Pp-Pp_{NORM})$$

- Assess trends relative to *in-situ* measurements and begin consideration of stress history such as uplifts, regional compression and mobile sequences where relevant.

This is an onshore field so there is a need to correct for depth of groundwater level rather than the seawater depth. A stress coupling effect from basement may be relevant for the deepest reservoir units due to short distance to basement. Regarding uncertainty range from lithological impact, a variation of K_0 of 0.6+/-0.2 may be useful, however, deep halite caprock at 1 km may experience higher K_0 up to 1. Furthermore, LOT, XLOT, break out analysis etc need to be used in updated refined analysis. The Decator and Quest CO_2 injections sites in Canada have experienced seismicity in the basement from injection of CO_2 in reservoirs positioned just above basement (Goertz-Allman et al., 2022), and it may be useful to compare to available stress data in those sites.

6.6 Summary of Field Cases

This evaluation indicates that workflow to assess the impact of lithology can be useful to highlight the expected natural range of K_0 and σh for CO2 storage sites. Based on knowledge of lithology and under assumption of uniaxial strain and drained conditions (hydrostatic pore pressure), profiles of σ_h vs. depth can be predicted at an early stage of storage evaluations (i.e. Lisa DK). When field stress data (XLOT/LOT) deviates significantly from expected average trends and variations range (K0=0.6+/-0.2), a potential tectonic impact may be checked closer and details on the structural history of the area can be determined and integrated into the assessment, as outlined in detail in this document. Higher values of K_0 (i.e. 0.6-1) may be expected in shallow uplifted areas (<1km maximum burial depth) and when salt formations are present.

7 Summary and Conclusions

A comprehensive discussion related to governing stress generating mechanisms and references to literatures is beyond the scope of this report, but summaries are documented in DV1.1a, DV1.1b, DV4.1. As there are ongoing investigations under WP1.3 and WP1.4, and developing links to WP2, WP3 and WP4, new results may also impact on the discussions and conclusions reported here.

7.1 Summary

7.1.1 Reginal evaluation- Impact of Burial History and Glacial Loading

Average trends from LOP are consistent with trends from XLOT data with limited variations in average trends over entire area when sorting on fields and main tectonic structures (1-7), and the average trends may therefore be used as stress indicator to increase number of stress observations significantly and give increased empirical confidence in both regional and local stress trends. From both XLOT data and LOP data there is a tendency towards a slight reduction in trend of σ_h vs. depth when moving eastwards from Rugne Basin towards the more uplifted areas in East. Deep pore pressure effect (likely diagenetic) that results in increased σ_h for depth > 3km is clearly present in the western part of investigation area in East Shetland platform and Rugne basin where XLOT and LOP show similar trend. Further east in Lomre Basin and Horda Platform where deep XLOT's (>3 km) are not available, deep LOP data are aligned with shallow LOP trends (and Thompson a and c trends from XLOT) with no indication of elevated pore pressure and increased σ_h. This may be related to a shift in the deep pore pressure regime east of Viking graben, trends (Thompson a and c) from over pressured in west to closer to hydrostatic in east. The boundary has not been thoroughly investigated but may be verified with other types of datasets (pressure trends from seismic or basin analysis).

The increase of σ_h during uplift (OCR effect) is most important in uncemented sands, clays and shallow mudstone (max burial <1-2 km) before significant chemical alteration occurs. The OCR effect is relevant in the Quaternary units, Oligocene/Eocene mudstone and sand formations and potentially also other mudstones in the shallower <1km depth. The shallow stress trend in east can be reconstructed through detailed analysis of well logs and uplift history in these shallower intervals.

Locally higher σ_h and K_0 ratios are indicated from LOP's in Hordaland Fm. including Troll and Aurora areas. The vertical load from ice loading may in some areas be larger than the load experienced during maximum burial depth. Oligocene age smectite-rich, high plasticity, low permeability clay formations underlying the URU in these areas may have been pressurized during ice age, and whether these high σ_h and K_0 is likely a result of overpressure or the high content of plastic smectite rich clay is analysed and reported in DV1.3. A combination of effects is also possible based on local drainage conditions and presence of permeable layers.

7.1.2 Insights from Constitutive Modelling

- The significance of friction angle in determining the value of K_0 during uniaxial normal consolidation has been demonstrated through detailed analysis, calibration and verification. This helps confirm the suitability of selecting indicators of sediment composition, such as clay fraction, as an input variable for establishing *in-situ* stresses in shallow, normally consolidated sediments that are not significantly overpressured (Chapter 3).
- The presence of plastic clay minerals like smectite has a profound influence on friction angle and by extension K_0. Considering lithologies of this type are often coincident with very low permeabilities suggests that further analysis of intervals of this type is advisable e.g. tertiary section at Horda Platform.
- Characterising the synthetic and unaltered samples and integrating understanding of the behaviour of altered samples provides a foundation for further systematic investigation of the influence of diagenetic processes on K_0. Accounting for changes to key constitutive properties due to diagenesis, established from analysis of experimental testing on deeply buried samples, indicates that they would exhibit significantly lower K_0 values during consolidation.
- Accounting for changing fundamental properties like Poisson's ratio, stiffness and, crucially, friction angle for key caprocks such as Draupne and Drake shale's demonstrated recovery of K_0 values that are not dissimilar to in-situ values derived from XLOT.
- An inference based on the above is that for shales, claystones and mudstones the effect of diagenesis is potentially to promote collapse of structure and assist compaction, but without significantly modifying strength – experimental evidence suggests that Draupne shale is essentially normally consolidated. Normal compaction therefore continues during/after diagenesis, but subsequent stress and volumetric changes are fundamentally different due to the modified fabric/texture post-diagenesis.
- Diagenesis may not alter the total amount of clay, but it may alter the friction angle and by extension K_0. For example Drake shale appears to have high clay content but also relatively high friction angle. This potentially indicates that methodologies based solely around clay fraction would overpredict K_0 at depth or in some scenarios.
- The unloading behaviour of altered sediments is sensitive to Poisson's ratio but importantly the lateral stress ratio prior to unloading. For the same Poisson's ratio an increase or decrease in the lateral stress ratio can be predicted based on the pre-unload K_0.
- The influence of anisotropy has not been considered in detail but may be significant, particularly for the Drake formation. Future investigation should accord some effort to how this might change interpretations undertaken to date.

7.2 Implications for stability and monitoring- Horda Platform.

The following finding need to be accounted for in the further work in models/predictions of fault stability/seismicity during CO_2 storage operations).

- A reduced eastwards average trend of σ_h vs. depth of reservoir and cap rock intervals (<3 km) is indicated).

- High σ_h in shallow units (<1km) in Smeaheia area indicates a high K_0 ratio resulting in better confinement which is likely positive for stability and sealing potential in the upper part of larger faults.
- High σ_h vs. depth trend in deep units (>3 km) should be accounted for in Western areas (Viking Graben and East Shetland Basin), however, may not be relevant in Lomre Terrace and Horda Platform (based on observations from LOT only).
- In west, the high σ_h from elevated pore pressure at larger depth may also influence stress field closer to basements i.e in combination with lateral stress component transferred through basement coupling (i.e. change from normal faulting towards strike-slip regime close to basement boundary may be more likely compared to hydrostatically pressurised deep units).

The following observation may have consequence for monitoring set-up. Shallow highly over-consolidated units in the Quaternary may act as stress barriers (K_0>1) influencing flow path of potential gas leaks which also have a consequence for monitoring set-up targeting surface leaks. Their lateral distribution can be regional over the area but OCR and K_0 may also vary locally depending on whether drainage was possible during glacial load for variations in grain size, permeability and drainage layers.

7.3 Lithology impacts- learnings for other CCS Assets

Average trends compare well between LOT and XLOT data, and in absence of high quality XLOT data the average trends from LOT data may give a good indication of σ_h trend. Local trends from this study are in line with regional trends from XLOT database (Thompson et. Al 2022a, b, c, d, e) and give further confidence in use of regional trends. However, local effects of excess pore pressure, large uplift, and diagenesis on σ_h should always be accounted for on a site-by-site basis.

The observed K_0 from XLOT data varies largely in range 0.4-0.8 (Andrews, 2016 and Thompson et., al 2022), which is same range as observed in experimental data for normally consolidated sediments ranging from sand to pure clays (DV3.2 and Grande et al., 2022). Average K_0 of 0.63 observed from XLOT database in entire North Sea (Thompson et al., 2022b) is close to 0.6 which is an average in observations from laboratory and empirical methods. For relaxed basin with hydrostatic pore pressure we may summarize; For normally consolidated areas and units (no uplift or glacial loading), a variation range of K_0 =0.6 +/-0.2 is expected. Uplifted areas can give depth dependent trend of K_0 with the higher values (K_0 =0.6-1) in shallow lithologies (<1km) and lower values (K_0 =0.4-0.6) in deep lithologies (max burial depth >2 km). Information on clay and smectite content can be a good indicator of σ_h for normally consolidated state (lithological impact) and detailed information of load history is useful for over consolidated state (impact previous loading). Analysis of constitutive properties suggests that altered samples may have certain constitutive properties that are closer to sands – lower Poisson's ratio, higher friction angle, higher dilation.

The above findings are based on siliciclastic sediments from Norwegian continental shelf. The presence of halite for instance may give high values of K_0 due to creep as indicated from LOT's in UK (i.e Williams et al., 2015). Adjacent sediments may also be influenced by loading from the salt structure, and boundary conditions may differ from uniaxial.

7.4 Conclusion

The following findings may be highlighted as conclusions from WP1.2;

- <u>LOT data reginal study;</u> Although less accurate than XLOT, the larger number of LOT datapoints may give valuable insight and "fill in" data gaps to increase confidence in local areas, as well as confirm depth dependent variations related to lithology and uplift. In this study using LOT data gave useful additional insights into depth dependent trends and lateral variations in average trends within the larger study area (i.e. across major structural elements, between fault blocks or CCS injection sites, shallow vs. deep).

- <u>In uplifted, eroded and glacially loaded areas</u>; 1) There is a tendency of <u>reduced average linear trend of σ_h vs. depth eastwards</u> towards the most uplifted areas along Norwegian coast, 2) A <u>reduced depth dependent trend</u> is indicated from both LOT data and K_0 from Poisson's. σ_h and K_0 may be high for the shallow lithologies from the effect of overconsolidation from uplift and glacial loading and reduced with depth as the impact of previous loading becomes less.

- <u>For, deeper lithologies</u> impact of diagenesis on constitutive behaviour may be accounted for through calibrated constitutive relationships (Chapter 4). The understanding of the requirements for this type of constitutive law is evolving and benefitting greatly from exposure to new data sets through WP3 and are further investigated and documented in under DV1.3 report.

- <u>Excess pore pressures</u> also contribute to depth dependent trend of σ_h and K_0 with a shift to higher stress at depth >3km in some areas (i.e., Thompson et. al 2022a and b). High deep trends are also indicated from LOT in Viking Graben and East Shetland Basin, however, in the Horda Platform, there is no shift in trend from LOP which may be attributed to an essentially hydrostatic pore pressure.

- <u>Early assessments of stress:</u> A workflow to assess stress from regional trendlines (Thompson et al 2022b) in combination accounting for the impact of lithology "lithological bounds" and burial history can be very useful to predict stress and determine the expected natural range of K_0 and σ_h for CO_2 storage sites as demonstrated for early-stage evaluations in the less mature Lisa sites (Denmark) where neither local LOT or XLOT data are in place.

- <u>Detailed assessment of stress:</u> Empirical relationships and constitutive modelling based on clay content, plasticity and previous loading history and diagenesis are found to be useful to address the expected impact of lithology on stress and detailed depth dependent and lateral variations. Evaluation may be done based on XRD data (report DV3.2), in combination with log-based methods (i.e. Grande et al., 2022) and through constitutive and numerical modelling methods (Chapter 4, DV3.2 and DV1.3). Such methods give additional insights in more mature CCS sites like in the more data rich Horda platform area.

- <u>Stability analysis and uncertainties:</u> Detailed profiles capturing depth dependent and lateral variations from lithology, uplift, glacial loading and pore pressure contributes to more precise best estimates and narrow down the span of uncertainties in the depth of interest for detailed analysis, where analysis may focus for shallow stress barriers (shallow), along fault flow (shallow to intermediate deep) and earthquake hazard evaluations and coupling to basement (deep). More precise input gives better ability to analyse/predict the geomechanical responses with less uncertainties during storage operations.

8   References

Aas G, Lacasse S, Lunne T, et al. (1986) Use of in-situ tests for foundation design on clay. Use of In-situ Tests in Geotechnical Engineering, 1–30.

Goertz-Allmann, B P., Nadège Langeta, Daniela Kühna,b, Alan Baird, Steve Oates, Carrie Rowed, Stephen Harveyd, Volker Oyea, Hilde Nakstad, 2022, Effective microseismic monitoring of the Quest CCS site, Alberta, Canada 16th International Conference on Greenhouse Gas Control Technologies GHGT-16, 23-27th October 2022, Lyon, France

Andrews, J., Fintland, T., Helstrup, O., Horsrud, P., Raaen, A., 2016. Use of unique database of good quality stress data to investigate theories of fracture initiation, fracture propagation and the stress state in the subsurface. 50th U.S. Rock Mechanics/Geomechanics Symposium, American Rock Mechanics Association.

Andrews J., and de Lesquen C., 2019, Stress determination from logs. Why the simple uniaxial strain model is physically flawed but still gives relatively good matches to high quality stress measurements performed on several fields offshore Norway, 53rd US Rock Mechanics/Geomechanics Symposium held in New York, NY, USA, 23–26 June 2019.

Andersen ES, Østmo SR, Forsberg CF, and Lehman S. 1995. Late- and post-glacial depositional environments in the Norwegian Trench, northern North Sea. Boreas 24: 47-64.

Baig, I., Faleide, J.I., Jahren, J., Mondol, N.H., 2016. Cenozoic exhumation on the southwestern Barents Shelf: estimates and uncertainties constrained from compaction and thermal maturity analyses. Mar. Petrol. Geol. 73, 105–130.

Baig I., Faleide J.I., Mondol N.H., and Jahren J., 2019, Burial and exhumation history controls on shale compaction and thermal maturity along the Norwegian North Sea basin margin areas, Marine and Petroleum Geology 104 (2019) 61–85

Bjerrum L. 1967. Engineering geology of Norwegian normally-consolidated marine clays as related to settlements of buildings (Seventh Rankine Lecture). Geotechnique 17: 81-118.

Bjerrum L, Andersen KH (1972) In-situ measurement of lateral pressures in clay. Nor Geotech Inst Publ, 29–38.

Bjørløkke, K and Høeg, K., (1997), Effects of burial diagenesis on stresses, compaction and fluid flow in sedimentary basins, Marine and Petroleum Geology, Vol. 14, No 3, pp. 267-276

Bjørlykke, K., 1998, Clay mineral diagenesis in sedimentary basins-a key to the prediction of rock properties. Examples from the North Sea Basin, Clay Minerals 33, page 15-34

Bjørslev Nielsen, O, Skovbjerg Rasmussen, E., and Thyberg B.I., 2015, DISTRIBUTION OF CLAY MINERALS IN THE NORTHERN NORTH SEA BASIN DURING THE PALEOGENEAND NEOGENE: A RESULT OF SOURCE-AREA GEOLOGY AND SORTING, PROCESSES, Journal of Sedimentary Research, 2015, v. 85, 562–581, DOI: http://dx.doi.org/10.2110/jsr.2015.40

Casagrande, A., 1936, The determination of the pre-consolidation load and its practical significance, Proceedings of the international conference on soil mechanics and foundation engineering. Vol. 3. Harvard University Cambridge. pp. 60–64.

Choi, J. C., Skurtveit, E., and Grande, L., Deep neural network based prediction of leak-off pressure in offshore Norway accepted for Offshore Technology Conference 2019, Huston, USA

Chuhan, F. A., Kjeldstad, A., Bjorlykke, K., and Hoeg, K. 2003 "Experimental Compression of Loose Sands: Relevance to Porosity Reduction during Burial in Sedimentary Basins," Canadian Geotechnical Journal, Vol. 40, pp. 995-1011. Hdoi:10.1139/t03-050

Croizé D., 2010, Mechanical and chemical compaction of carbonates - An experimental study , Dissertation for the degree of Philosophiae Doctor (Ph.D.), Faculty of Mathematics and Natural Sciences, Department of Geosciences, University of Oslo, Norway

Cuffey and Paterson (2010). The Physics of Glaciers (4th edition). Publ: Butterworth-Heinemann.

Crook, A. J. L., S Willson, J Yu, and D Owen. 2006. "Predictive Modelling of Structure Evolution in Sandbox Experiments." Journal of Structural Geology 28 (5): 729–44

Johnson, J., Hansen, J. A.,Rahman, MD. J.,Renard, F. Mondol, N, H,M 2022 Mapping the maturity of organic-rich shale with combined geochemical and geophysical data, Draupne Formation, Norwegian Continental Shelf, Marine and Petroleum Geology, Volume 138, 105525, ISSN 0264-8172,.

Day-Stirrat, R. J., A. McDonnell, and L. J. Wood. 2010. "Diagenetic and Seismic Concerns Associated with Interpretation of Deeply Buried 'Mobile Shales.'" AAPG Memoir, no. 93: 5–27. https://doi.org/10.1306/13231306M93730.

Dewhurst, D.N., Cartwright, J.A., Lonergan, L. 1999. "The development of polygonal fault systems by syneresis of colloidal sediments" Marine and Petroleum Geology, 16, 793-810.

Ewy, R., Dirkzwager, J., Bovberg, C. 2020. "Claystone porosity and mechanical behavior vs. Geologic burial stress." Marine and Petroleum Geology, Volume 121, 104563, https://doi.org/10.1016/j.marpetgeo.2020.104563.

Forsberg CF, Planke S, Tjelta T, Svanø G, Strout J, and Svensen H. 2007. Formation of Pockmarks in the Norwegian Channel. Paper presented at 6th International Offshore Site

Investigation and Geotechnics Conference: Confronting New Challenges and Sharing Knowledge, 221-230.

Gateman, J.H.M., 2016, Relationship between burial history and seismic signatures in the Horda Platform area, Norwegian North Sea, Master thesis University of Oslo, URN:NBN:no-55594

Gateman J.H.M., and Avseth. P, 2016, Net uplift estimation using both sandstone modeling and shale trends, on the Horda Platform area in the Norwegian North Sea, SEG International Exposition and 86th Annual Meeting.

Grande, L., N. H. Mondol, and T. Berre. 2011. "Horizontal Stress Development in Fine-Grained Seimdents and Mudstones during Compaction and Uplift." In 73rd EAGE Conference & Exhibition Incorporating SPE EUROPEC, Vienna, Austria, 1–5.

Grande, L., and N. H. Mondol. 2013. "Geomechanical, Hydraulic and Seismic Properties of Unconsolidated Sediments and Their Applications to Shallow Reservoirs." In 47th US Rock Mechanics/Geomechanics Symposium, San Francisco, CA, USA, 1–10.

Grande L., Forsberg C F., Mondol N., Skurtveit E., Singh R.M., Thompson N., 2023, Impact of glacial loading and uplift on ground stresses in the Horda-Platform area, TCCS-12, Trondheim 19-21st June 2023

Griffith L., Thompson N., Skurtveit E., Smith H., Grande L., 2023 Rock mechanical testing of core from Eos CCS validation well, TCCS-12, Trondheim 19-21st June 2023, published for CO2 datashare

Grollimund B, Zoback. M.D, Wirput D.J, and Arnesen. L, 2001, Stress orientation, pore pressure and least principal stress in the Norwegian sector of the North Sea, Petroleum Geoscience, Vol 7, 2001, pp. 173-180.

Grande, L., Mondol, H. N., Skurtveit, E., Thompson, N., 2022, Stress estimation from clay content and mineralogy-Eos well in the Aurora CO2 storage site, offshore Norway, 16th International Conference on Greenhouse Gas Control Technologies, GHGT-16 23rd -27th October 2022, Lyon, France

Gundersen, A.S., Hansen, R.C., Lunne, T., L'Heureux, J.-S., & Strandvik, S.O., 2019, Characterization and engineering properties of the NGTS Onsøy soft clay site, AIMS Geosciences, 5(3):665-703. doi:10.3934/geosci.2019.3.6

Gyllenhammar, Carl Fredrik (2003) A critical review of currently available pore pressure methods and their input parameters: glaciations and compaction of north sea sediments., Durham theses, Durham University. Available at Durham E-Theses Online: http://etheses.dur.ac.uk/4090/

Halland, E. et al. 2014. CO2 storage Atlas, Norwegian Continental Shelf. http://www.npd.no/en/Publications/Reports/Compiled-CO2-atlas/

Huggett J.M. (1992) Petrography, mineralogy and diagenesis of overpressured Tertiary and Late Cretaceous mudrocks from the East Shetland, Basin. Clay Miner. 27, 487-506

Holden, N., 2021, Structural characterization and acrossfault seal assessment of the Aurora CO2 storage site, northern North Sea, Master Thesis UiO

Jalali, R., 2022, Consolidation and stress history in shallow sediments in the northern North Sea, Master thesis NTNU

Janbu, N. 1969. The resistance concept applied to deformation of soils. In Proceedings of the 7th International Conference on Soil Mechanics and Foundation Engineering, Mexico City, 25–29 August 1969. A.A. Balkema, Rotterdam, the Netherlands. Vol. 1, pp. 191–196.

King, J.J., Roberts, D.T., Cartwright, J.A., Levell, B.K. 2022. Numerical modelling of the growth of polygonal fault systems, Journal of Structural Geology, 162, 104769.

Larionov, V. (1969). Borehole radiometry. Nedra, Moscow , 127.

Lerche, I., Yu, Z., Toerudbakken, B. and Thomsen, R.O., 1997, Ice loading effects in sedimentary basins with reference to the Barents Sea: Marine and Petroleum Geology, v. 14, n. 3, p. 277-338.

L'Heureux, J-S; Ozkul, Z; Lacasse, S; D'Ignazio, M; Lunne, T, 2017, Bestemmelse av hviletrykk (K0) i norske leirer – anbefalinger basert på en sammenstilling av lab-, felt- og erfaringsdata, Fjellsprengningsteknikk - bergmekanikk - geoteknikk. Oslo 2017. Lecture 35. English Title: "Determination of the earth pressure at rest (K0)-in Norwegian clays-recommendations based in lab-, field, and experience data"

Lloyd, C., Huuse, M., Barrett, B. J., Stewart, M. A., & Newton, A. M. (2021). A regional CO2 containment assessment of the northern Utsira Formation seal and overburden, northern North Sea. Basin Research.

Lunne T, Powell JJ, Robertson PK (1997) Cone penetration testing in geotechnical practice. CRC Press.

Lunne, T., Long M., and Forsberg C.F., 2002, Characterization and engineering properties of Onsøy clay

Lunne, T., Long, M., and Uzielli., M, 2006, Characterisation and engineering properties of Troll clay, Proceedings Workshop in Singapore Nov. 06

Løseth, H., Nygård, A., Batchelor, C.L., and Fayzullaev, T., 2022, A regionally consistent 3D seismic-stratigraphic framework and age model for the Quaternary sediments of the northern North Sea, Marine and Petroleum Geology, Journal pre-proof Accepted Date: 20 May 2022.

Marchetti S (1980) In-situ tests by flat dilatometer. J Geotech Eng Div 106: 299–321.

Marchetti S, Monaco P, Totani G, et al. (2001) The flat dilatometer test (DMT) in soil investigations. A report by the ISSMGE Technical Committee 16 on Ground Property, Characterisation from In-situ Testing. International Conference on Insitu Measurement of Soil Properties. Bali, Indonesia, 95–131.

Marsland A, Randolph MF (1977) Comparison of the results from pressuremeter tests and large in-situ plate tests in London Clay. Géotechnique 27: 455–477.

Maystrenko, Y., Ottesen, D. & Olesen, O. 2021: 3D thermal effects of Cenozoic erosion and deposition within the northern North Sea and adjacent southwestern Norway. Norwegian Journal of Geology 101, 202115. https://dx.doi.org/10.17850/njg101-4-1.

Mazzini A, Svensen HH, Planke S, Forsberg CF, and Tjelta TI. 2016. Pockmarks and methanogenic carbonates above the giant Troll gas field in the Norwegian North Sea. Marine Geology 373: 26-38.

Mazzini A, Svensen HH, Forsberg CF, Linge H, Lauritzen SE, Haflidason H, Hammer Ø, Planke S, and Tjelta TI. 2017. A climatic trigger for the giant Troll pockmark field in the northern North Sea. Earth and Planetary Science Letters 464: 24-34.

Mikalsen, H. (2015). Reservoir structure and geological setting of the shallow PEON gas reservoir (Master's thesis, UiT The Arctic University of Norway).

Muir-Wood, D. 1990 Soil behaviour and critical state soil mechanics. Cambridge [England] ; New York: Cambridge University Press (Cambridge core).

Mullrooney, M.J., Osmond, J.L., Skurtveit, E., Faleide, J.I., Braathen, A. 2020. "Structural analysis of the Smeaheia fault block, a potential CO2 storage site, northern Horda Platform, North Sea" Marine and Petroleum Geology, 121, 104598.

Mondol, N. H., 2009, Porosity and permeability development in mechanically compacted silt-kaolinite mixtures: 79th Annual International Meeting, SEG, Expanded Abstracts, 2139–2143, https://doi.org/10.1190/1.3255280.

Mondol, N.H., Grande. L., Bjørnarå T.I., and Thompson. N., 2022, Rock Physics analysis for the Northern Lights CCS project, Offshore Norway, EAGE annual 83rd conference and exhibition, Madrid Spain

Mondol, N.H., Grande. L., Bjørnarå T.I., and Thompson. N., 2022, Caprock characterization of the Northern Lights CO2 storage project, offshore Norway, EAGE GeoTech 2022, 4-6 April 2022

Myhrvold J.A.T., and Kopperud A.E.V., 2023, Consolidation and stress history in shallow sediments in the northern North Sea, Master thesis NTNU

NGI 1990, HYDRAULIC FRACTURE AND CONDUCTOR INSTALLATION COLLATION AND ANALYSIS OF FIELD TESTS, Tom Lunne and Trond By, NGI Report 521620-2 10 December 1990

Obradors-Prats, J., Rouainia, M., Aplin, A. C., & Crook, A. J. L. (2019). A Diagenesis Model for Geomechanical Simulations: Formulation and Implications for Pore Pressure and Development of Geological Structures. Journal of Geophysical Research. Solid Earth, 124(5), 4452-4472.

Rahman, J.,Fawad, M., Mondol N.H., 2020, Organic-rich shale caprock properties of potential CO2 storage sites in the northern North Sea, offshore Norway, Marine and Petroleum Geology 122 (2020) 104665.

Rahman, M.J., Fawad, M., Jahren, J. Mondol, N.H. 2022. Influence of Depositional and Diagenetic Processes on Caprock Properties of CO2 Storage Sites in the Northern North Sea, Offshore Norway. Geosciences, 12, 181. https://, doi.org/10.3390/geosciences12050181.

Rise, L., K. Rokoengen, A.C. Skinner and D. Long (1984), Northern North Sea. Quaternary geology map between 60°30' and 62°N, and east of 1°E, IKU, Norway.

Roberts, D. T., A. J.L. Crook, J. A. Cartwright, M. L. Profit, and J. M. Rance. 2014. "The Evolution of Polygonal Fault Systems: Insights from Geomechanical Forward Modeling." 48th US Rock Mechanics / Geomechanics Symposium 2014 1 (May 2016): 488–502.

Rose, P., Byerley, G., & Vaughan, O. (2018, January). The Bacchus development: dealing with geological uncertainty in a small high-pressure–high-temperature development. In Geological Society, London, Petroleum Geology Conference series (Vol. 8, No. 1, pp. 319-337). Geological Society of London.

Rose, P., Byerley, G., Vaughan, O., Cater, J., Rea, B. R., Spagnolo, M., & Archer, S. (2018, January). Aviat: a Lower Pleistocene shallow gas hazard developed as a fuel gas supply for the Forties Field. In Geological society, London, petroleum geology conference series (Vol. 8, No. 1, pp. 485- 505). Geological Society of London.

Thompson, N., Andrews J.S., Wu, L., Meneguolo, R., 2022a, Characterization of the in-situ stress on the Horda platform – A study from the Northern Lights Eos well, International Journal of Greenhouse Gas Control 114 (2022) 103580

Thompson, N. Andrews, J.S., Teixeira Rodrigues, N.E., Reitan, H. 2022b, Data mining of in-situ stress database towards development of regional and global stress trends and pore pressure relationships. SPE Norway Subsurface Conference 2022. 27 April, Bergen, SPE-209525.

White Rose, 2016. K43: Field Development Report, Technical: Storage. Capture Power and National Grid. 234pp.

Williams, J.D.O., Fellgett, M.W., Kingdon, A. and Williamson, J.P. 2015. In-situ stress orientations in the UK Southern North Sea: Regional trends, deviations and detachment of the post-Zechstein stress field. Marine and Petroleum Geology, 67, 769–784.

Wu, L., Skurtveit, E., Thompson, N., Michie, E., Fossen, H., Braathen, A., Fisher, Q., Lidstone, A., and Bostrøm, B., 2022, Containment Risk Assessment and Management of

CO2 storage on the Horda platform, 16th International Conference of Greenhouse Gas Control Technologies, GHGT-16, 23rd-27th October 2022, Lyon, France.

Yang, Y., Aplin, A.C. 2010. A permeability-porosity relationship for mudstones. Marine and Petroluem Geology 27 (8), 1692-1697.